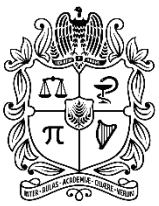

UNIVERSIDAD
NACIONAL
DE COLOMBIA

Desarrollo de un material tipo Starbon® a partir de almidón de origen colombiano para su uso como catalizador en esterificación de ácidos grasos

Milena Alexandra Zabala Vásquez

Universidad Nacional de Colombia

Facultad de Ingeniería, Departamento de Ingeniería Química y Ambiental

Bogotá, Colombia

2024

Development of a Colombian starch based Starbon® type material for its use as catalyst in fatty acid esterification

Milena Alexandra Zabala Vásquez

Tesis presentada como requisito parcial para optar al título de:

Magister en Ingeniería – Ingeniería Química

Director (a):

PhD. Alvaro Orjuela Londoño

Línea de Investigación:

Procesos catalíticos y petroquímicos

Grupo de Investigación:

Procesos Químicos y Bioquímicos

Universidad Nacional de Colombia

Facultad de Ingeniería, Departamento de Ingeniería Química y Ambiental

Bogotá, Colombia

2024

A mi hermana y mi mamá, que siempre me dan fuerza para seguir adelante.

“The more clearly we can focus our attention on the wonders and realities of the universe about us, the less taste we shall have for destruction”.

— Rachel Carson

a

Acknowledgments

First of all, I would like to express my deep appreciation to my family, especially my mother, Leyla Vásquez, and my sister, Sandra Zabala. Their constant support and encouragement have been my rock throughout this academic journey. Special thanks to Lucy, Nelly, Gladys, Alcira, Leonor, Cecilia, Mario, Javier, and Violeta for their unwavering concern for my wellbeing throughout this time. I am sure you have gone above and beyond your own areas to contribute to the development of my project.

Likewise, a sincere thank you to my supervisor, Professor PhD. Álvaro Orjuela, for his continuous support, guidance, and confidence in my academic endeavours and for motivating me to continue my academic journey. I'm also grateful to Professors PhD James Clark and PhD Suranjana Bose from the University of York for their willingness to share their insights into the synthesis of Starbon materials.

I am grateful to my research colleagues - Felipe Bohórquez, Alexander Baena, Angélica Rodríguez, Andrés Cabeza and Sebastián Rodríguez - with whom I have grown academically, sharing laboratory space, discussing research results, and making the journey of knowledge creation more agreeable. Equally important, the direct support of Laura Panqueba and Laura Ávila in the laboratory was crucial in understanding the nuances of Starbon® materials. Special thanks to colleagues Luis Salas and Liliana Ávila, whose research converged with mine in the materials field, for their valuable suggestions and for sharing their knowledge of the behaviour of carbon and starch, which contributed to the methodological understanding.

In addition, I would like to thank the laboratory technicians, especially Ricardo Cortés, whose attention, support, and knowledge of the equipment were crucial during the experiments. In addition, the characterisation of the synthesised materials would not have been possible without the support of Professor Carlos Trujillo, who made every effort to

keep the nitrogen adsorption equipment operational. Finally, the characterisation of the materials was completed thanks to the support of Professor Sonia Rincón and her team, including Fabio Moreno and Kevin Camacho. They were always open to helping me and learning about my process.

Part of this research was developed thanks to a scholarship granted by the BAYLAT organisation, which allowed me to carry out research at the Friedrich-Alexander University of Erlangen-Nürnberg in Erlangen, Germany. I appreciate the guidance in the field of materials and starches provided by my supervisor Professor PhD. Alexandra Inayat and PhD. student Katrin Städtke. I would also like to thank Lizeth Loaiza, Pedro Martínez and Camila Mejía, who became my family and supported me during my stay in Germany.

Finally, I would like to express my gratitude to my friends, for their unconditional support on this journey and for their attention to the progress of my research. Their company have been a constant source of motivation and encouragement. Special thanks to Alejandro Cárdenas, Daniela Vargas, Danna Gómez, Daniel Lavado, Diana Jiménez, Federico García, Felipe Munar, Giovany Rubio, Jenny Mateus, Luis Gil, Miguel Castelblanco, Neiry Martínez, Paula Triana, and Roque Jiménez.

To all mentioned and those inadvertently omitted, thank you for your dedication, support, and unconditional commitment. I hope to have your closeness in my future research endeavours.

Abstract

Mesoporous materials are attractive supporting structures for heterogeneous catalysis as they facilitate access and mobility of large molecules, thus improving yields in a variety of chemical reactions. Among different materials, Starbon® materials are mesoporous carbons which can be advantageously synthesized from biobased sources, be further acid-activated to be used as catalysts in esterification reactions. Conventionally, Starbons® are produced using a high-amylose-content starch, which guarantees a high mesopore volume due to the arrangement of amylose molecules during the synthesis process. Looking for the valorisation of waste streams and low-cost raw materials, the use of starch derived from common roots and tubers needs to be studied. According to Colombian National Planning Department, nearly 5 Mton of roots and tubers are produced in the country, nevertheless, nearly 30% are discarded during production stages as they do not meet quality standards. In this regard, this work focused on understanding and optimizing the surface properties of Starbon® materials derived from cassava starch for its subsequent use as catalyst in long-chain esterification reactions. The synthesis of Starbon materials involves gelatinization, retrogradation, solvent exchange and carbonization steps, which conditions were assessed, firstly by an exploratory analysis, and subsequently by a Factorial 3^2 and Box-Behnken experimental designs, taking surface area, pore volume and pore size as response variables. A method for the synthesis of cassava-derived Starbon was proposed. The obtained cassava-Starbon exhibited a surface area of 263 m^2/g, with a mean pore diameter of 3.7 nm and a pore volume of 0.2cm^3/g. Subsequently, the material was sulfonated and tested in the batch esterification of stearic acid with isopropyl alcohol, considering the growing market in fatty acid esters industry. Cassava-Starbon catalyst enabled slightly higher conversion and higher turn-over number (0.15 mol/s H^+Eq) compared to widely used ion exchange resins.

Key-words: Carbon, catalyst, cassava starch, esterification, mesoporous, porosity, Starbon.

Resumen

En la catálisis heterogénea, materiales mesoporosos son soportes atractivos al facilitan el acceso y la movilidad de moléculas de gran tamaño, mejorando así los rendimientos en diversas reacciones. Entre diferentes materiales, los materiales Starbon® son carbones mesoporosos que pueden sintetizarse ventajosamente a partir de fuentes biobasadas, y luego activarse con ácido para utilizarse como catalizadores en reacciones de esterificación. Convencionalmente, los Starbons® se producen utilizando almidón con alto contenido de amilosa, lo que garantiza un alto volumen de mesoporos debido a la disposición de las moléculas de amilosa durante el proceso de síntesis. En busca de la valorización de corrientes de residuales, es de interés estudiar el uso de almidón derivado de raíces y tubérculos comunes en la síntesis de estos materiales. Según el Departamento Nacional de Planeación de Colombia, se producen casi 5 millones de toneladas de raíces y tubérculos en el país, sin embargo, cerca del 30% se descartan durante las etapas de producción por no cumplir con los estándares de calidad. En este sentido, este trabajo se centró en comprender y optimizar las propiedades superficiales de los materiales Starbon® derivados del almidón de yuca para su uso posterior como catalizador en reacciones de esterificación de cadenas largas. La síntesis de los materiales Starbon implica gelatinización, retrogradación, intercambio de solventes y carbonización de los almidones. Estas condiciones fueron evaluadas para la síntesis empleando almidón de yuca, primero mediante un análisis exploratorio y luego mediante un diseño Factorial 3^2 y Box-Behnken, tomando la superficie, el volumen de poros y el tamaño de poros como variables de respuesta. De esta manera, fue posible proponer un método para la síntesis de Starbon derivado de yuca. El Starbon de yuca obtenido mostró una superficie de 263 m2/g, con un diámetro de poro promedio de 3.7 nm y un volumen de poro de 0.2cm^3/g. Este material fue sulfonado y probado en la esterificación batch de ácido esteárico con alcohol isopropílico, considerando el creciente mercado en la industria de ésteres de ácidos grasos. El catalizador Starbon de yuca permitió una conversión ligeramente superior y un TOF más

alto (0.15 mol/s H+Eq) en comparación con las resinas de intercambio iónico ampliamente utilizadas.

Palabras clave: Carbón, catalizador, almidón de yuca, esterificación, mesoporoso, porosidad, Starbon.

Content

List of Figures

Pág.

List of Tables

Pág.

List of Abbreviations

Abbreviation	Term
ANOVA	Analysis of variance
AV	Acid value
BET	Brunauer, Emmett and Teller method
BJH	Barrey-Joyner-Halenda model
Cat.	Catalyst
Carb.	Carbonization
CH_4	Methane
Cl-	Chloride
CO	Carbon monoxide
CO_2	Carbon dioxide
DFT	Density function theory
DPN	National Planning Department
H_2SO_4	Sulfuric acid
H_3PO_4	Phosphoric acid
IPA	Isopropyl alcohol
IUPAC	International Union of Pure and Applied Chemistry
KOH	Potassium hydroxide
Mg	Magnesium
MgO	Magnesium oxide
$Mg(OH)_2$	Magnesium hydroxide
MSA	Methanesulfonic acid
NaOH	Sodium hydroxide
N_2	Nitrogen
PET	Polyethylene terephthalate
PF	Phenol- formaldehyde
PI	Polyimide
p-TSA	p-toluenesulfonic acid
PVA	Polyvinyl alcohol
RF	Resorcinol-formaldehyde
S	Starch
SA	Stearic acid
SEM	Scanning Electron Microscopy
S_{BET}	Specific surface area
SO_3	Sulphur trioxide
SO_3H	Sulfonic group
T	Temperature
TBA	Tert-butyl alcohol
TEM	Transmission electron microscopy
TGA	Thermogravimetric analysis
TOF	Turnover frequency

Abbreviation	Term
TON	Turnover number
wt.	Weight
X	Reaction conversion
$ZnCl_2$	Zinc Chloride
4-BDS	4-benxene-diazonium sulfonate
γ-Al_2O_3	Gamma aluminium oxide
ΔH	Enthalpy

Prologue

This document is structured in four chapters, each dedicated to exploring the synthesis of Starbon®-type materials from Colombian cassava starch and its catalytic application in the esterification of long-chain fatty acids. For this purpose, in Chapter 1 a solid theoretical framework is established, providing essential insights necessary for comprehending topic presented in subsequent chapters. Chapter 2 focus in the understanding and adaptation of relevant variables in the Starbon® synthesis process, specially emphasizing on tailoring these processes to the use of Colombian cassava starch as precursor. Once this understanding was completed, Chapter 3 is dedicated to present a systematic optimization process aimed at enhancing the surface properties of the cassava starch derived Starbon® material. Finally, Chapter 4 brings together the insights gained from the previous chapters, wherein the synthesized Cassava-Starbon is tested as a catalyst for the esterification of long-chain fatty acids. This chapter is dedicated to presenting the results of these tests, coupled with a comparative analysis against commercially available heterogeneous catalysts. Written in the format of scientific papers, Chapters 2, 3, and 4 seamlessly integrate relevant portions of the introduction. The document concludes with a summary of the key findings and implications of the research. The closing chapter provides insights for future exploration and advancements in this field.

Introduction

Fatty acid esters (FAEs) are important oleochemicals employed in the manufacture of personal care, pharmaceutical and food products. FAEs constitute a global market valued at $ 2.4 billion USD per year, projected to reach $ 3.2 billion USD by 2027 (Grand View Research, 2020). These compounds are typically synthesized through esterification reactions, often employing homogeneous catalysts such as sulfuric acid, p-toluenesulfonic acid (p-TSA), or methanesulfonic acid (Chandane et al., 2017). Nevertheless, the use of these catalysts involves energy- and materials-intensive separations and downstream processing for neutralization and disposal. Alternatively, following to green chemistry principles, heterogeneous catalysts as ion exchange resins and zeolites have been explored for esterification of fatty acids in the pursuit of minimizing waste generation. The use of heterogeneous catalysis not only intends to increase productivity, but also to reduce or eliminate generation of hazardous substances (Díaz et al., 2000).

Among the variety of heterogeneous catalysts used for esterification, mesoporous acid catalysts are of special interest as they can facilitate the access of large molecules (e.g. fatty acids) to active sites, thereby enhancing reaction yields. In particular, mesoporous carbons have emerged as favorable catalyst supports for this reaction as their high surface area and extended porous matrix enable high conversions despite the presence of water in the reactive medium. These mesoporous carbonaceous materials are typically synthesized by using sacrificial templates to induce the required porosity, followed by carbonization al high temperatures to eliminate the template and preserved the desired structure. However, this conflicts with the above-mentioned green chemistry principles, particularly waste prevention and design for energy efficiency. Consequently, investigations into the production of template-free mesoporous carbon have boosted during recent years. As a result, the synthesis of aerogels, xerogels and cryogels was found as a template-free alternative due to the mechanical resistant and high surface area per volume unit of the obtained materials (Członka et al., 2018). The most common precursor materials used for

the synthesis of organic gel structures are resorcinol-formaldehyde (RF) polymers, which are thermally treated to obtain the desired mesoporous carbons. Nevertheless, RF does not allow an easy optimization of carbonaceous material characteristics due to the limited availability of its physicochemical properties; also, RF materials are non-renewable (Tamon et al., 1999).

In this context, polysaccharides have emerged as a sustainable alternative precursor for the synthesis of mesoporous carbons considering their natural abundance, low cost, functional groups, and its possibility to form aqueous gels. All these characteristics are well aligned with the principles of green chemistry: less hazardous synthesis, and use of renewable feedstock. In their natural state, polysaccharides exhibit low surface area and poorly developed porosity. However, when aqueous gels are formed, they expand, increasing the surface area per unit volume, which is suitable for the production of mesoporous carbons (White & Clark, 2015). Particularly, when the polysaccharide used for mesoporous carbon production is starch, the resulting material is commercially known as Starbons® (starch-derived mesoporous carbons). Starbon® materials were developed at the Green Chemistry Centre of Excellence at the University of York in England, in conjunction with the Department of Organic Chemistry at the University of Cordoba in Spain.

Starbons® can be considered promising biobased mesoporous materials that can be activated by mean of sulfonation to be used as catalyst in esterification, particularly of large acid or alcohol molecules. Advantageously, the hydrophilic-hydrophobic character of Starbon® can be tuned by controlling the degree of carbonization, enhancing catalytic properties and water removal capacity. As a result, when tested on different reactions, Starbon® has shown higher reaction rates than other commercial acid catalysts. Additionally, it has demonstrated to be stable and reusable in petrochemical and fine chemical reactions (Mena & Macquarrie, 2014). It is worth mentioning that despite the fact that the use of sulfonation agents (e.g. sulfuric acid, oleum, SO_3) is not completely aligned with green chemistry principles, such agents are cost-effective and readily available for the activation of Starbon® catalysts (Clark, 2002). To minimize their potential environmental impacts, the sulfonating agents used during the activation process could be recycled and reused in the preparation of the sulfonated materials.

To promote a circular economy in the catalytic sector and to employ more sustainable processes based on green chemistry principles, Starbon® production can also be carried out using residual biomass. In this case, waste products and residual streams containing starch could be treated for starch extraction and further transformation into suitable catalytic materials. Colombia, as an agricultural country (contributing to 21% of national exports), has a significant production of starch-rich farm products —especially roots and tubers—. According to Colombian National Planning Department, 38.1% of the total area cultivated in the country is dedicated to produce around 5 Mton of roots and tubers annually (DPN, 2016). However, one of the main challenges in the production and marketing of tubers is their degradation, which typically occurs 48 hours after the extraction from the soil (Folgueras et al., 2012). In addition, only products of a certain size can be sold into the market due to consumers' preferences. Because of the previously mentioned, approximately 30% of the roots and tubers produced are discarded during production stages or sold at a value that does not cover production costs, as they fail to meet quality standards. Moreover, industrial processing of some tubers, such as flour production, precooked foods, and snacks, generates waste streams with a high content of usable starch. Some of those are aqueous waste streams which are rich in non-precipitated starch that are disposed in sewage (García et al., 2020). Therefore, exploring utilization alternatives for these agricultural residues, especially those with high valorization, is important for economic growth of the country.

Consequently, this project focuses on the study of a suitable method for the production of Starbon® materials using Colombian starch as feedstock, and in their further activation to produce effective catalysts for fatty acid esterification. Particularly, cassava starch was chosen due to its commercial availability in the country and the extensive use in the food industry which implies the existence of associated residual streams (Canales & Trujillo, 2021). In this regard, the project will apply the green chemistry concept to develop active solid-acid catalysts based on renewable materials. The synthesis process for the Starbon®-type materials follows previous reports using corn-based starches as precursors.

The Starbon® production method, developed using Hylon VII starch (corn-based 70%-amylose starch), take advantage of starch's expansion capacity to form a mesoporous structure, which is subsequently carbonized under an inert atmosphere. This process

involves a gelatinization stage in water to get expanded starch, followed by retrogradation and drying to obtain an aerogel mesoporous structure, which is finally carbonized. As Starbons® are tunable materials, changes introduced in the synthesis method can affect their characteristics including their final mesoporosity, total volume pore, and surface area. Those characteristics also depends on the nature of the starches, and their content of amylose and amylopectin. The use of low amylose content starches as precursors has been reported as a limitation in the surface properties of Starbon® materials, as amylose chains are responsible of prompting porosity when they leave the granule in the expansion stage (White et al., 2008). Nevertheless, no studies have delved into the understanding of production nuances when low amylose content starches are employed. This is the case of cassava starch, which has approximately 70% amylopectin and 21% of amylose content (depending on the variety). Therefore, to assess the impact of low-amylose content starches in the synthesis of Starbon® materials, this project aims to assess different operating conditions -such as gelatinization temperature and mass ratio, retrogradation time, and carbonization temperature- in the production of cassava-based Starbons®. Considering the previously mentioned and in order to establish a suitable preparation method, a preliminary study on the synthesis of cassava based Starbon® is carried out focusing on understanding pore's structure and surface characteristics.

Once a basic understanding of the relation between the synthesis variables and the surface characteristics of the cassava-Starbon® is acquired, it will be possible to focus on a greener synthesis for its use as catalyst in fatty acid esterification. In this regard, the mesoporosity of the material will be optimized by a factorial design of experiments and a Box-Behnken methodology, looking for pore sizes that allow big molecules to reach active sites. Finally, the material obtained under the most suitable conditions will be subjected to sulfonation, characterized for its surface parameters and exchange capacity, and tested in the esterification of fatty acids. As a benchmark, a comparison will be done by performing esterification reactions using commercial homogeneous and heterogeneous catalysts.

1. Background and Theoretical Framework

1.1 Carbon Materials

After oxygen, carbon is the most abundant element in the biosphere. Carbon materials, including diamond, graphite, carbon nanotubes, fullerenes, carbynes and graphene, share a common carbon composition, but exhibit varying degrees of crystallinity and macro- and micromorphology, which influence their physical properties (Inagaki & Kang, 2016). Naturally, carbonaceous materials are derived from the thermal degradation of fossil-derived precursors and biomass, under high energy-intensive conditions (Titirici et al., 2015). The process primarily occurs through thermal decomposition (e.g., pyrolysis) at temperatures of 800 – 1500°C under inert atmospheres (Inagaki, 2013), and it can take place in gas, liquid, and solid phases, leading to diverse carbon materials (Table 1-1).

As a result of the carbonization process, different morphologies are generated at the nanoscale which are highly responsible for the porous characteristics of the material. The nanotexture in carbon materials is classified as oriented and non-oriented according to their origin, with oriented further divided into planar, axial, and point schemes. Each nanotexture results in different types of carbon materials, such as glass-like carbon, kish graphite, pyrolytic carbons, cokes, carbon fibres, activated carbons, and carbon blacks (Figure 1-1). Many of these carbon materials consist of anisotropic particles, of which the orientation creates another variety of microtextures in bulk materials (Inagaki & Kang, 2016). In solid-phase carbonization, resins (e.g. phenol-formaldehyde and of furfuryl alcohol) and biomass (e.g. cellulose-rich materials) can be converted to carbon materials. Fast carbonization results in porous carbon, represented by activated carbons, while slow carbonization results in glass-like carbons, containing significant closed pores (Inagaki, 2013).

Table 1-1: Carbon materials obtained by gas, liquid and solid phase carbonization (Inagaki, 2013).

	Precursors	Carbon Material	Characteristics
Gas-phase carbonization	Hydrocarbon gases, decomposition in space	Carbon black	Fine particles
	Hydrocarbon gases, deposition on substrate	Pyrolytic carbon	Various textures, preferred orientation
	Hydrocarbon gases with metal catalysts	Vapor-grown carbon fibers Carbon nanofibers	Fibrous morphology, various nanotextures
	Hydrocarbon gases, without catalyst	Diamond-like carbon	Thin film, sp^3 bond, amorphous structure
	Carbon vapor	Carbon nanotubes	Tubular, single-wall and multiwalled
		Fullerenes	Spherical, molecular nature
Solid-phase carbonization	Plants, coals, and pitches	Activated carbons	Highly porous adsorptivity
	Furfuryl alcohol (FA), phenol resin, cellulose	Glass-like carbon	Amorphous structure, conchoidal fracture, gas impermeability
	Poly(acrylonitrile), pitch, cellulose, and phenol resin	Carbon fibers	Fibrous morphology, high mechanical properties
	Polyimide films	Carbon films	Film wide range of graphitizability
Liquid-phase carbonization	Pitch, coal tar	Cokes Mesocarbon microbeads	Spherical particles
	Cokes with binder pitches	Polycrystalline graphite blocks, including high density isotropic graphite	Various densities, various degrees of orientation

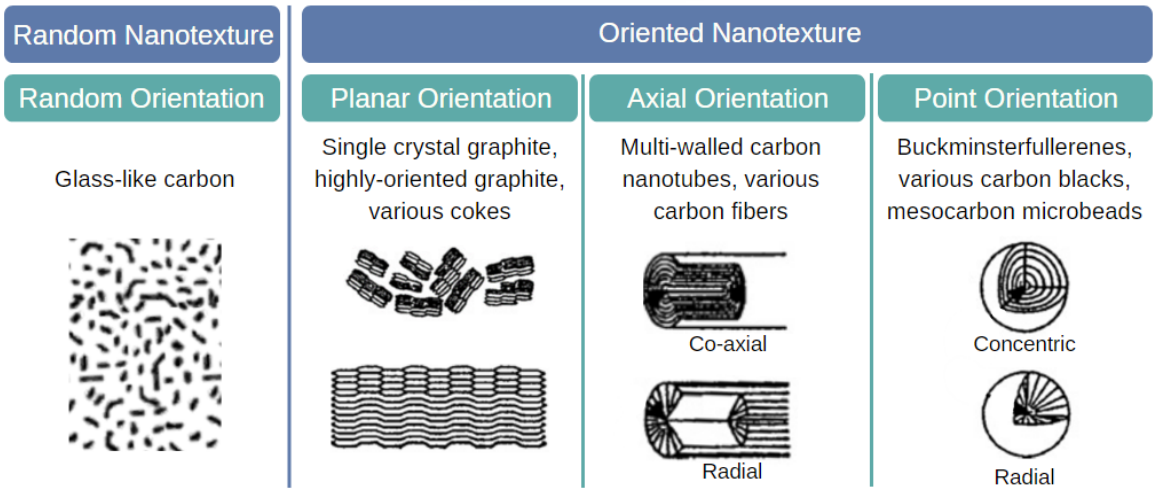

Figure 1-1. Nanotextures in carbon materials. Adapted from: Inagaki, 2013.

1.1.1 Activated Carbons

Activated carbons, known by their high porosity and extended surface area, find extensive industrial applications as adsorbents in water treatment (Mohan & Pittman, 2006), carbon capture (Choi et al., 2009), energy storage (Pandolfo & Hollenkamp, 2006) and heterogeneous catalysis (Auer et al., 1998; Rodriguez, 1998). In all these applications the pore texture is the most important property to be controlled (Inagaki, 2013). Considering the standardized classification of The International Union of Pure and Applied Chemistry (IUPAC) presented in Table 1-2, porous carbons can contain micropores (<2 nm), mesopores (2 - 50 nm), and macropores (>50 nm). The pores in such structures are interconnected in bi-dimensional and tri-dimensional patters as schematically illustrated in Schematic representation of the structure of porous carbon tridimensional (left) and bidimensional (right)

Figure 1-2.

Table 1-2: IUPAC classification of pore size, condensation mechanism, and application (Sing et al., 1985).

Pore type	Size /nm	Condensation mechanism	Application
Micropore	<2	Tridimentional	Adsorption in liquid phase and gas phase
Mesopore	2 - 50	Capillary	Liquid phase – heterogeneous catalysis or chromatographic separation
Macropore	>50	No Condensation	Filtration of a system

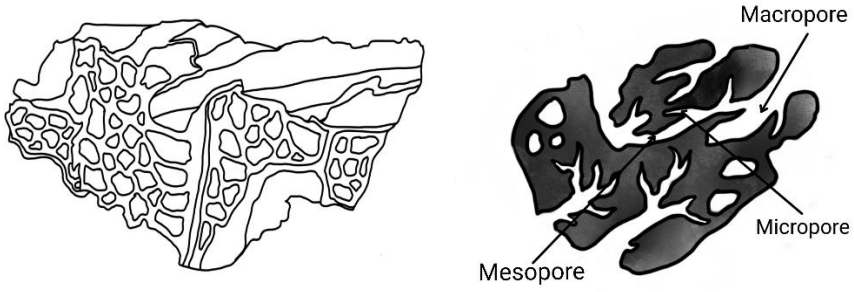

Figure 1-2. Schematic representation of the structure of porous carbon tridimensional (left) and bidimensional (right).

Similar to other solids, the characterization of the porous structure in carbonaceous materials is carried out by mean of adsorption of a probe gas. Nitrogen adsorption is commonly employed in most commercial equipment and the adsorption isotherms enable to determine features such as surface area and pore volume of the materials. As the adsorption mechanism differs for microporous, mesoporous, and macroporous materials, this is manifested in the isotherm profiles which enables to elucidate porous types and some morphology features. Microporous materials undergo tri-dimensional adsorbate condensation within a strong electromagnetic field induced by narrow pores. In contrast, mesoporous materials rely on the formation of successive layers of adsorbate ending with capillary condensation. In the case of the macroporous materials, they exhibit properties similar to conventional flat surfaces unfilled by capillary condensation (Gregg & Sing, 1982). The above indicates that absorption isotherms could be used to elucidate the effects of different synthesis variables in the pore distribution and morphology of the starch-based carbons before and after activation.

Besides synthesis, activation has also a major impact in the structure of carbonaceous materials. Typically, commercial activated carbons are derived from low-cost renewable materials (e.g. nut shells, wood ships), and the activation can be carried out by using physical/thermal treatments or by chemical methods. Physically activated carbon involves selective gasification using CO2 or steam at temperatures between 800-900°C, while chemically activated carbon results from impregnation of reagents such as NaOH, H_3PO_4, $ZnCl_2$, etc., followed by carbonization, commonly at temperatures above 650°C (White & Clark, 2015). Both routes lead to economical and highly microporous carbons from various organic precursors. Regardless the synthesis and activation methods, understanding of the process is paramount to enable obtaining controlled morphology and surface characteristics for the desired applications. Commercial activated carbons span from catalytic supports to adsorbents for separation applications (e.g. adsorption, bleaching, chromatography) also including their use in electrochemistry applications. In general, they are obtained by physical and chemical methods from various organic precursors, offering a wide range of properties, with a high degree of microporosity and being economically viable (De et al., 2015). Nevertheless, the scope of activated carbons is somewhat limited in applications such as large-molecule catalysis, fuel cells, biomedical devices, and automotive components because of small pore sizes and morphology. This underscores

the need for developing novel precursors and methods to obtain tunable mesoporous carbon materials.

1.1.2 Mesoporous carbons

Mesoporous materials correspond to solid matrixes with an interconnected network filled with either gas or liquid, with pores sizes ranging from 2 nm to 50 nm (Sing et al., 1985). When the network is constituted of a carbonaceous material it is considered a mesoporous carbon, and such type of materials have gained attention for their versatility in preparation from relatively inexpensive precursors. The main advantage of such structures is that their pore sizes facilitate high loadings of chemicals to the active sites, and an efficient diffusion/mass transfer of analyte or substrate in liquid-phases. This enables a more effective adsorption of a wide range of molecules than in conventional micropore-activated carbons.

Recently, different carbonization processes have been proposed for the synthesis of mesoporous carbons, including the replication of a porous inorganic template (hard template method), self-assembly and carbonization of polymer blends (polymer blend or soft template method), defluorination of fluorinated hydrocarbons, and carbonization of a preformed organic polymer aerogels. The template carbonization initially developed for thin oriented graphite films, reveals high potential to control morphology by selecting suitable template materials (Inagaki, 2013). The hard template approach involves replicating various ordered inorganic templates generating ordered mesoporous carbons. However, this method results in the loss of particle morphology and low micropore content. The synthesis steps include the preparation of an inorganic template with a controlled pore structure, the impregnation/infiltration of the sacrificial template with a carbonizable or polymer precursor, followed by a thermal carbonization leading to the crosslinking and condensation of organic precursors, forming the carbon material. The last step is typically performed at temperatures above 600 °C to chemically toughen the carbon product against the acidic or caustic solutions used in dissolving the inorganic matrix (White & Clark, 2015). To control the pore structure in carbon materials, various templates were developed as summarized in Table 1-3. As observed, different carbon precursors, and characteristics of the pore structure are obtained in the resultant carbons from the different templates.

Table 1-3: Reported studies on the synthesis of mesoporous carbon by template method.

Template		Carbon precursor	Carbon obtained	Ref.
Mesoporous silica	MCM-48, MCM-41, SBA-1, SBA-15	Impregnation of sucrose, FA, PF, mesophase pitch. Chemical vapor infiltration of acetylene.	Ordered or disordered mesopores. Channel-like.	[1]
MgO	MgO, Mg acetate, Mg citrate, $Mg(OH)_2$	Mixing with polyvinyl alcohol (PVA), coal Tar pitch, polyethylene terephthalate (PET), polyimide (PI)	Disordered mesopores.	[2]
Surfactants	Diblock and triblock copolymers	Mixing with RF, triethyl orthoacetate (EOA)	Ordered or disordered mesopores.	[3]

[1] Bazuła et al., 2008; Joo et al., 2001; Jun et al., 2000; Kruk et al., 2000; Peng et al., 2010.
[2] Morishita et al., 2010; Morishita, Ishihara, Kato, Tsumura, et al., 2007; Morishita, Ishihara, Kato, & Inagaki, 2007.
[3] Kosonen et al., 2006; Liang et al., 2004; Tanaka et al., 2005; Zhang et al., 2005.

The hard template approach is attractive due to the potential to generate a wide range of accessible mesophases and morphologies, coupled with chemical inertness, stability, and advantages over classical microporous activated carbons. However, it involves sacrificial templates, necessitating high carbonization temperatures for their removal and to render the carbon structure inert. In contrast, the soft template method results in carbons with small mesopore size (<10 nm) and developed microporosity. However, challenges related to mass transfer/diffusion limitations and active-site accessibility often persist (Li et al., 2013; Saha et al., 2013).

An alternative involves the preparation of porous carbon materials without using templates, creating aerogels, xerogels, and cryogels, based on the thermal carbonization of organic/polymeric gel precursors. These non-fluid networks are primarily composed of interconnected colloidal particles in a gas (Kistler, 1932), exhibiting low densities (≥100 kg m−3) surface areas in the region of 1000 m2 g−1 and very high resistance (Pekala, 1989). These gels are typically obtained through the polycondensation of resorcinol-formaldehyde mixtures. The gel can be dried under atmospheric conditions and temperatures below 100 °C forming xerogels. When using supercritical drying above the liquid's critical point aerogels are produced. In the case of freeze drying the liquid to prevent its crystallization, cryogels are produced (Tamon et al., 1999).

Aerogels and cryogels present various types of porosity depending on the synthesis process and subsequent treatment (Hanzawa et al., 1996). Carbonization under non-

oxidizing conditions yields high-surface-area carbon structures with interconnected interparticle mesopores (Bekyarova & Kaneko, 2000). The resultant carbon aerogels often show adsorption isotherms of type IV with clear hysteresis, influenced by precursor gel composition, drying method, time, and carbonization temperature (Pekala et al., 1991). While the porous dimensions of parent organic gels do not automatically transfer into carbon aerogels, the shrinkage, pore closure, and pseudo-graphitization that may occur during carbonization are crucial considerations (Yamamoto et al., 2001).

1.1.3 Carbon materials as acid catalysts

The use of acid catalysts is widespread in the chemical and pharmaceutical industries and traditionally they correspond to homogeneous inorganic acids difficult to recover or remove. Instead, solid acids, including mixed oxides, acidic clays, zeolites, and hybrid organic–inorganic materials, offer a greener alternative to concentrated acid solutions due to lower corrosiveness, their environmental friendliness, ease of separation, and minimized hazardous waste generation. As a result, nowadays solid-acid catalysts like zeolites are well-established in the petrochemical industry (Clark, 2002; Marziano et al., 1998). In addition to zeolites, activated carbons are also widely used in different applications, either as catalysts or as supports of other active species. Carbon-based solids have demonstrated remarkable catalytic activity for acid-catalyzed reactions such as hydration, hydrolysis, and esterification of higher fatty acids (Mena, 2014). In particular sulfonated carbons are widely used for these applications. Sulfonated carbons are primarily synthesized through incomplete carbonization of sulfoaromatic rings (Hara et al., 2004), sulfonation of microporous or mesoporous carbons, by treatment of char using sulfuric acid (Okamura et al., 2006; Suganuma et al., 2008; Toda et al., 2005), and hydrothermal carbonization (Hu et al., 2008).

Generally, the catalytic activity of sulfonated carbons depends on the precursors used. Carbonization is usually done at high temperature under an inert atmosphere for a long time to form polycyclic aromatic carbon sheets. Several studies have explored the synthesis of carbon-based acid catalysts from different precursors, employing methods like incomplete carbonization, thermal treatment, and hydrothermal carbonization. Such catalysts, derived from diverse sources such as glucose, starch, sucrose, and cellulose, exhibit significant catalytic activities in esterification reactions and have potential

applications in biodiesel production, hydrolyzing cellulose, and other organic transformations. Table 1-4 summarizes some studies for the synthesis of carbon-based acid catalysts mentioning the precursor employed, synthesis method and performance in reaction.

Table 1-4: Reported studies on the synthesis of carbon-based acid catalysts from different biobased precursors.

Precursor	Synthesis method	Performance	Ref.
D-glucose	Incomplete carbonization at 300-450°C.	Remarkable for the esterification of higher fatty acids. Higher activity than commercial acid catalysts for biodiesel production.	(Okamura et al., 2006; Takagaki et al., 2006; Zong et al., 2007)
D-glucose	Thermal treatment of the mixture of p-toluenesulfonic acid (p-TSA)/glucose at 180 °C.	Higher catalytic activity than sulfonated active carbon in the reaction of esterification of succinic acid with ethanol.	(B. Zhang et al., 2010)
D-glucose	Heating a mixture of D-glucose, p-toluenesulfonic acid and diphenyl- ammonium tosylate.	Good activity for esterification reaction of carboxylic acids with acid-sensitive alcohols.	(Zhan et al., 2014)
D-glucose and starch in aqueous solution	Carbonized at 400 °C under N_2. Sulfonated using concentrated sulfuric acid at 150–160°C under N_2.	Highest acid density and esterification activity was obtained from mixture of glucose and corn powder.	(Chen & Fang, 2011)
Sucrose and alumina	γ-Al_2O_3 impregnated with aqueous solutions of sucrose. carbonized at 600 °C under N_2. Immersed in hydrofluoric acid (HF) solution. Mixed with aqueous solution of 4-BDS in HCl at 5 °C.	High efficiency for the esterification of oleic acid with methanol. Higher TOF than sulfonated activated carbon and Amberlyst-15 ($109h^{-1}$ vs. $44h^{-1}$ vs. $15h^{-1}$).	(Geng et al., 2011)
High amylose corn starch	Heated in water. Cooled to 5°C. Doped with a catalytic amount of an organic acid. Heated under vacuum at a 180 °C. Suspended in H_2SO_4 99.999% purity for 4 h at 80°C.	Active and reusable catalysts for the aqueous phase esterification of dicarboxylic acids	(Budarin, Clark, Luque, Macquarrie, Koutinas, et al., 2007)
Cellulose	Heated at 450°C under N_2. Boiled in fuming sulfuric acid (15 wt% SO_3) at 80°C under N_2.	Highly active in hydrolyzing cellulose: up to 68.9% of reducing sugars in a ionic liquid medium (130 °C for 3 h) and 51% in aqueous medium (180 °C for 9 h).	(Suganuma et al., 2008)
Cellulose	Heated at 600°C under N_2. Sulfonated by the addition of 98% sulfuric acid at 150 °C. Cl^- ions adsorb onto cellulose.	Highly selective in hydrolyzing cellulose under hydrothermal conditions. Active groups have no leaching problem.	(Pang et al., 2014)
Wood powder with $ZnCl_2$	Immersion in HCl aqueous solution with $ZnCl_2$. Heated for 1 h at 250-600°C in a furnace.	High catalytic performance for the esterification of acetic acid	(Kitano et al., 2009)

Precursor	Synthesis method	Performance	Ref.
	Heated in fuming sulfuric acid at 80°C under N_2.	(70°C). High catalytic activity for the benzylation of toluene.	
Camphor tree branches	Immersed with10% sulfuric acid. Carbonized in toluene at high temperature.	Excellent performance in the ketalization of cyclohexanone with glycol	(Ouyang et al., 2014)
Waste of Bahia pulp fibers	Impregnated with H_3PO_4 aqueous solution. Carbonized at 250–450 °C under N_2. Heated in H_2SO_4 at 90 °C under N_2.	Good activity for the transesterification of methyl acetate with butanol. Higher performance than Amberlyst and H-ZSM-5.	(Fu et al., 2012)
Furfural	Hydrothermal carbonization of a mixture of furfural–sodium dodecylbenzene sulfonate at 180 °C in an autoclave.	Highly active in esterification reactions involving bulky organic acids.	(Jia et al., 2014)
Sulfoaromatic hydrocarbons	Incomplete carbonization. Heating in sulfuric acid at 200–300°C.	High activity in the esterification of acetic acid.	(Hara et al., 2004)
Activated carbon	Reaction of 4-benzene-diazonium sulfonate (4-BDS) with activated carbon using hypo-phosphorous acid (H_3PO_2).	Comparable and higher catalytic activities than commercial catalysts in esterification of aliphatic acids with long carbon chains. Leaching of SO3H group during the reactions.	(X. Liu et al., 2010)
Graphene oxide	Reduced with 80% hydrazine hydrate at 100°C. Mixed with 4-Benzene-diazonium-sulfonate and H_3PO_2 aqueous solution.	High catalytic activity in the hydrolysis reaction. Keep their activity through several cycles.	(Ji et al., 2011)

1.2 Starbon® materials

Starbon® are mesoporous structures obtained by carbonizing starch and other expanded polysaccharide forms under inert atmospheric conditions by the methods described in **Table 1-4**. Those materials were developed at the Green Chemistry Centre of Excellence at the University of York in England, in collaboration with the Organic Chemistry Department at the University of Córdoba, Spain. In 2006, Budarin et al. reported a novel approach for the generation of a new family of mesoporous carbonaceous materials with surfaces ranging from hydrophilic to hydrophobic, which is controlled by the degree of carbonization (Budarin et al., 2006). Aligned with the principles of green chemistry, Starbon® materials offer biogenic origins and reduced environmental impact in both usage and preparation. A notable characteristic is their independence from sacrificial templates, as they inherently form a mesoporous network. Additionally, these materials enable the production of pore sizes ranging from 8 to 16 nm, surpassing those achieved with templating methods (Lu et al., 2005).

Mechanically stable and featuring controllable electrical conductivity, Starbons® exhibit remarkable versatility in functional groups, modifiable based on the carbonization degree. This allows the production of polysaccharide-like structures with abundant hydroxyl groups, akin to starch at low carbonization temperatures. Conversely, higher temperatures yield more aromatic, graphite-like materials. This adaptability ensures stability across a broad spectrum of conditions, from polar solvents like alcohols to acidic and basic solutions. The tunable hydrophilic/hydrophobic balance of Starbon® is a direct outcome of carbonization degree control (Budarin et al., 2006). Given these properties, Starbon® materials find applications in diverse fields such as nanotechnology, heterogeneous catalysis, energy storage, water treatment, and phase separation (chromatography). In nanotechnology frame, investigations have explored applications with palladium and ruthenium supported on Starbons® as catalysts (Luque et al., 2009). In chromatography studies, efficiency has been demonstrated in the separation of enantiomers, including substituted ferrocene compounds (Okamoto & Yashima, 1998). Areas such as water treatment and energy storage continue to be under study and hold promising applications for the future (Parker et al., 2013).

Commercial nomenclature of Starbons® provides insights into the synthesis process; for instance, Starbon®-400-SO_3H indicates sulfonation with sulfuric acid and carbonization at 400°C. Specifically, this material boasts a BET surface area of 386 m^2g^{-1}, a BJH pore diameter of 4.1 nm, and a BJH pore volume of 0.62 cm^3g^{-1} (Clark et al., 2008).

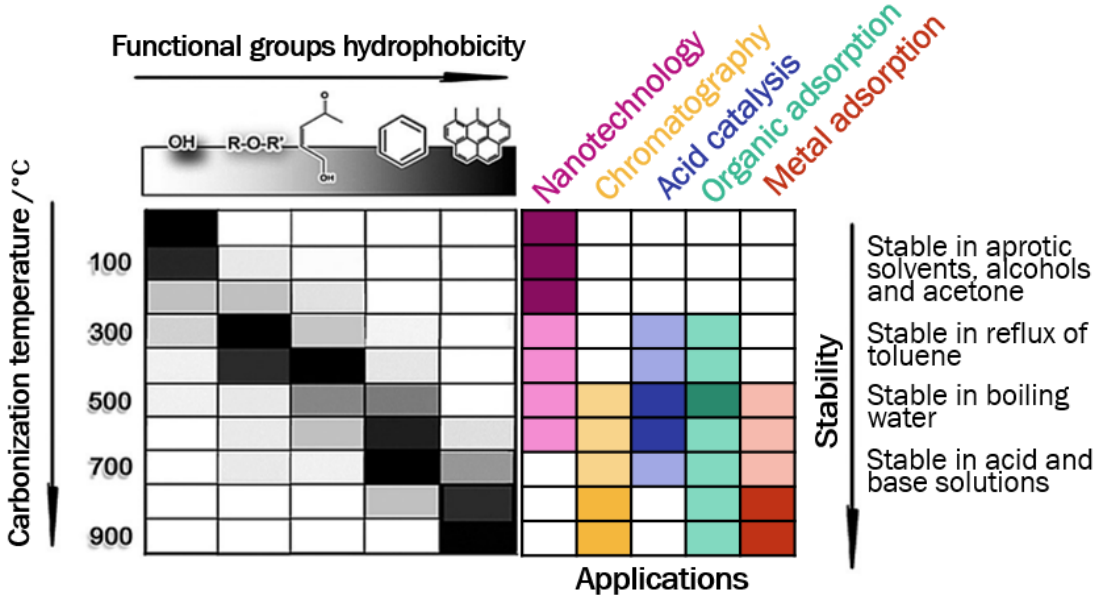

Figure 1-3. Starbon® functional groups, stability and applications range according to carbonization degree. Adapted from: Budarin et al., 2006.

Starbon® are synthesized through the inert atmosphere carbonization of biobased matrices. The utilization of low-cost or residual biomass aligns with the green principles governing their synthesis. Particularly, polysaccharides, have garnered attention due to their inherent advantages, including natural abundance, cost-effectiveness, and the ability to form expanded aqueous gels with diverse functional groups (–OH, –C (O) OH, $–NH_2$. In their native form, polysaccharides have a low surface area and underdeveloped porosity. However, as polysaccharides are composed of microscopically clustered networks; by converting them into expanded gels the polysaccharide opens up through reassociation and rearrangement of chains to generate a porous "aqueous" gel with a large surface area per unit volume (White & Clark, 2015) .

The preparation of Starbon® materials has been extensively studied not only using starch but also employing other polysaccharides such as alginic acid and pectin as precursors (Luque et al., 2012). These biopolymers exhibit distinctive properties that make them intriguing candidates for the development of advanced catalyst materials. The exploration of starch, alginates, and pectin as precursors underscores the commitment to sustainable and eco-friendly practices in catalyst design and production. The textural and physicochemical properties of the final material obtained are influenced by preparation conditions such as the of polysaccharide employed, the heating mechanism (microwave or

conventional), the gelatinization temperature, the solvent and drying mechanism, as well as the carbonization temperature.

1.2.1 Synthesis of Starbon® materials from starch

Starch composed of amylose and amylopectin, is a neutral polysaccharide suitable for the synthesis of Starbon® materials. Native starch granules, however, do not yield mesoporous materials upon carbonization. The synthesis process involves the formation of expanded starch as a precursor to Starbon® utilizing a sol-gel method. This method takes advantage of the expansion capacity of the polysaccharide to create a mesoporous structure, which is then preserved and carbonized in an inert atmosphere. Aerogels and cryogels are prepared from starch through a process involving thermal gelatinization in water and partial recrystallization through retrogradation, where the gel is cooled to 5°C producing a porous gel. Subsequently, the trapped water is exchanged with a solvent of lower surface tension, such as t-butanol, to prevent the structural collapse during the drying. The last can be carried out through vacuum or by freeze drying (White et al., 2009). The choice of starting materials is crucial, as high amylose content in polysaccharides is responsible for the formation of the expanded network and mesoporosity. Hylon VII starch extracted from high amylose corn (70% amylose) is an example of a suitable precursor, resulting in expanded mesoporous starch with a surface area of approximately 180 m2g-1 and an average pore diameter of around 6 nm (White et al., 2008). The final step involves carbonization and sulfonation. The expanded starch is doped with an organic acid, such as p-toluenesulfonic, and heated under vacuum for rapid carbonization, fixing the mesoporous structure. After carbonization, the pore size distribution indicates a predominance of mesopores with a volume between 0.4 and 0.6 cm^3g^{-1} and a pore diameter ranging from 8 to 16 nm (White et al., 2008). A summary of the Starbon® synthesis process is represented in Figure 1-4 (Luque et al., 2012).

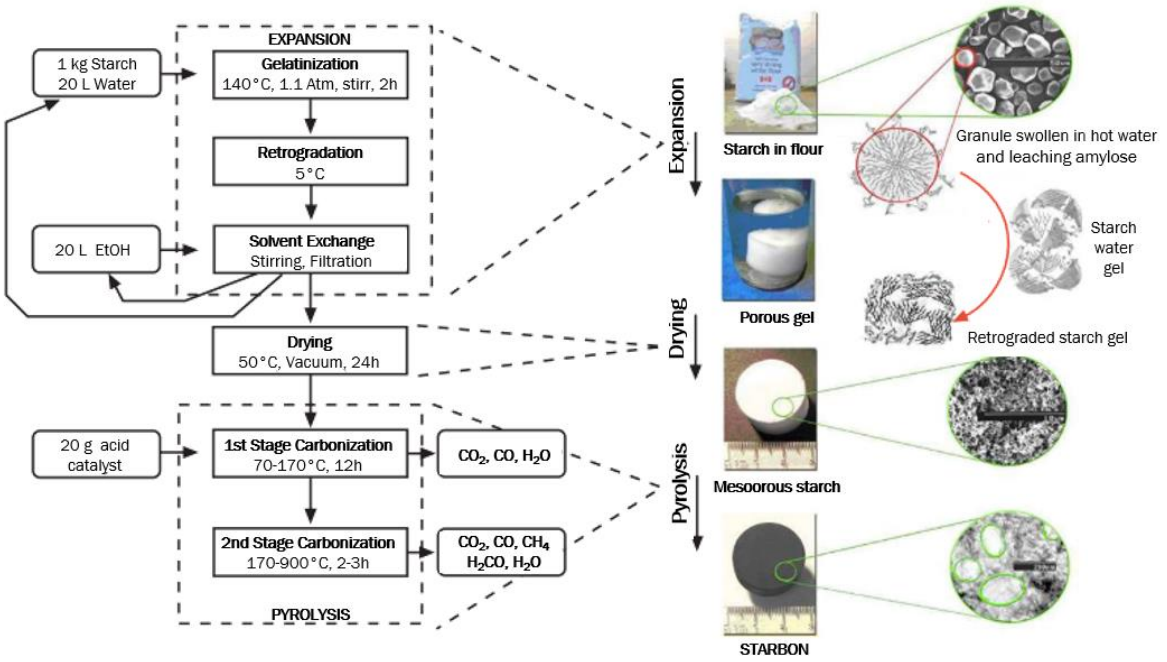

Figure 1-4. Starbon® synthesis method using starch as precursor. Adapted from: Luque et al., 2012.

For the activation of the mesoporous carbon obtained after carbonization, the synthesized Starbon® is suspended in pure sulfuric acid for 4 hours at 80°C to anchor SO3H groups to the carbon surface. Subsequent washes with distilled water are performed to remove residual acid until achieving a neutral pH (Mena, 2014). The carbons are then conditioned with boiling toluene at 150°C for 4 hours and then with water at 80°C for 3 hours to remove free organic or sulfonated compounds. Finally, oven drying is carried out at 100°C for approximately 8 hours, resulting in a material with a BET surface area of 386 m2g-1, a BJH pore diameter of 4.1 nm, and a BJH pore volume of 0.62 cm3g-1 is obtained (Budarin et al., 2006).

1.2.1.1 Starch

Starch is a plant-derived polysaccharide widely used in the industry, as it serves various purposes in stabilizing processed foods, coating for paper, and acting as an adhesive. Its applications extend to the textile industry, ethanol production, and concrete applications, showcasing its versatility.(Intriago & Muñoz, 2014). Starch is abundantly present in various plant varieties such as cereal grains, tubers, leaves, legume seeds, and fruits. For instance, cereal grains contain between 60 and 75% of their dry weight as starch. The concentration

of starch varies with the maturity state of these sources (Hernández et al., 2008). Structurally, starch is a high-molecular-weight macromolecule composed of biopolymer chains of amylose and amylopectin (Figure 1-5 and Figure 1-6). Amylose, a linear polymer of glucose units linked by α (1-4) bonds, can form hydrated micelles through hydrogen bridges, generating a helical structure. On the other hand, amylopectin, a branched polymer of glucose units, exhibits partial solubility in hot water and is composed of 94-96% α (1-4) bonds and 4-6% α (1-6) linkages (Guan & Hanna, 2004).

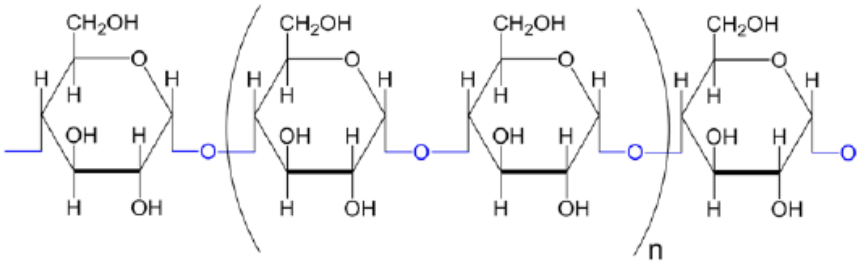

Figure 1-5. Amylose. ∝(1→4) glycosidic bonds are represented in blue (Zobel, 1988).

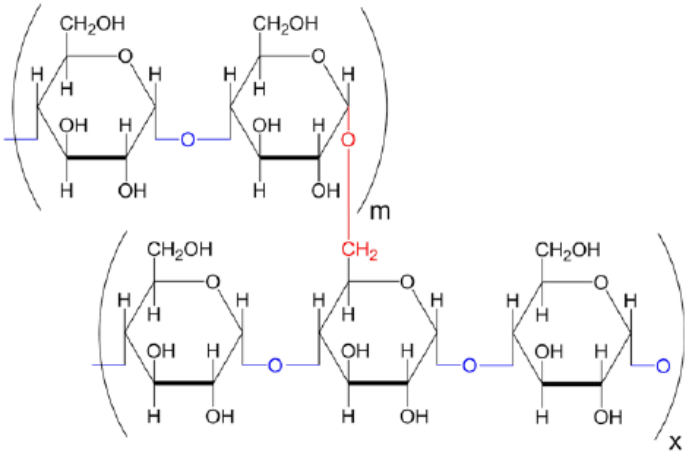

Figure 1-6. Amylopectin. ∝(1→4) glycosidic bonds are represented in blue, and ∝(1→6) glycosidic bonds are represented in red (Zobel, 1988).

The rheological and functional properties of starch are influenced by the ratio of amylose to amylopectin in its structure. The amylose content is particularly associated with the gelatinization process of starch crystal aggregates and serves as the mesopore former (White et al., 2008). Table 1-5 presents the amylose content in starch from different plant sources.

Table 1-5: Amylose content in starch from different sources (Hernández et al., 2008).

Starch source	Amylose content (%wt.)
Plantain	25.0 – 30.0
Sweet potato	19.6
Cassava	15.9 - 22.4
Achira	22.7
Corn	23.9 – 32.5
Potato	16.0 – 28.0
Andean potato	26.0

The physicochemical and functional properties of native starches, including gelatinization and retrogradation are influenced by their granular and molecular structures. Starch granules are part of a semicrystalline polymeric system characterized by concentric alternating rings of crystalline and amorphous region. Typically, starch granules have a specific surface area (S_{BET}) of s <10 m^2g^{-1} in their native extracted form (Juszczak et al., 2002). The crystallinity of native starch granules ranges from 14% to 45%, and different polymorphs with distinct crystalline structures are identified. Starch can exhibit A-type, B-type, or C-type crystalline structures depending on the source. A-type crystalline structure is common in cereal starches, featuring left-handed parallel-stranded double helices in a monoclinic unit cell. B-type crystalline structure characterizes high-amylose starches found in tubers, fruits, and stems, exhibiting six left-handed parallel-stranded double helices in a loosely packed hexagonal unit cell. C-type crystalline structure is present in starch extracted from legumes or plant roots, showing coexisting A- and B-type crystallites (Figure 1-7) (Bekyarova & Kaneko, 2000).

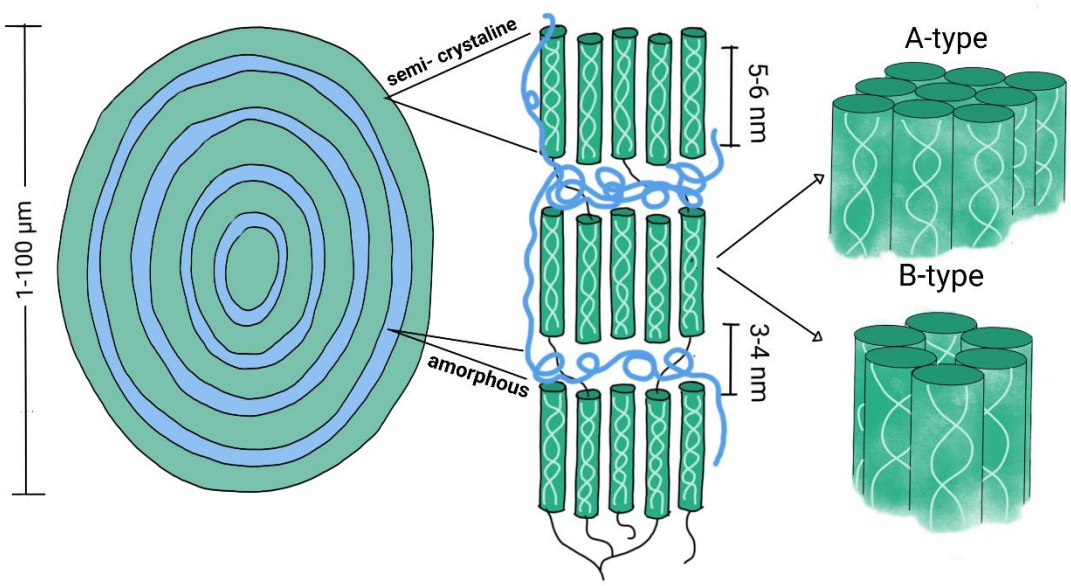

Figure 1-7. Schematic representation of starch structure from granules to glucosyl units. Adapted from: Dome et al., 2020.

In the early 2000s, research done at the Centre of Excellence in Green Chemistry at the University of York demonstrated that corn starch, when prepared under microwave conditions, has the potential to yield xerogels with low density, surface areas around 120 m^2g^{-1}, high mesoporosity (95%), and a mesopore volume exceeding 0.6 cm^3g^{-1} (White et al., 2008). This discovery opened avenues for novel applications of starch-based materials.

1.2.1.2 Gelatinization

The transformation of low-surface native starches into expanded gels involves a critical process known as gelatinization. This process aims to create a porous "aqueous" gel characterized by a large surface area and volume. The crystalline structure inherent in starch necessitates breaking it down to form gels. Gelatinization is initiated by the addition of excess water, promoting the expansion of starch granules. Heat is then applied to increase the solubility of starch granules, leading to water absorption (Figure 1-8).

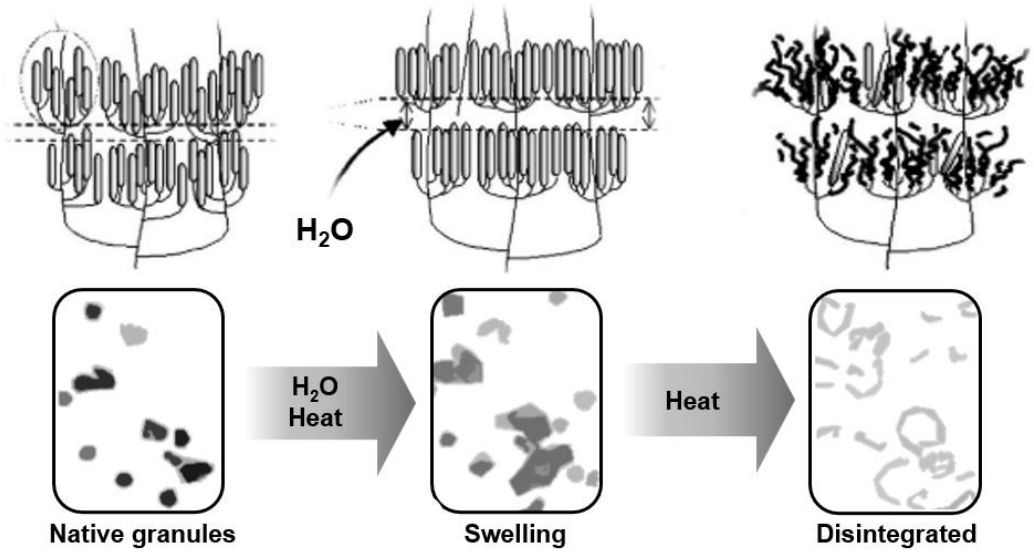

Figure 1-8. Scheme of starch gelatinization. Adapted from: Knorr et al., 2006.

During gelatinization, starch granules swell due to water absorption in the amorphous region, causing the growth ring structure to disintegrate. Simultaneously, the crystalline regions undergo melting, with amylose leaching out and amylopectin undergoing reordering through the breaking of hydrogen bonds. The result is an increase in particle size, re-association of solubilized amylose, and the formation of a gel with increased viscosity. Continued heating leads to the breaking of the granular envelope, causing dispersion (Knorr et al., 2006).

The entire gelatinization process is endothermic, with each type of starch having a characteristic gelatinization temperature. This temperature is primarily determined by the glass transition of the amorphous fraction of the starch. Differential Scanning Calorimetry (DSC) studies have shown that approximately 10 mJ mg^{-1} of starch is required to complete the gelatinization process (Biliaderis et al., 1985). Table 1-6 provides insights into the thermodynamic properties of starches from different precursors during the gelatinization stage. The properties include the Initial Temperature (T_i), Peak Temperature (T_p), Final Temperature (T_f), and gelatinization enthalpy (ΔH), all determined through DSC (Hernández et al., 2008).

Table 1-6: Thermodynamic properties of starch in the gelatinization stage (Hernández et al., 2008)

Starch type	T_i /°C	T_p /°C	T_f /°C	ΔH /kJ kg^{-1}
Sweet potato	55.2	61.3	68.2	14.9
Yam	55.2	61.3	68.2	9.2
Corn	62.3	66.3	72.9	10.3
Taro	72.5	78.4	84.0	14.9
Potato	60.0	69.0	80.0	4.6
Plantain	65.0	79.0	100.0	9.4
Canna	62.2	74.9	89.2	12.5
White sorghum	66.2	71.0	75.5	11.1
Cassava	57.8	65.2	75.3	10.0

For Starbon® material synthesis, the polysaccharide is heated in water above the gelatinization temperature as it is needed to reach the critical point of swelling for the starch granule to produce a disordered coil polymer solution (White et al., 2016). Higher gelatinization temperatures are desirable to avoid remnants of the starch granule structure that could act as nucleation points for the recrystallizing porous polysaccharide phase during gel preparation (White et al., 2014) . Figure 1-9 is a schematic representation of the reported starch gelatinization process in Starbon® materials synthesis. There are two possible pathways: by common thermal gelatinization and the use of microwaves (Budarin, Clark, Luque, Macquarrie, Koutinas, et al., 2007). The gelatinization stage significantly influences the final Starbon® porosity. Variables such as gelatinization temperature, starch precursor, and mass ratio (starch: water) directly impact swelling conditions, resulting in differing textural properties in the resulting dried expanded starch.

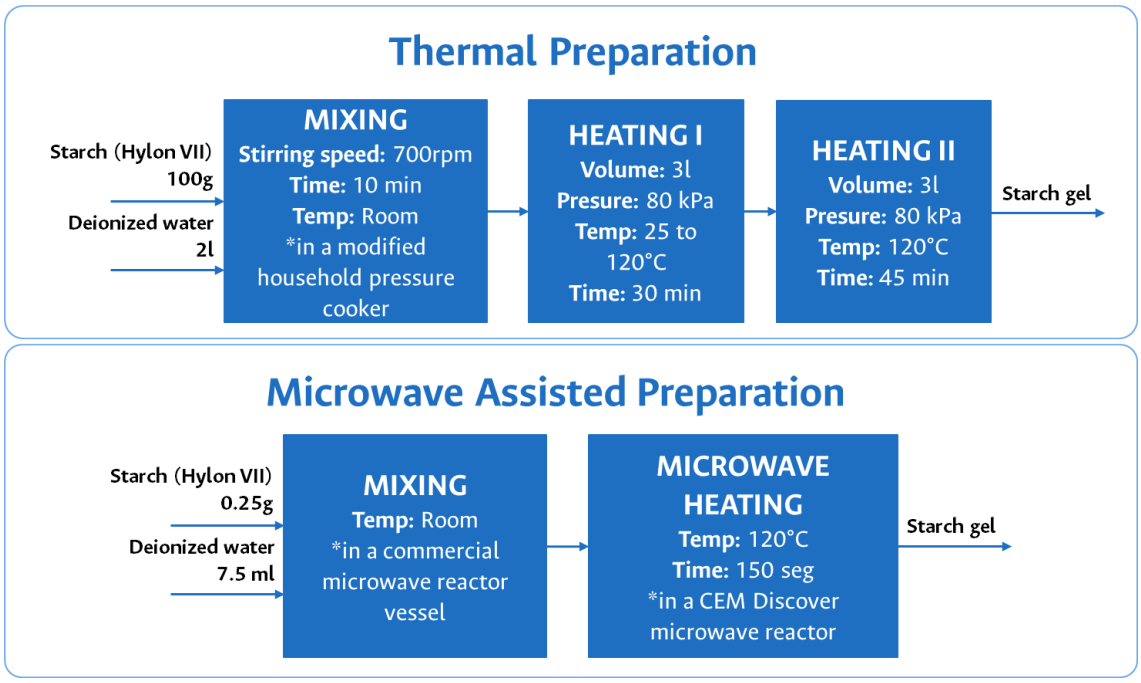

Figure 1-9. Diagram of the gelatinization process employed by Budarin and coworkers in the obtention of expanded starch gel.

1.2.1.3 Retrogradation

Following gelatinization, starch gels undergo retrogradation, involving the reorganization and association of amylose and amylopectin chains in the gel. Retrogradation occurs during cooling, promoting the restoration of hydrogen bonds and the establishment of localized ordered polymer associations, producing a predominantly amorphous aqueous gel phase (White et al., 2016). A schematic representation of expansion of granule in water and subsequent retrogradation is shown in Figure 1-10. Generally, retrogradation implies an increased degree of crystallinity with the appearance of B-type crystalline polymorphs (Figure 1-7) (S. Wang et al., 2015).

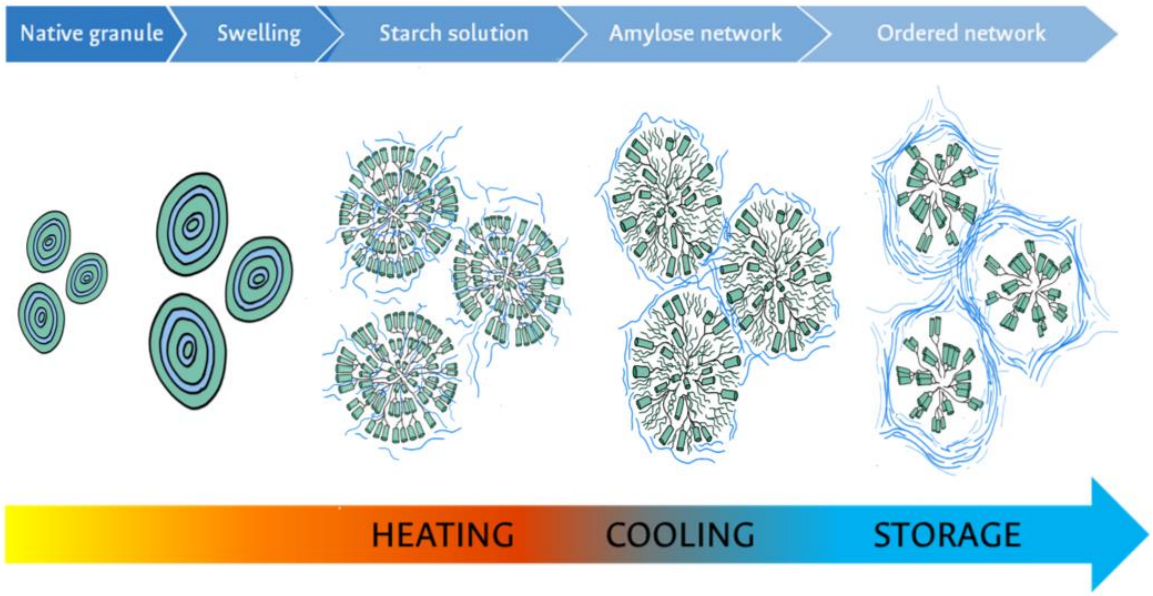

Figure 1-10. Schematic representation of changes in molecules arrangement during expansion of granule in water and subsequent retrogradation. Adapted from: Wang et al., 2015.

The long-range order present in the starch granule is lost during gelatinization and not recovered during retrogradation. The new network formed during retrogradation is a result of short-range inter- and intra-molecular interactions. Amylose retrogradation influences the initial hardness of a starch gel, while amylopectin is more responsible for long-term changes (Sandhu & Singh, 2007). When high temperatures are used during the gelatinization, the recrystallization of the amylopectin serves as seed upon which a highly mesoporous, amylose-rich phase is deposited, leading to the formation of regularly sized (~5 mm), mesoporous xero- or aerogel spheres (White et al., 2014).

Various factors can influence starch retrogradation including water content, starch source, and storage conditions. The optimum saccharides size range for retrogradation is reported to be between about 14 and 24, with chains that are too short or too long not favouring retrogradation (Shi & Seib, 1992). Water content plays a crucial role, with retrogradation not observed for corn starch when the water content is below 20% or above 90%. Maximum retrogradation occurs in starch gels at 40% to 45% water content (S. Wang & Copeland, 2013). Storage conditions also impact retrogradation, with longer storage times facilitating the formation of more starch crystallites with a higher degree of perfection. Lower storage temperatures induce faster crystallization of amylopectin (S. Wang et al., 2015).

Understanding starch retrogradation can be aided by techniques such as Fourier transform mid-infrared (FTIR) spectroscopy, where bands at 1047 and 1022 cm^{-1} reflect the amounts of ordered and amorphous regions, respectively (van Soest et al., 1994). The ratio between infrared bands 1047 cm^{-1}/1022 cm^{-1} increases during retrogradation, indicating an increased organization of the structure (S. Wang et al., 2015).

1.2.1.4 Solvent exchange and drying

After the synthesis of the retrograded gel, the next crucial step in the production of Starbons® is solvent exchange and drying. This process aims to transform the retrograded gel into either aerogel or cryogel while preserving the gel structure. Solvent exchange is vital to prevent the collapse of the pore structure during drying by reducing the high surface tension of pore-bound water (White et al., 2014). Different solvent exchange and drying methodologies for the synthesis of Starbons® are presented in Table 1-7. Two main pathways are proposed for drying the retrograded gel: vacuum drying to produce an aerogel or freeze-drying for cryogel formation.

Table 1-7: Reported solvent exchange method on the synthesis of Starbon® materials.

Solvent Exchange Method	Solvent	Drying method	Ref.
5 solvent exchanges	Ethanol	Vacuum oven	(Parker et al., 2012) (Parker et al., 2013)
Budarin and coworkers patented method	Ethanol Acetone	Vacuum oven	(White et al., 2016)
Addition de TBA and mixing.	TBA	Freeze drying	(Borisova et al., 2015)
No solvent exchange. Direct gelation of the polysaccharide in aqueous TBA	TBA	Freeze drying	(Borisova et al., 2015)

In 2007, Budarin and coworkers patented a method involving solvent exchange through several washes using ethanol and acetone, schematized in Figure 1-11. It was found that the choice of solvent and the number of exchanges were variables that affected the final porosity of the materials.

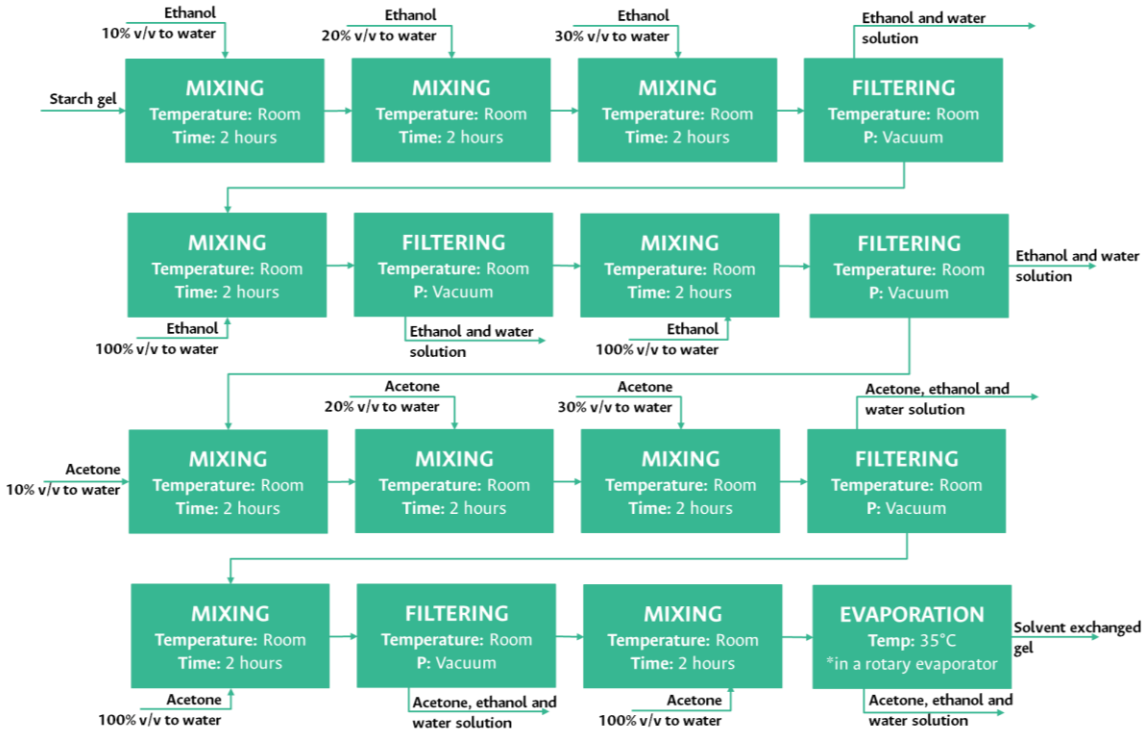

Figure 1-11. Solvent exchange method patented by Budarin and collaborators.

Freeze-drying is an alternative method for obtaining expanded porous starch by adding an organic solvent to the retrograded gel, deep freezing it, and sublimating the solvent to preserve the pores. This approach helps to overcome surface tension issues related to liquid-vapor interfaces (Elkhatat & Al, 2011). Particularly, tert-butyl alcohol (TBA) was found to be an adequate solvent for generating hierarchical porosity. The mesoporosity increased towards the eutectic points, where maximum values were achieved. The increase in mesoporosity was associated with the presence of very fine microstructured eutectic phases preserving the mesopores. An aqueous solution of tert-butanol (25% w/v) resulted in the formation of fine crystals, leading to better preservation of mesoporous structures in the freeze-dried gels (Borisova et al., 2015).

1.2.1.5 Carbonization

Once the porous material derived from polysaccharides is obtained, it undergoes a carbonization process to transform it into more stable carbonaceous forms. The principal reactions in carbon precursors involves pyrolysis up to about 800°C and carbonization above 800°C. These processes continuously overlap, collectively referred to as

"carbonization". The carbonization of starch-based materials involves the release of aliphatic and aromatic hydrocarbons, cyclization, and aromatization. From around 600°C, foreign atoms such as oxygen and hydrogen are released. Above 800°C, the main evolved gas is H_2 due to polycondensation of aromatics (Inagaki, 2013). As the carbonization temperature increases, carbon materials become harder due to the growth and stacking of carbon chains. The elemental composition of starch-derived materials is dependent on the carbonization temperature, transitioning from a starch-like material at low temperatures to a graphitic-like structure at high temperatures (Okamura et al., 2006).

Two principal carbonization/decomposition transitions occur:

- In the range 180–300 °C: Induced via intermolecular crosslinking/dehydration of hydroxyls leading to ethers and carbonyls. Heterolytic scission of glycosidic linkages yields levoglucosan and shortened “dehydrated” polysaccharide chains.
- In the range 300–550 °C: Intramolecular dehydration induces the formation of C=C (olefinic) double bonds conjugated with a carbonyl group. Condensation of sugars (i.e. glucose, levoglucosan) with their decomposition products such as furfural and hydroxymethylfurfural.

At the final transition above 550 °C, the conversion of 1D linear conjugated groupings to 2D (surface plane) increasingly condensed aromatic structures, results in the formation of structures with increased long-range order typical of classical carbon materials (White & Clark, 2015). The thermal decomposition products of starch at different temperatures are illustrated in Figure 1-12. For Starbon® synthesis, the porous material derived from starch undergoes carbonization through thermally catalyzed decomposition facilitated by acid. Expanded starch is doped with an organic acid enabling fast carbonization and fixing of the mesoporous structure (Budarin et al., 2006).

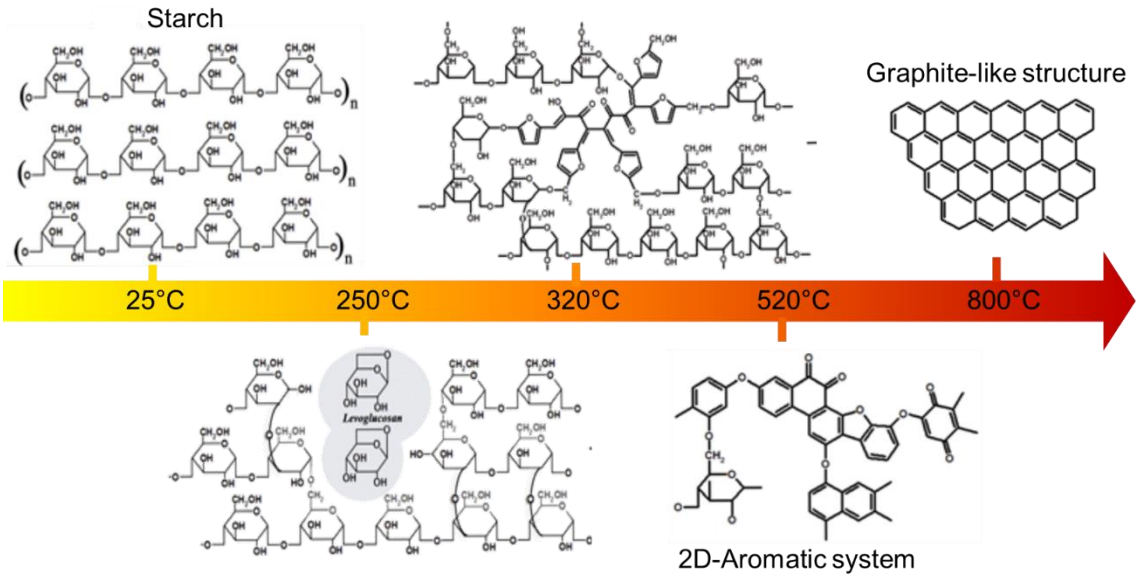

Figure 1-12. Products of thermal decomposition of starch at different temperatures. Adapted from: White & Clark, 2015.

Transmission electron microscopy (TEM) performed on Starbon® during carbonization reveals the structural evolution at different temperatures (Figure 1-13). Image A shows expanded starch with a homogeneous structure around the mesopore. Images B to F show Starbons® prepared at progressively higher temperatures. Dark areas around the mesopores in B and C indicate small carbon particles, suggesting the carbonization process begins around the pores. Images from D to F demonstrate how the carbonization reaction gradually moves towards the rest of the material (Budarin et al., 2006). The material morphology of the carbonized Starbon® resembles the nanoscale morphology of the parent porous starch before carbonization. It results in maintenance of the total pore volume around 0.4 to 0.6 $cm^3g^{-1,}$ with a predominance of mesopores (8 to 16 nm) (White & Clark, 2015). The correlation between carbonization temperature and the porosity of the final material is observed. Interconnected network structures and increased microporosity are evident in Starbons® carbonized at 300°C or lower temperatures. Temperatures higher than 300°C promote interconnection between pores, and temperatures exceeding 600°C result in well-defined micropores with 500 m^2g^{-1} (White & Clark, 2015). The selection of a carbonization temperature is crucial and depends on the final application. For catalyst applications, Starbon® carbonized in the range from 300°C to 700°C can be utilized based on the specific reaction requirements (Figure 1-3).

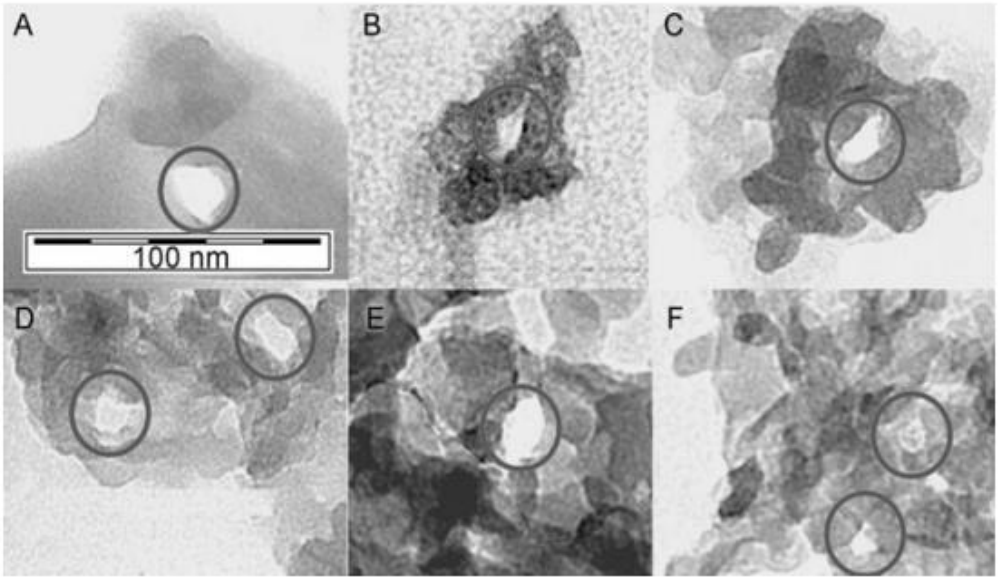

Figure 1-13. TEM of starbons® produced at a range of temperatures: A) expanded starch; B) 100°C; C) 150°C; D) 220°C; E) 300°C; F) 450°C (Budarin et al., 2006).

1.2.1.6 Sulfonation

When Starbons® are treated with sulfuric acid, a solid acid with promising properties as a heterogeneous catalyst is obtained. Different routes for the sulfonation of Starbons® have been proposed, involving the submersion of the carbon on concentrated sulphuric acid. This contact should be carried out at temperatures above 35°C to achieve a proper anchoring of the SO_3H sites on the surface. The resulting mesoporous sulfonated carbon must be washed until a neutral pH is achieved, removing residual acid. Subsequent conditioning with boiling toluene and hot water may be performed before final drying (Luque et al., 2012; Mena, 2014). The functionalization of carbons is intricately tied to the initial structure, influencing the surface and properties of sulfonated carbons. Sulfonated carbons, containing SO_3H groups, retain all the textural properties and defects of the original carbon support. This enables the production of both hydrophilic and hydrophobic acidic carbons with a wide range of superficial SO_3H acidity, porosity, and carbon framework structures.

Acidic carbons, especially those derived from incompletely carbonized materials, possess various oxygen functional groups such as -COOH and OH-, which contribute to the material's ability to adsorb or retain significant amounts of hydrophilic molecules, in addition to the SO_3H groups attached to the flexible carbon structure. Lower carbonization temperatures result in smaller carbon sheets. Consequently, lower temperatures lead to

higher –SO_3H densities, primarily located at the edges of the carbon sheets (Konwar et al., 2019). Hence, it is pertinent to understand some characteristics of different types of SO_3H-functionalized acidic carbons obtained through sulfonation of diverse carbon supports, as highlighted in Table 1-8. As observed, sulfonation of Starbon® materials results in acidic carbons with varying properties, including SO3H acidity, porosity, and carbon framework structures. The resulting materials can be tailored for specific applications based on their properties.

Table 1-8: Overview of different types of SO3H-functionalized acidic carbons (Konwar et al., 2019).

Carbon	SO_3H Acidity /mmol g^{-1}:	Specific Surface Area /m^2g^{-1}:	Average Pore Size /nm:
Non-Porous Sulfonated Carbons	0.56 - 4.90	< 2	Not specified
Macroporous Sulfonated Carbons	0.56 - 4.90	Up to 120	>50
Mesoporous Sulfonated Carbons	0.14 – 1.88	75-1191	3.1 – 28.1
Microporous Sulfonated Carbons	0.50 – 1.10	800-2000	<2
Nanostructured Sulfonated Carbons	0.68 – 2.00	215-500	Not specified

1.2.2 Starbon® materials as catalysts

The mesoporous nature of Starbon® implies lower surface energies compared to microporous materials. This characteristic enhances accessibility to active sites and facilitates efficient mass transfer, resulting in higher diffusion rates and mass transfer coefficients. Starbon®, as a mesoporous catalyst, is well-suited for the conversion of larger molecules, particularly in petrochemicals and fine chemistry (Luque, 2010). The ability to tailor its structure and functional groups makes it valuable for controlling selectivity in reactions, especially in liquid-phase applications (White & Clark, 2015). This type of material has been tested for its activity as a heterogeneous catalyst in various acid-catalysed reactions under thermal or microwave conditions. Additionally, various studies have shown that reaction rates obtained with acid Starbon® are considerably higher than those achieved with commercial solid acids, and it also exhibits greater selectivity. Furthermore, Starbon® acids have demonstrated exceptional stability and reusability in the investigated reaction medium. It can be easily recovered from the aqueous reaction mixture

and has been reused up to three times, maintaining reaction rates almost identical to the original ones.

1.2.2.1 Performance in esterification, transesterification, and other reactions

Treating Starbon® with sulfuric acid yields a solid acid with promising properties as a heterogeneous catalyst in esterification and transesterification reactions. In esterification, it demonstrates significantly higher reaction rates compared to alternative commercial solid acid catalysts. For diacid esterification, the rates are 5 to 10 times higher, with an improved diester selectivity. The reaction time is notably shorter for Starbon-400-HSO3, ranging from 3-5 hours compared to over 12 hours for other carbonaceous solid acids (Budarin, Clark, Luque, Macquarrie, Koutinas, et al., 2007). Moreover, in simultaneous esterification of free fatty acids and transesterification of triglycerides for second-generation biodiesel production, it has been verified that Starbon® surpasses other commercial solid acid catalysts, showcasing remarkable activity and reusability. Despite a decline in activity with successive use, the catalyst maintains effectiveness, especially under microwave-assisted processes (Luque & Clark, 2011).

In a recent study conducted by Clohessy and Witold in 2020, carbonaceous catalysts were compared to traditional catalysts in the context of biodiesel production. The research demonstrated that partially carbonized materials such as glucose, sucrose, cellulose, or starch exhibit superior reaction rates and activity compared to conventional catalysts like Amberlyst 15 ion exchange resins and sulphated zirconias. Remarkably, starch proved to be the most effective polysaccharide in both esterification and transesterification reactions, exhibiting activities approaching to those achieved with sulfuric acid, a potent traditional catalyst (Clohessy & Kwapinski, 2020).

Starbon® also excels in other liquid-phase reactions, such as the acylation of alcohols and alkylation of aromatic compounds under microwave conditions. In the acylation of benzyl alcohol with acetic acid, Starbon-400-SO3H exhibited reaction rates 5 to 10 times higher than commercial catalysts and twice as fast as similar sulfonated microporous carbon materials. In the alkylation of aromatic compounds with benzyl chloride, sulfonated Starbon provided high yields and selectivity, outperforming various tested catalysts, including zeolites and mesoporous Al-MCM-41 materials (Luque et al., 2011).

2. Understanding Starbon® synthesis using cassava starch as precursor

2.1 Introduction

Starbons® represent a class of porous materials derived from renewable resources. Its name stands for "starch-derived mesoporous carbon" as they were originally obtained using starch as precursor. The synthesis process entails the controlled pyrolysis of polysaccharides, resulting in materials characterized by high porosity, large surface areas, and the ability to adsorb a diverse range of molecules (Budarin et al., 2006). While natural polysaccharides possess low surface areas and poorly developed porosity, Starbons® can be obtained by expanding polysaccharides through the production of aqueous gels. As these materials are derived from renewable resources, they present an environmentally sustainable alternative to conventional materials and catalysts derived from fossil fuels. Additionally, owing to the abundance of polysaccharides and cost-effective production processes, Starbons® are economically viable compared to other porous materials. This characteristic positions them as potential replacements for conventional materials in various applications, leading to more sustainable, cost-effective, and efficient processes (Budarin et al., 2006). Various Starbons® have been produced primarily using high amylose corn starch (Hylon VII) as a raw material for diverse applications, as summarized in Table 2-1.

Different factors in each stage affect the final surface properties of the Starbon® materials. Among them, the type of starch used for the synthesis influences the final pore volume according to the amylopectin content of the starch: lower amylopectin contents promote higher porosity as the amylose leaches the granule and forms higher pores (White et al., 2008).

Table 2-1: Reported studies of applications for Starbon® materials.

Research	Starch type	Application	Ref.
Towards a Bio-Based Industry: Benign Catalytic Esterifications of Succinic Acid in the Presence of Water	High amylose corn starch	Catalysis	(Budarin, Luque, et al., 2007)
Water-tolerant Ru-Starbon® materials for the hydrogenation of organic acids in aqueous ethanol	High amylose corn starch	Catalysis	(Luque & Clark, 2010)
Use of Starbon for the Adsorption and Desorption of Phenols	High amylose corn starch	Organic adsorption	(Parker et al., 2013)
Mesoporous Carbons from Polysaccharides and Their Use in Li-O2 Batteries	Maize and high amylose corn starch	Batteries	(Uriburu-Gray et al., 2020)
The role of surface functionality of sustainable mesoporous materials Starbon® on the adsorption of toxic ammonia and sulphur gasses	High amylose corn starch	Gas adsorption	(Milescu et al., 2020)

To valorise waste streams and second-generation raw materials, the utilization of waste starches becomes of primary interest for industrial applications. In Colombia, major starch sources include potatoes, cassava, and bananas. Despite producing nearly 5 million tons of roots and tubers, approximately 30% are discarded due to quality standards (DPN, 2016). These materials present an opportunity for valorization through starch extraction, with subsequent transformation into high-value products such as bio-based catalysts. Specifically, cassava starch contains 17–20% amylose. It is differentiated from other starches by its low residual content (1.2% lipids, 0.1% protein, 0.08% ashes), lower amylose compared to other varieties, and high molecular weights of amylose and amylopectin (Manrique, 2006). As cassava starch content of amylopectin is around 73%, there are limitations on the production of Starbon® by the conventional method and the synthesis conditions need to be studied. Therefore, the gelatinization, retrogradation, solvent exchange, and carbonization conditions must be assessed to adapt them for low-amylose content starches.

2.2 Materials and methods

2.2.1 Materials

Cassava starch was purchased from a local supplier (Yucarina, Unilever®). Deionized water used for the gelation process was obtained in the laboratory. Tert-butyl alcohol (99.7% wt., PanReac AppliChem ITW Reagents) and ethanol (99.5% wt., PanReac AppliChem ITW Reagents) were employed for solvent exchange, and p-toluenesulfonic acid monohydrate (97% wt., Fisher Scientific) was used as a carbonization promoter.

2.2.2 Methods

2.2.2.1 Cassava starch characterization

The amylose and amylopectin content in cassava starch was determined using the enzymatic method K-AMYL 06/18 (Megazyme, 2018). Additionally, the morphology of starch granule was analysed by Scanning Electron Microscopy (SEM) using FEI Quanta 200 equipment.

2.2.2.2 Conventional synthesis

Expanded cassava starches were synthesized according to the conventional method reported in the literature (Borisova et al., 2015; Budarin et al., 2006). A defined amount of starch was added to deionized water in a 1:10 mass ratio, and the mixture was heated at 80°C under atmospheric pressure for 1 hour. Subsequently, the resulting gel was retrograded at 5 °C for 48 h. A solvent exchange was performed by adding tert-butyl alcohol up to 25% wt. in the mixture and *p*-toluenesulfonic acid (5% wt.) as a doping agent. The material was then freeze-dried at -107°C and 1mbar to yield the expanded starch. The procedures are schematically presented in Figure 2-1.

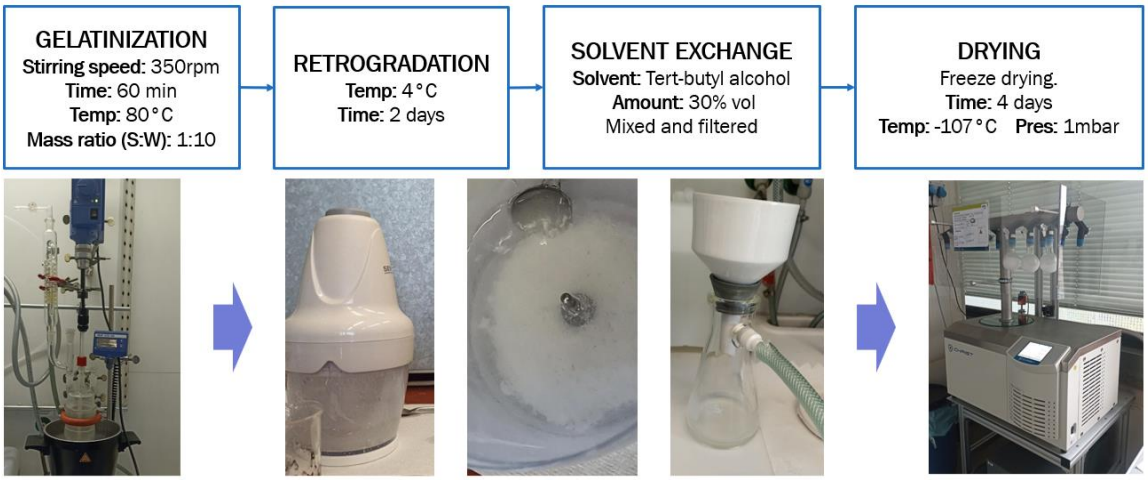

Figure 2-1. Conventional synthesis method for Starbon® production, until drying step for expanded starch obtention.

2.2.2.3 Study of synthesis variables

Gels were synthesized by stirring 15g of cassava starch in 150 ml of water for 1h at 110°C and 125°C, in a three-neck round-bottom flask using a half-moon overhead stirrer. The obtained sample was divided into 3 beakers and put in a freezer for its retrogradation at 4°C. The first sample was taken out after 4 days, the second after 8 days and the third after 16 days. When samples were removed from the fridge, they were immediately subjected to solvent exchange using two proposed methods, namely using ethanol or TBA.

When solvent exchange was performed using ethanol, 100 ml of ethanol were added to the gel, blended, and subsequently stirred magnetically at 500 rpm for 1h at room temperature. It was filtered under vacuum to remove water-ethanol solvent. New ethanol (100 ml) was added, and the procedure was repeated. The number of solvent exchanges was evaluated. Samples were then placed in a vacuum oven at 30°C for 24h. When solvent exchange was done using freeze drying method, TBA was heated at 30°C for melting, as it crystallizes at room temperature. It was observed that rapid addition to the mixture separated it in two phases, so it was compared to slow addition, at 2ml every 10 minutes until reaching 20% wt. with respect to the initial water used for gel preparation. Subsequently, it was pre-frozen using liquid nitrogen and freeze-dried in an Alpha 3-4 LSC basic Christ freeze-dryer for 48 hours. A portion of dried materials in both routes was doped using 5% wt. of p-TSA solved in a small volume of acetone as promotor of carbonization. Carbonization was executed at

450°C and 700°C in a Thermo Scientific Lindberg/Blue Mini-Mite tubular oven, at different ramps as presented in Figure 2-2 (Mena, 2014). A schematic representation of the steps in the synthesis, their conditions and the assessed variables is presented in Figure 2-3.

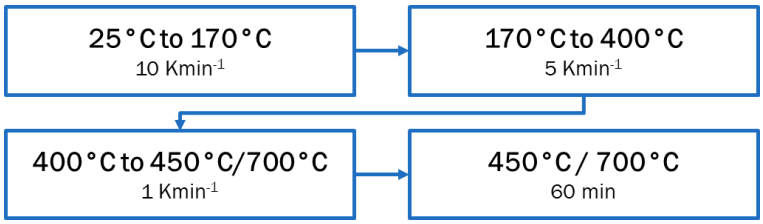

Figure 2-2. Temperature ramps for carbonization in Starbon® synthesis.

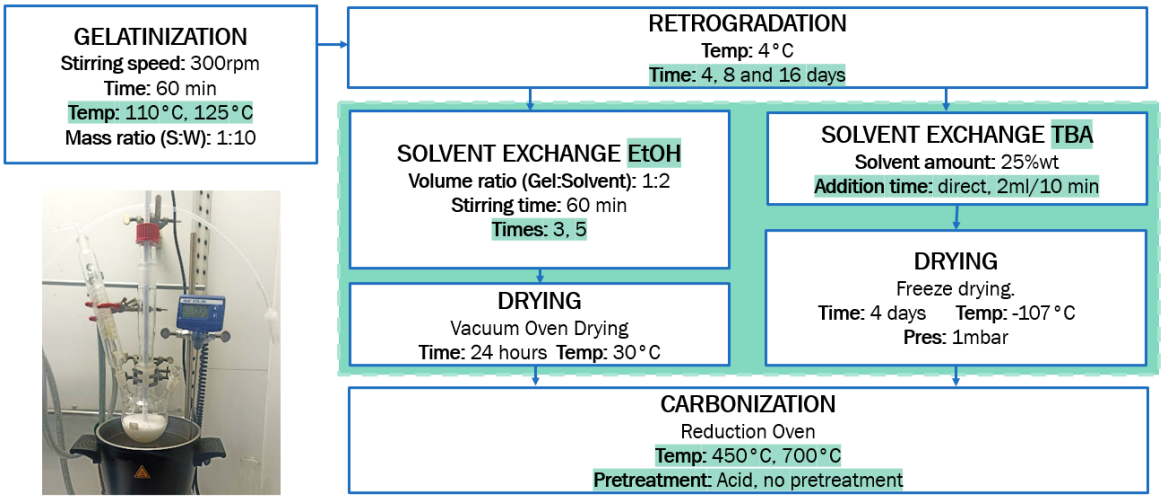

Figure 2-3. Modified synthesis method for Starbon® production using cassava starch. Assessed variables are highlighted in green.

2.2.2.4 Expanded cassava starch and Cassava-Starbon characterization

Expanded starch samples and carbonized samples were characterized using nitrogen adsorption at 77K using Quadrasorb (Quantachrome Instruments). The expanded starch samples were outgassed using a vacuum degasser for 24 h at 50 °C and subsequently analysed, while the carbonized starch samples were outgassed at 250°C. The surface area was calculated using Brunauer, Emmett and Teller (BET) method in the relative pressure range from 0.05 to 0.30, and the pore volume was determined using the Barrett-Joyner-Halenda (BJH) model. Pore size distributions were calculated using the non-linear density function theory (DFT) model for slit-cylindrical pores on carbon materials, from the

adsorption and desorption branches of the isotherms. Organic compounds on the materials were characterized by Fourier transform infrared spectra (FT-IR), obtained by a Perkin Elmer FT-IR 1760 Spectrometer in the wavenumber range from 2000 cm^{-1} to 500 cm^{-1}. The thermal stability of the cassava starch was tested by thermogravimetric analysis (TGA). The analysis was conducted using a simultaneous DSC-TGA TA Instruments STD 2960 V3.0F. The operation was performed from 30 ◦C to 600 ◦C at a heating rate of 10 ◦C/min under nitrogen. A sample mass of 19.4 mg was kept throughout the test.

2.3 Results and discussion

2.3.1 Cassava starch characterization

The amylose content of Colombian cassava starch was determined to be 20.75% wt., while the amylopectin content was estimated in 79.25% wt., which is consistent with literature values for this starch (Fallahi et al., 2016). Based on SEM images, it was observed that cassava starch granules were spherical and truncated, with an average size of 16 µm and a range of 8 to 22 µm (Figure 2-4).

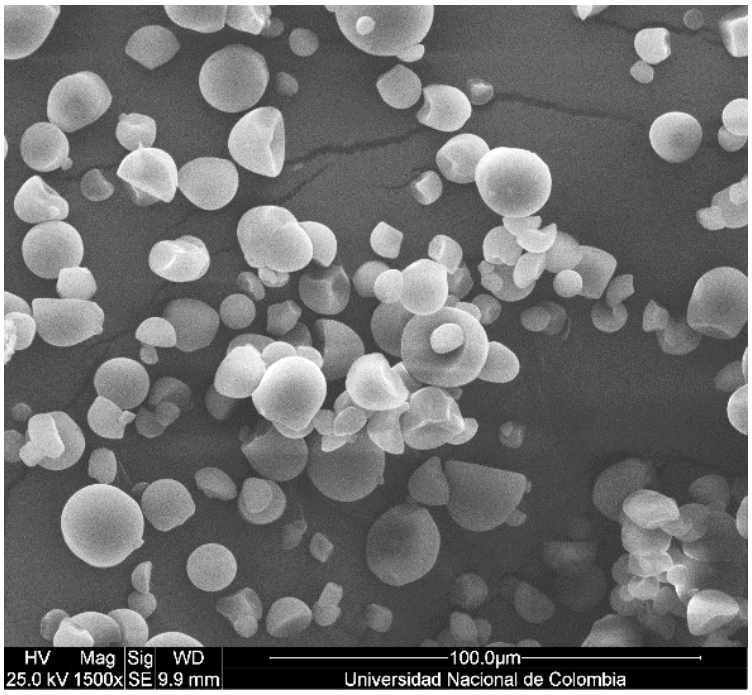

Figure 2-4. SEM image of native cassava starch granules.

2.3.2 Conventional synthesis

The conventional synthesis method as reported by Budarin and colleagues (2006) was implemented, including drying by freeze drying proposed by Borisova (2015) using Colombian cassava starch as the precursor. However, some steps in the synthesis remain unclear due to the patent on the Starbon® production process, such as the stirring speed and the type of mechanical stirrer used during gelatinization. Moreover, it may be beneficial to provide additional details regarding the process of mixing the obtained gel with t-butyl alcohol prior to freeze drying, particularly given its solid state at atmospheric conditions. The absence of such information has been found to pose challenges during the synthesis process, as even minor variations can significantly impact the final porosity of the material. Consequently, although several attempts in the production of the material were done, those conducted to expanded cassava starch samples with inadequately developed porosity and a negligible surface area (approx. 1.3 m^2g^{-1}). Nitrogen adsorption isotherms for the expanded cassava starch samples synthesized via the conventional method revealed a structural collapse during the synthesis process, leading to a loss of intrinsic porosity compared to the native cassava starch, as illustrated in Figure 2-5.

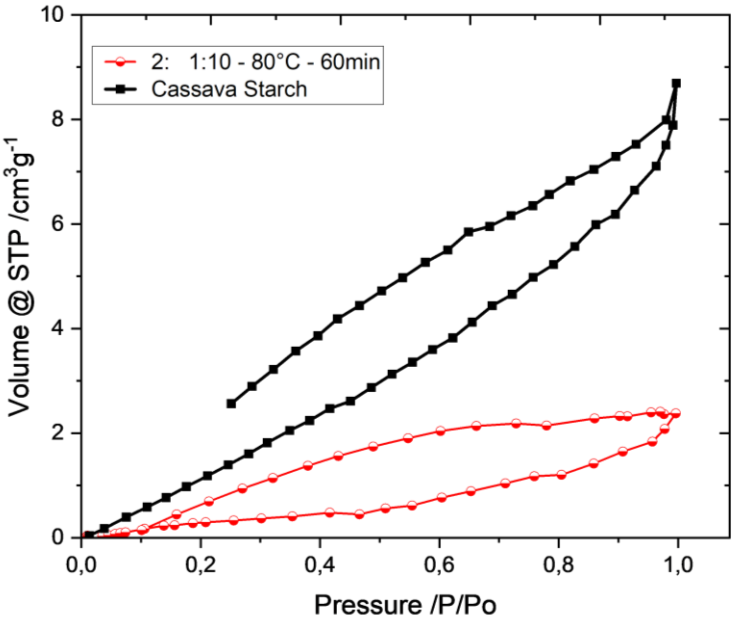

Figure 2-5. Nitrogen isotherm of expanded cassava starch produced by conventional synthesis (red) compared to native cassava starch (black).

Similar challenges were encountered by other researchers attempting to produce Starbon® materials, underscoring the critical need for a detailed understanding of synthesis variables. Brouwer in 2017, at Wageningen University in the Netherlands, synthesized starbons® under different conditions including freeze-drying and vacuum oven drying, finding that the starbons® and dried gels contained significantly lower values for the BJH mesopore volumes compared to literature (Brouwer, 2017) Similar results were obtained by Sreedhar and coworkers, in the Department of Chemical Engineering at BITS Pilani Hyderabad Campus, Hyderabad, India, who carried out Starbon® synthesis for its implementation on carbon capture. They followed the method reported by Budarin and collaborators (2006), and obtained surface areas around 2 m^2g^{-1} when carbonizing at 350°C, with a maximum of 13 m^2g^{-1} when increasing carbonization temperature until 550°C (Sreedhar et al., 2019). In this regard, a systematic study of the synthesis variables and adapting them to cassava starch is important for achieving the valorization of Colombian biomass.

The observed reduction in porosity during synthesis can be attributed to several synthesis variables. One hypothesis posits that a low gelatinization temperature may have left the starch granules partially intact, creating nucleation sites that facilitate the alignment of amylose and amylopectin chains, thereby reducing porosity. A second hypothesis concerns the retrogradation time; given that cassava starch contains less amylose compared to other starches, it may exhibit a diminished propensity for retrogradation, necessitating a longer duration than starches with higher amylose content, such as Hylon VII. A third hypothesis suggests that the incorporation of TBA during the solvent exchange phase could reduce porosity achieved during gelatinization and retrogradation, as the rapid addition of TBA induces phase separation within the gel. Furthermore, it is proposed that doping with p-TSA may lead to the collapse of the porous structure. Based on these hypotheses, modifications were implemented in the synthesis process, and various conditions were systematically evaluated.

2.3.3 Study of synthesis variables

The optimization of the synthesis process for cassava starch involved testing different gelatinization temperatures, retrogradation times, and solvent exchange methods. Cassava starch is considered a waxy starch due to its high amylopectin content. As a result, waxy starches generally have a greater capacity to form transparent and viscous gels compared

to other starches that contain higher levels of amylose. This characteristic was demonstrated during the gelatinization of cassava starch. When a starch gel is formed with amylose-based networks, it achieves elasticity and resistance to deformation. In contrast, softer gels with amylose-free aggregates tend to be more penetrable, exhibiting higher stickiness and adhesion. These characteristics make such gels easier to penetrate, sticky to the touch, and prone to adhering to surfaces. The reduced content of amylose groups to form hydrogen bonds between molecules in the gel disrupts long-distance interactions within the gel structure, leading to a decrease in gel cohesion. Consequently, soft gels containing aggregates without enough amylose networks are likely to have lower cohesion, making them more penetrable, sticky, and adhesive. As cassava starch gel is less cohesive and more penetrable, it became more susceptible to collapsing or losing its porous structure during drying, resulting in lower porosity. Experimentation with different drying conditions and adjustments to the gel formulation becomes crucial for obtaining aerogels with the desired porosity.

The influence of gelatinization temperature was previously studied, increasing it so as to ensure the complete expansion of the starch granules and reorganization of the amylose and amylopectin chains (White et al., 2008). Additionally, the influence of retrogradation time on the final porosity was examined considering that longer retrogradation times promote a better organization of the network (Tian et al., 2011). Solvent exchange and drying by both routes proposed in literature (using EtOH and vacuum oven, and TBA and freeze-drying) were compared (Borisova et al., 2015; Budarin, Clark, Luque, Macquarrie, Milkowski, et al., 2007). The expanded starches under those conditions were characterized by its surface properties. Subsequently, carbonization was done at 450°C and 700°C adding p-TSA as doping agent and without the use of p-TSA for understanding its function during the process.

Based upon the preliminary results, and the conditions previously evaluated in the gelation and retrogradation stages, a complete set of experiments was carried out to explore the impact on the surface characteristics of expanded cassava starch. As observed in Table 2-2 , and differently from the preliminary tests, the variations in the synthesis method were successful in achieving an expansion of the granule and the preservation of the pores

produced in expanded gels. Additional results are presented in Figures 2-6 to 2-13, and the corresponding analysis on each variable is presented in the following sections.

Table 2-2: Synthesis parameters and textural properties of expanded cassava starch materials.

Gelatinization temperature /°C	Retrogradation time /days	Solvent exchange method	Surface area /m^2g^{-1}	Pore size /nm	Pore volume /cm^3g^{-1}
110	4	EtOH	17	13.5	0.07
125	4	EtOH	14	9.4	0.05
110	8	EtOH	6	5.7	0.01
125	8	EtOH	10	8.8	0.01
110	16	EtOH	6	4.7	0.03
125	16	EtOH	7	4.6	0.01
110	4	TBA	32	4.0	0.08
125	4	TBA	56	4.6	0.13
110	8	TBA	19	4.4	0.01
125	8	TBA	43	7.3	0.02
110	16	TBA	26	6.7	0.06
125	16	TBA	13	8.4	0.03

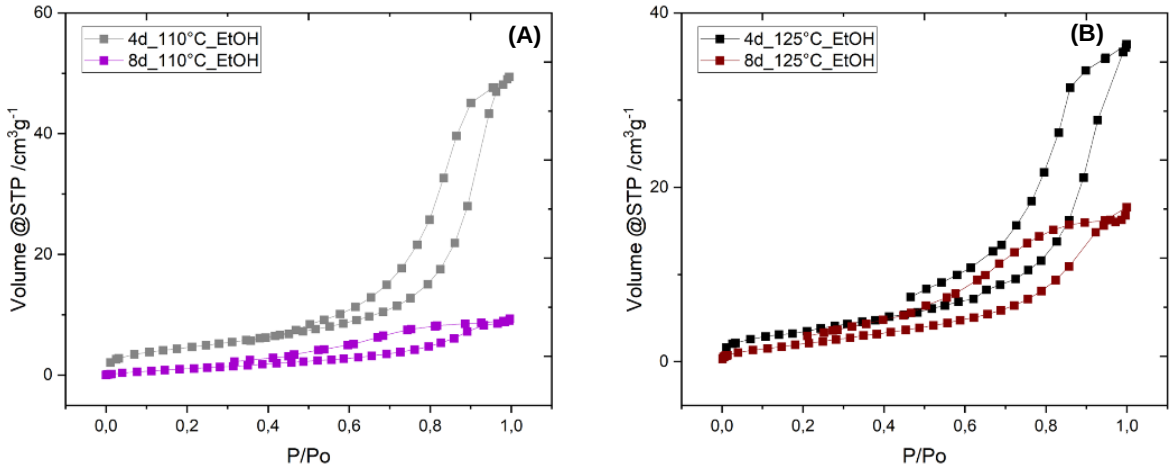

Figure 2-6. Nitrogen isotherms of expanded cassava starch samples obtained by EtOH solvent exchange method.

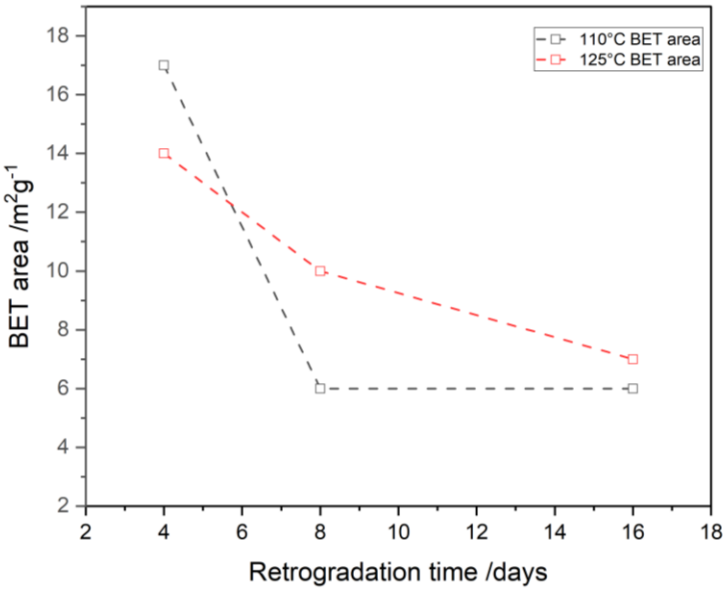

Figure 2-7. Surface area of expanded cassava starch samples obtained by EtOH solvent exchange method.

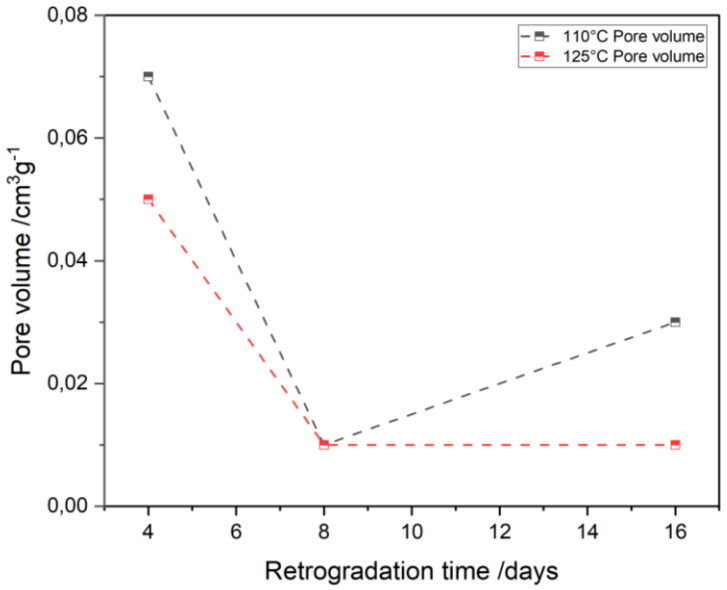

Figure 2-8. Pore volume of expanded cassava starch samples obtained by EtOH solvent exchange method.

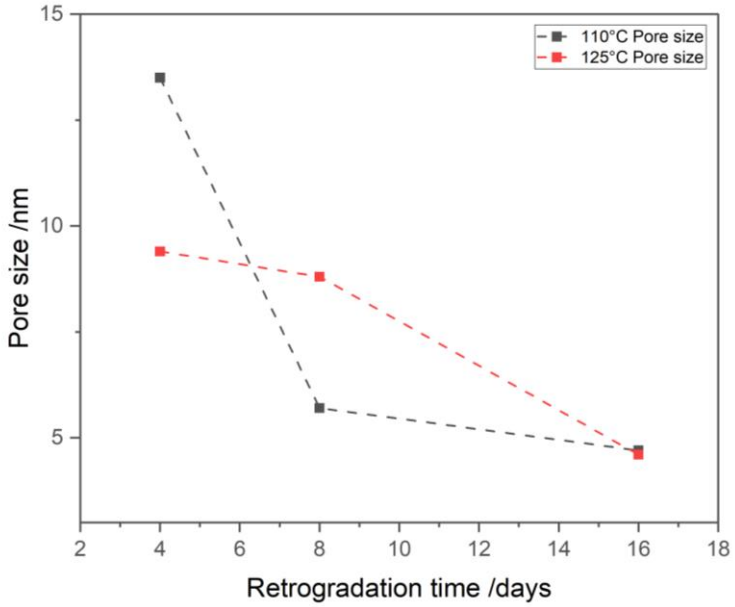

Figure 2-9. Pore size of expanded cassava starch samples obtained by EtOH solvent exchange method.

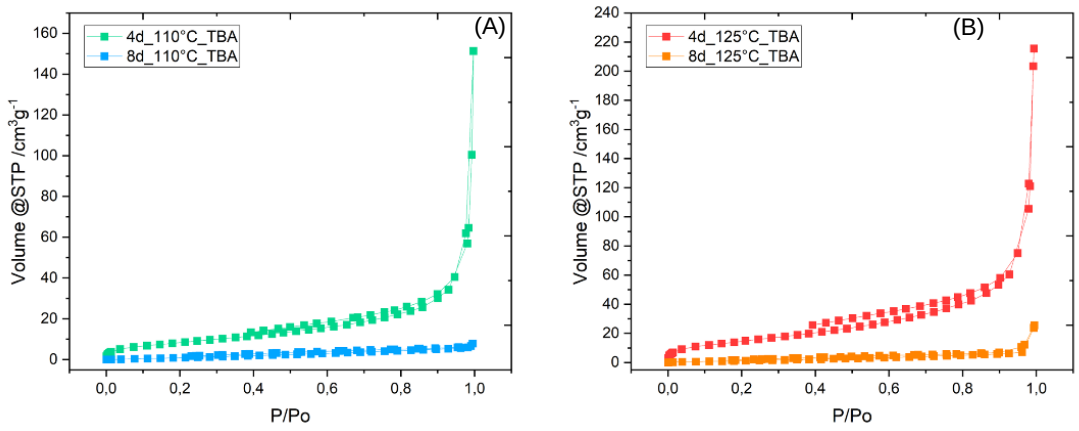

Figure 2-10. Nitrogen isotherms of expanded cassava starch samples obtained by TBA solvent exchange method.

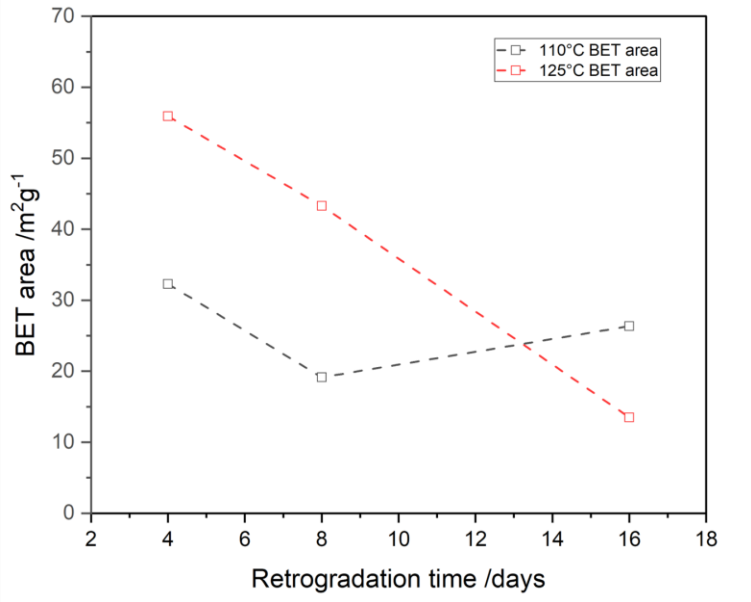

Figure 2-11. Surface area of expanded cassava starch samples obtained by TBA solvent exchange method.

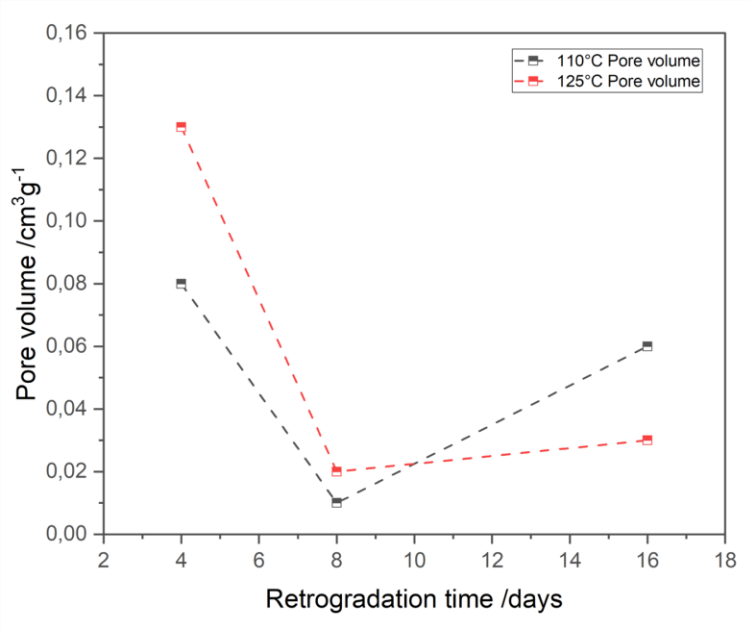

Figure 2-12. Pore volume of expanded cassava starch samples obtained by TBA solvent exchange method.

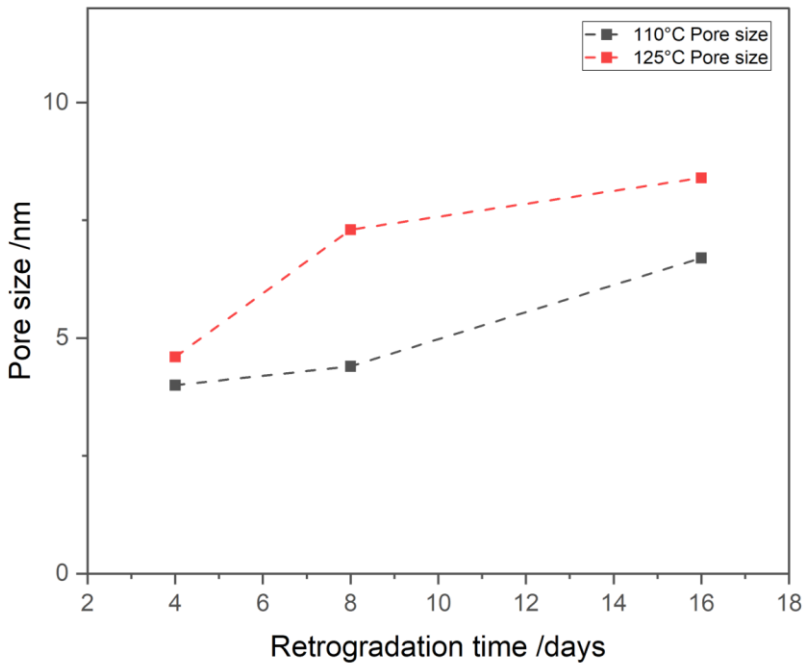

Figure 2-13. Por size of expanded cassava starch samples obtained by TBA solvent exchange method.

2.3.3.1 Gelatinization temperature

Gelatinization is the main and most important step in Starbon® synthesis as it is responsible for the dispersion of amylose and amylopectin chains as granule swells and water is integrated in the structure. The gelatinization temperature is therefore an important variable, as it affects the diffusion of water into the granule and the polymer recrystallization behaviour. Cassava starch gelatinization temperature ranges from 62°C to 86°C, presenting a peak at 68°C (Cheng et al., 1998). This range was surpassed in the selected gelatinization temperatures (110°C and 125°C). It was possible to evidence that increasing the gel temperature could have promoted the complete solution of the granule in the mixture, avoiding the loss of porosity related to partial crystallization of the net. Two temperatures: 110°C and 125°C were studied, nevertheless, it is possible to evidence in Figures 2-7, 2-8, 2-9, 2-11, 2-12 and 2-13 that there are no clear trends of surface area, pore volume and pore size mainly because temperature ranges were closely clustered. In this sense, this variable had minor influence on the final porosity of the material in the assessed range.

Starbon® materials have generally been produced using high-amylose corn starch known as Hylon VII, which gelatinization temperature ranges from 130°C to 150°C. White et al. used Hylon VII starch for preparing gels by microwave gelatinization at different temperatures from 100°C to 180°C to understand the influence of gelatinization temperature on final porosity of the dried expanded starch (White et al., 2008). They found that when temperature was higher than gelatinization range for Hylon VII at 180°C, the formation of regular spherical particles with a higher order of polysaccharides was observed. It was suggested that, at this temperature, amylopectin melts and then depolymerizes through a hydrolysis of 1-6 bonds. Consequently, similar phenomenon should be taken place in the cassava starch studied. As the synthesis temperatures used are much higher than gelatinization temperature of cassava starch, at 110°C and 125°C, breaks in amylopectin chains have occurred and the formation of spheres conducts to the no-significant effect of the variable in the assessed range. TGA was performed to cassava starch to understand its depolymerization temperature. The results suggested that the decomposition of chains when starch is still on its granule form starts at around 180°C, nevertheless, when the granules are dispersed in water the envelope has been remove, the structure is less crystalline and the depolymerization of amylopectin molecules should start at lower temperatures. Contrasting with literature, for Hylon VII starch, the TGA results suggested that the decomposition of starch starts at 275°C (Labelle et al., 2023), and White et al. are reporting the depolymerization in water at 180°C (White et al., 2008).

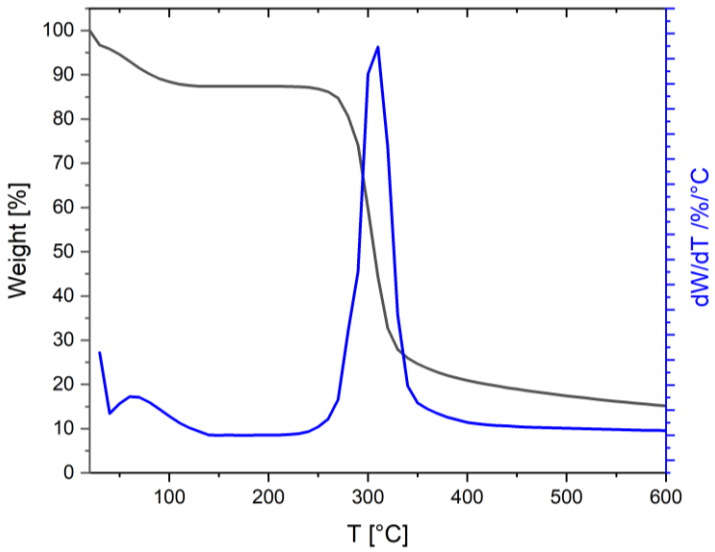

Figure 2-14. TGA and DTG curve for cassava starch.

2.3.3.2 Retrogradation time

After retrogradation, cassava starch gels were sticky and soft due to the starch's high amylopectin content In contrast to the firm gel obtained when amylose is abundantly present in starch, waxy starch pastes on retrogradation form a soft gel, which contains aggregates but no network (Tang & Copeland, 2007). Since cassava starch has a lower amylose content compared to other starches, it may have a lower tendency to retrograde and harden over time. The amylose's tendency to reorganize promotes nucleation in retrogradation, making the gel firmer in less time. Being a linear molecule, it is more prone to organize itself and form crystals, while branched starch is less likely to do so, and therefore will be pasty.

The retrogradation time was manipulated, revealing a notable impact on porosity. According to Tian et al., 2011, who studied the starch retrogradation by thermogravimetric analysis on different starches including low-level amylose starches, there is a correlation between the retrogradation time and the order of the chains on the expanded starch. As a result, shorter retrogradation times are desirable to promote the formation of pores. It is possible to confirm the previous mentioned on the isotherms obtained for both solvent exchange methods, where for both gelatinization temperatures, higher nitrogen adsorption is evidenced when gels were retrograded in shorter times (4 days) (Figure 2-6A and B, Figure 2-10A and B), which is an indicative of increased mesopore formation. Ethanol solvent exchange exhibited a decrease in surface area, pore volume, and pore size with extended retrogradation times (Figures 2-7, 2-8 and 2-9). In contrast, TBA solvent exchange resulted in an increased pore size with longer retrogradation times, suggesting that more ordered networks enhances the mixing between the water in the gel and the TBA added, promoting easy formation of microstructured eutectic phases and preserving the mesopores (Figures 2-11, 2-12 and 2-13) (Borisova et al., 2015).

2.3.3.3 Solvent exchange and drying method

Two synthesis routes employing ethanol and TBA as solvents were compared, focusing on the solvent exchange step. Both methods leaded to porous expanded materials. In the first route, wherein TBA was employed as solvent, the formation of a unique phase between t-butanol and water was the key of mesopores production. Consequently, the solvent addition must guarantee a final composition in which the eutectic point is reached (Borisova et al.,

2015). It was observed that the gradual addition of this solvent may be crucial in generating an emulsion that preserves the pore structure, while the fast addition of the solvent leaded to phase separation and the destruction of the porosity (Figure 2-15).

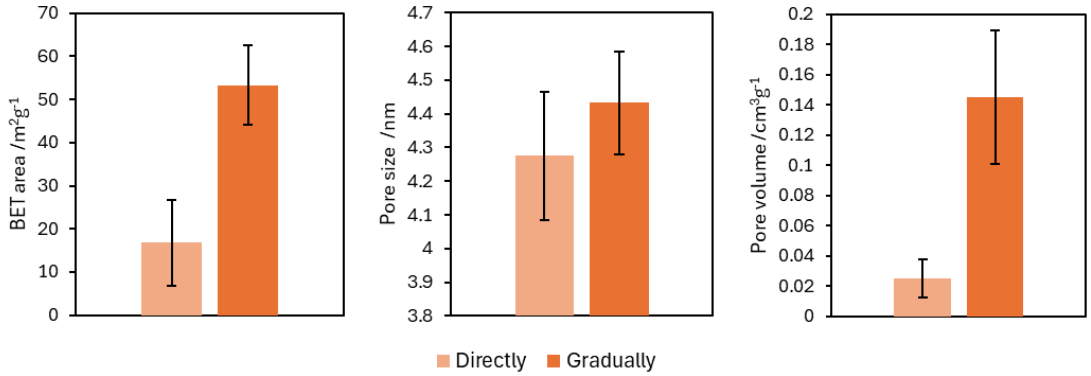

Figure 2-15. Surface area, pore size and pore volume of dried cassava gels prepared by TBA method, with TBA added directly (left) and at 2ml/10min (right).

Furthermore, during the exchange utilizing ethanol as solvent, it was concluded that both the number of exchange cycles significantly impacted the final porosity of the material, in contrast with the porosity obtained when three exchanges were made, the increase to five exchanges conducted to higher surfaces and pore volumes with an small reduction in pore size (Figure 2-16).

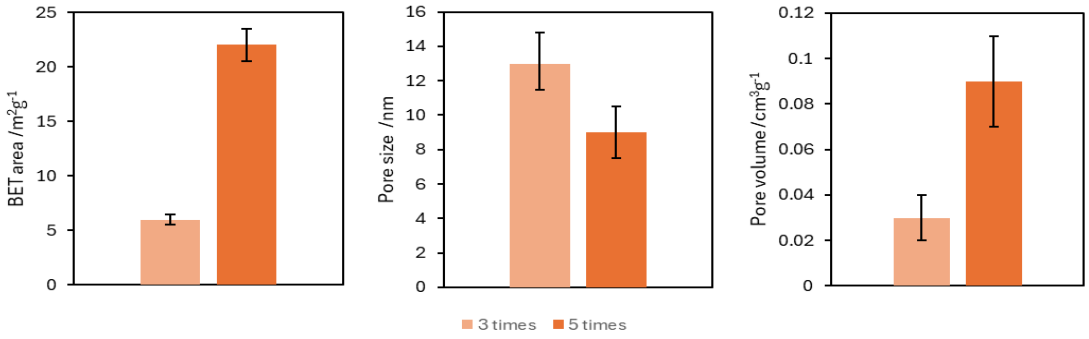

Figure 2-16. Surface area, pore size and pore volume of dried cassava gels prepared by EtOH method, with solvent exchange done 3 times (left) and five times (right).

When retrograded for 4 days, the ethanol method conducted to mesoporous materials with higher pore sizes (9-13 nm) than the obtained by TBA method (4nm). Consequently,

smaller pores but similar pore volumes implies that surface area available in samples exchanged by TBA method was higher than the obtained by ethanol method (33% higher). Additionally, it has been demonstrated that pores reduce their size during carbonization, leading to higher surface areas and the appearance of microporosity in carbons (White & Clark, 2015). Having that on mind, the recommendation of one of the two routes will be linked to the final application of the Starbon® material. Materials prepared by TBA method will be suitable for applications in the adsorption or reaction of small molecules and will have a high surface area which will enhance the acidity or adsorption capacity of the material. On the other hand, materials synthesized by EtOH method will be suitable for applications involving larger molecules such as long chain fatty acids esterification.

2.3.3.4 Carbonization pretreatment and temperature

During the carbonization process, it was observed that the presence of an acidic agent (p-TSA), enabled carbonization initiation within the pores of the expanded material, resulting in the formation of carbonized powder. In contrast, the absence of this acid leads to foam production, yielding to a coke-like material (Figure 2-17). When the acid is not used, carbonization results in melting of the polysaccharide network before the necessary dehydration-initiated mechanism (required to maintain the porosity) occurs. The use of the acid catalyst allows the decomposition mechanism to proceed at lower temperatures (e.g. < 150 °C) before the network melting, and the successful conversion of the porous starch phase into stable nanostructured, porous carbonaceous materials (White & Clark, 2015).

Figure 2-17. Product of carbonization of expanded starch: without doping with acid (A) and with doping with acid (B).

Once proved the effect of acid pretreatment and its importance during synthesis, all materials were pretreated before carbonization. Yield during this process resulted in around 22-35% of the weighted material remaining after carbonization. Higher carbonization

temperatures promoted the decomposition of material, leading to smaller yields. In **Table 2-3** are presented the surface area, pore size and pore volume for cassava starch gelatinized at 110°C and retrograded for 4 days.

Table 2-3: Synthesis method, carbonization temperature and textural properties of Cassava-Starbon materials.

Solvent exchange method	Carbonization temperature /°C	Yield /%	Surface area /m^2g^{-1}	Pore size /nm	Pore volume /cm^3g^{-1}
EtOH	Before carbonization	NA	17	13.5	0.07
EtOH	450	29.9	92	4.3	0.10
EtOH	700	23.9	360	2.4	0.21
TBA	Before carbonization	NA	32	4.0	0.08
TBA	450	31.6	202	1.8	0.17

When samples were carbonized, an increase on its surface occurs thanks to the formation of microporosity resulting of the degradation of the starchy matrix. Thus, producing a decrease in average pore size and an increase in the pore volume of the samples. This is also related to carbonization temperature. Higher carbonization temperatures produce a significant reduction in pore sizes (Figure 2-18A). This limits the use of materials carbonized at 700°C in applications with large molecules but make then suitable for adsorption of small molecules.

IR spectroscopy in Fourier transform mode (FTIR) spectroscopy of expanded cassava starch and its corresponding carbonized samples at 450°C and 700°C is presented in Figure 2-18B. Through the obtained spectra it is possible to evidence the conversion of the hydrophilic hydroxyl-rich polysaccharide precursor into carbonyl and aromatic rings in the surface. Hydroxyl groups (OH) are identified at the range of 1000-1100cm^{-1} in expanded starch precursor. Subsequently, when carbonized at 450°C ether and carbonyl groups are evidenced at 1209cm^{-1} and 1700cm^{-1} respectively, remaining hydrophilic and hydrophobic. Finally, in the sample carbonized at 700°C the conversion into aromatic structure is done and aromatic groups are predominant in the band of 700-950cm^{-1}, being mainly hydrophobic (Shuttleworth et al., 2013).

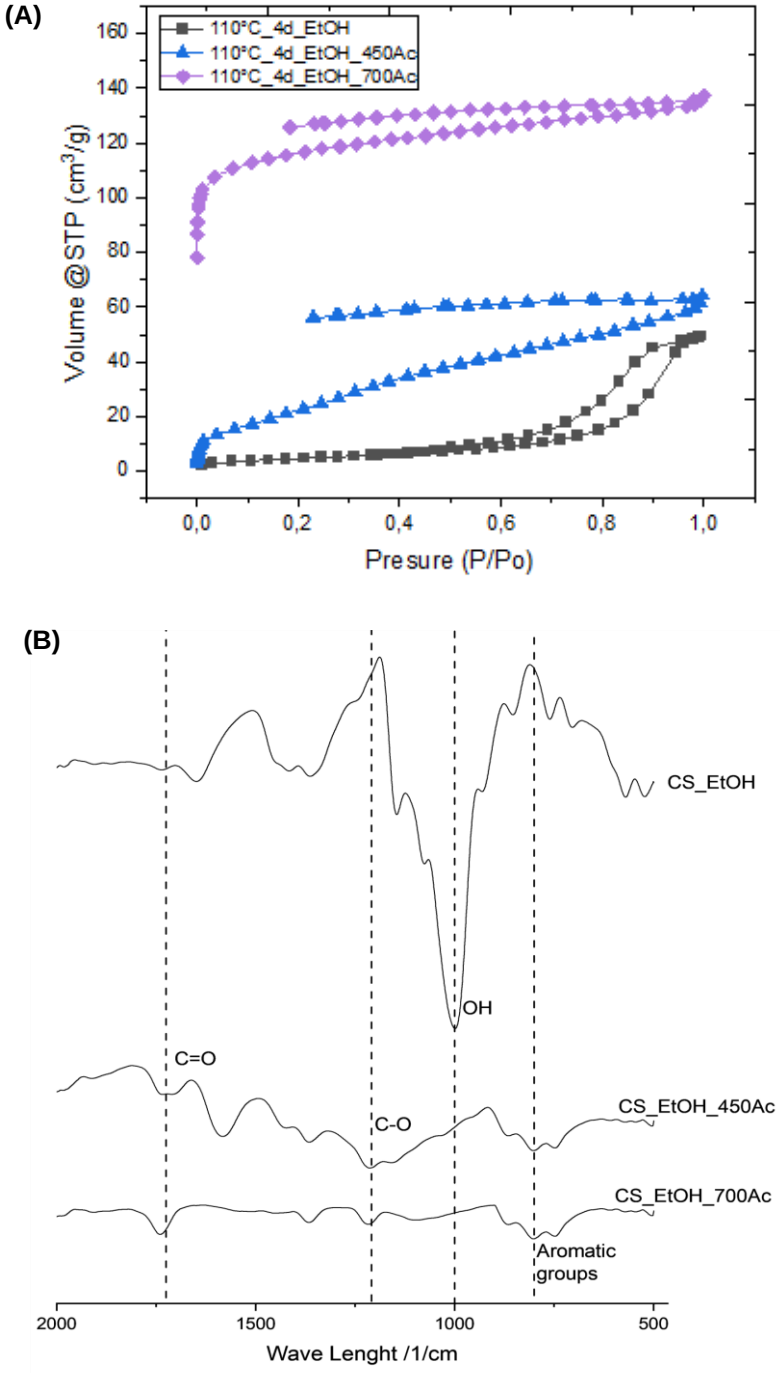

Figure 2-18. Nitrogen isotherm and FTIR spectra for Cassava-Starbon materials produced by EtOH method. Before carbonization and carbonized at 450°C and 700°C.

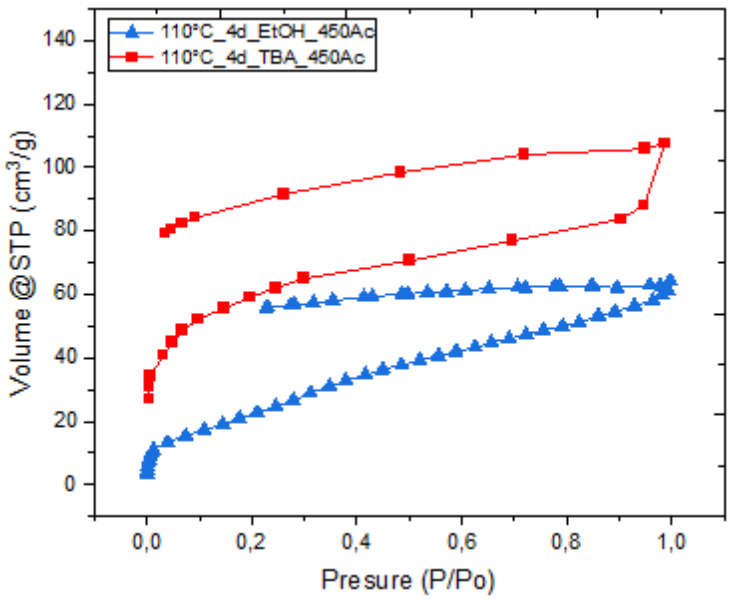

Figure 2-19. Nitrogen isotherm for Cassava-Starbon materials using EtOH and TBA synthesis method, carbonized at 450°C.

Through Figure 2-19 it is possible to compare the nitrogen isotherm of carbonized samples al 450°C synthesized by ethanol solvent exchange and TBA solvent exchange. Both samples present a behaviour of a type III isotherm with hysteresis, which demonstrates pores are slit shaped. The higher volume adsorbed in TBA isotherm is associated to the presence of a higher microporosity than in material obtained with EtOH as solvent. While EtOH remain mesoporous (av. pore size of 4.0 nm), most of the surface area in TBA material is associated to a microporous surface (av. pore size of 1.8 nm).

2.4 Conclusions

Conventional synthesis method reported by Budarin and coworkers (2006) for the production of Starbon® materials was implemented using Colombian cassava starch as precursor. Nevertheless, samples exhibit poorly developed porosity and insignificant surface area which was expected as the reported methodology was developed for high-amylose starches. In the case of Colombian starches, it was verified that they had 20.75% wt. amylose and 79.25% wt. amylopectin. Therefore, new conditions for the gelatinization, retrogradation, solvent exchange and carbonization steps were proposed according to literature and different experimental conditions were assessed. The obtained materials were characterized by their surface area, pore volume and pore size distribution. As a

result, suitable synthesis parameters were defined for obtaining high mesopore volumes and surface areas in the low-amylose-starch-derived Starbons®.

No clear influence of gelatinization temperatures above 110°C was observed, but further analysis of this variable is suggested considering the narrow range of temperatures evaluated in this study. In contrast, increasing the retrogradation time leaded to striking in porosity and a loss of surface. Nonetheless, by using a four-days retrogradation was suitable for cassava starch, despite it was expected that longer times were required to obtain organization of the polysaccharides' chains. Regarding the solvent exchange method, it was found that using ethanol and vacuum oven enable to obtain materials with higher pore sizes. In comparison, the use of freeze-drying and TBA leaded to the formation of smaller pores but with higher surfaces.

During the carbonization, the use of acid precursor demonstrated to avoid the melting of polysaccharide and formation of foam, leading to a porous carbonized powder. Carbonization temperature affected the functional groups in the surface of the cassava-Starbon® material, changing its hydrophobic-hydrophilic ratio. Additionally, when higher temperatures were used, the micropore content in the cassava-Starbon® increased. Consequently, the selection of the solvent exchange/drying method and the carbonization temperature should be done considering the final application of the cassava-Starbon® material. Once carbonized at 450°C the cassava-derived Starbon® synthesized using EtOH solvent exchange, it was possible to achieved remarkable surface areas of approximately 160 m^2g^{-1} and a pore volume of 0.13 cm^3g^{-1} with pore sizes of 4nm. These materials are still susceptible to improve its porosity as common Starbon® materials can reach until 400 m^2g^{-1}. Nonetheless, the developed procedure was found successful considering that the precursor had a very low amylose content.

3. Optimization of the surface properties for Colombian cassava starch based Starbon®

3.1 Introduction

Starbon® materials are mesoporous carbons obtained from polysaccharides, originally discovered at the Green Chemistry Centre of Excellence at the University of York in collaboration with the University of Córdoba in Spain (Budarin et al., 2006). Due to their unique surface properties, these materials have gained industrial significance for their mechanical resistance and versatility, finding applications in water treatment, nanotechnology, energy, and catalysis (Luque et al., 2009; Okamoto & Yashima, 1998; Parker, 2013). The name "Starbon" is a combination of "starch" and "carbon," highlighting the material's origin from starch, which transforms into carbon upon carbonization. Starch, particularly high-amylose starch like Hylon VII, has been the primary precursor for Starbon® synthesis, leading to notable porous materials (Budarin, Luque, et al., 2007; Luque & Clark, 2010; Milescu et al., 2020; Uriburu-Gray et al., 2020). However, to broaden the application and value of the agroindustry, there is growing interest in studying second generation, lo cost and low-amylose raw materials for Starbon® production.

Exploiting roots and tubers that may not meet the required standards and specification for the food industry (including cassava) for starch extraction could enhance agro-industrial capabilities in countries like Colombia. Cassava starch, with its lower amylose content, holds potential yet to be explored as a precursor for Starbon® materials. Today, Colombian agricultural and industrial processes generate large amount of cassava residues that can be valorised through such endeavours (DPN, 2016). However, challenges persist as most typically Starbon® based mesoporous carbons are produced from high amylose content starches. The process involves starch expansion in water, followed by retrogradation, drying to preserve a porous network, subsequently carbonization, and final activation when the material is intended for catalytic purposes. In this chapter, an exploratory analysis was

conducted on described process using cassava starch as the precursor. Initial attempts led to materials with negligible porosity, prompting adjustments in retrogradation, solvent exchange, and drying conditions. Therefore, a general method was devised to create porous materials, nevertheless, further studies on gelatinization during starch expansion and final carbonization were suggested for optimizing surface properties, especially when considering their application as catalysts for large-molecules conversion.

Given the boost of the cosmetics and food industries in recent years, production of fatty esters for these markets is of particular interest mainly for countries like Colombia which has vast oleaginous resources. Nonetheless, suitable materials must be developed to enable an effective transformation of fatty acids into value-added esters. In the esterification of large fatty acids with linear or branched alcohols there is need for highly active acid catalysts with a lipophilic surface and suitable porous structure to facilitate accessibility and high mass transfer rates. For this application, mesoporous materials such as ion exchange resins might seem promising, however they are mostly hydrophilic, and the porous matrix shrinks under organic media. Alternatively, biobased mesoporous carbons such as sulfonated Starbon® can become promising catalysts for the synthesis of fatty esters. Specifically, fatty acids esters obtained from lauric, palmitic, and stearic acid have kinetic diameters in the range of 0.8-1.5 nm (Dimian & Rothenberg, 2016). In general, it is required pore diameters of at least five times the kinetic diameter of a molecule to avoid diffusional issues, but smaller than 100 nm, which could result in poor activation of the material (Bosley, 1997). Consequently, mesoporous Starbon® materials with pore sizes exceeding the kinetic diameters of fatty acids and fatty esters would be desired, as those would ensure unimpeded access to active sites without steric hindrance while maintaining high surface areas for optimal catalytic performance. In this regard, this study delves into a comprehensive analysis of the synthesis process of Cassava-Starbon materials for its use as catalyst in the industry of fatty acid esters.

3.2 Materials and methods

3.2.1 Materials

Cassava starch was purchased from a local supplier (Yucarina, Unilever®). Deionized water used for the gelatinization process was obtained in the laboratory. Ethanol (99.5% wt.,

PanReac AppliChem ITW Reagents) was employed for solvent exchange, and p-toluenesulfonic acid monohydrate (97% wt., Fisher Scientific) was used as a carbonization promoter.

3.2.2 Methods

3.2.2.1 Variables selection and experimental design

In preliminary experiments it was found that gelatinization temperature, starch to water ratio, type of starch (i.e. nature and molecular weight), and carbonization temperature play a key role in the morphology of the Starbon® materials. The gelatinization of cassava starch starts at 60°C and finish at 80°C (depending on the variety and cultivation conditions of each specie) (Cruz et al., 1996). In the preliminary study, temperatures above 110°C were found to have no significant effect on the porosity obtained at the end of the starch gelatinization process as the complete dispersion of the granule occurred. Therefore, a lower range is investigated in the current research (70, 90, and 110°C). In the case of mass ratios starch to water (S:W), different values have been employed in Starbon® material preparation ranging from 1:5 to 1:20 (Borisova et al., 2015; Budarin et al., 2006; Budarin, Luque, et al., 2007; Luque et al., 2012; Parker et al., 2013; White et al., 2016). The molecular weight of starch influences the starch-water interaction during gelatinization, making it a variable to consider when establishing a mass ratio. Specifically, molecular weight in starches is influenced by the amount of amylose and amylopectin on its structure, as well as their chain length and ramifications, which varies for one starch to another. Consequently, to consider the effect of the molecular weight in the interaction between amylose, amylopectin and water molecules during gelatinization, the mass ratio should be studied, and determining the most suitable to enhance the porosity in cassava-derived Starbon®. Therefore, the influence of using 1:5, 1:10, and 1:20 S:W ratios in the final porosity of Starbon® from cassava starch will be evaluated.

Furthermore, carbonization temperatures were investigated at 450°C and 700°C. Although higher carbonization temperatures leaded to higher surface in the materials, they became predominantly microporous at 700 °C, making them not adequate for its use in esterification reactions. According to the surface groups in the Starbon® material, the carbonization in the range from 300°C to 500°C is suitable for its use in esterification reactions, also

promoting the removal of water from the active sites thanks to the hydrophobicity obtained at this temperatures, enhancing the reaction rates (White & Clark, 2015). Three carbonization temperatures (300°C, 400°C and 500°C) were assessed to determine the surface properties of the Cassava-Starbon.

A 2^3-factorial design of two independent variables and 3 levels was implemented to assess the gelatinization conditions. In this design the influence of gelatinization temperature and mass ratio starch to water (S:W) over the pore size, surface area and pore volume was evaluated for a total of 18 experiments (9 tests and their duplicates). Additionally, the factorial design was combined with a standard Box-Behnken design (BBD) with three independent variables at three levels, to add the carbonization temperature as variable and analyse the impact of carbonization on the previously synthesized gels (15 trials). The experimental design is schematized in the Figure 3-1, and the runs performed for the experimental design are presented in Table 3-1 and Table **3-2**. In order to determine if there is a significant effect of the variables selected on the final porosity of the material, and to understand potential interactions, an analysis of variance (ANOVA) was implemented, followed by and Tukey test for means comparison. Before ANOVA analysis, normality was verified using the Shapiro-Wilk test. Statistical software such as Minitab® 18.1 and R Studio® were used for the data processing and analysis.

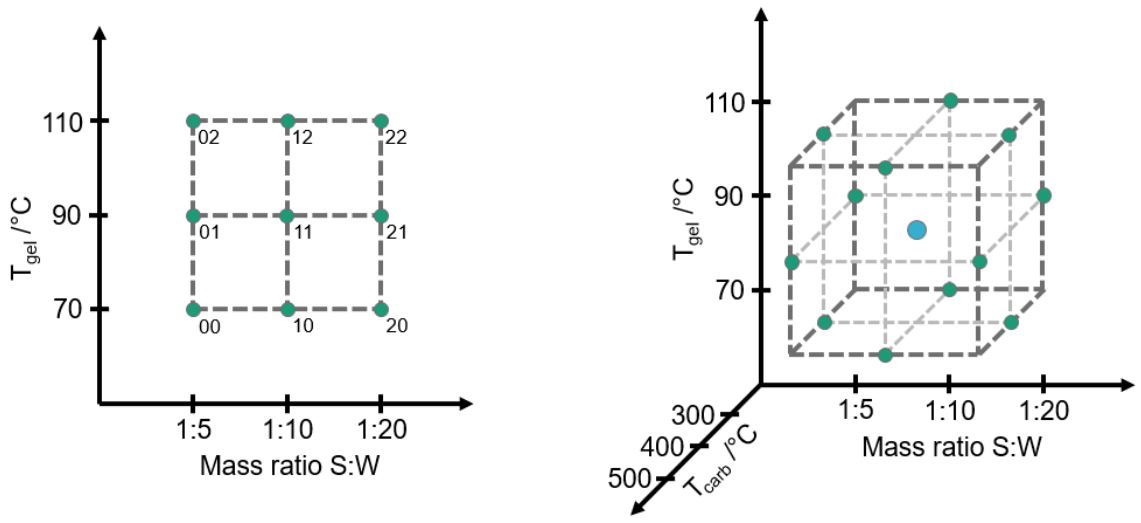

Figure 3-1. Scheme of the experimental design for gelatinization and carbonization conditions. Factorial 3^2 (left) and Box-Behnken (right).

Table 3-1: Levels and variables for factorial 3^2 experimental design.

Run	Mass ratio S:W (X_1)	T_{Gel} /°C (X_2)
F1	1:5	70
F2	1:10	70
F3	1:20	70
F4	1:5	90
F5	1:10	90
F6	1:20	90
F7	1:5	110
F8	1:10	110
F9	1:20	110

Table 3-2: Levels and variables for three factor Box-Behnken experimental design.

Run	Mass ratio S:W (X_1)	T_{Gel} /°C (X_2)	T_{Carb} /°C (X_3)
BB1	1:5	70	400
BB2	1:20	70	400
BB3	1:5	110	400
BB4	1:20	110	400
BB5	1:5	90	300
BB6	1:20	90	300
BB7	1:5	90	500
BB8	1:20	90	500
BB9	1:10	70	300
BB10	1:10	110	300
BB11	1:10	70	500
BB12	1:10	110	500
BB13	1:10	90	400
BB14	1:10	90	400
BB15	1:10	100	400

3.2.2.2 Samples preparation

Gels were synthesized stirring 10g, 20g and 40g of cassava starch in 200 ml of water for 1h at 70°C, 90°C and 110°C in a three-neck round-bottom flask using a half-moon overhead stirrer. The obtained sample was put in a freezer for its retrogradation at 4°C for 4 days.

When samples were removed from the fridge, they were immediately subjected to solvent exchange using ethanol. In this case, 400 ml of ethanol were added to the gel, blended, and subsequently stirred magnetically at 500 rpm for 1h at room temperature. It was filtered under vacuum to remove water-ethanol solvent. Afterwards, more ethanol (400 ml) was added and the procedure was repeated until five solvent exchanges were performed. Finally, samples were placed in a vacuum oven at 30°C for 24h. Once dried, the materials were doped using 5% wt. of p-TSA dissolved in a small volume of acetone as promotor of carbonization. Carbonization was executed at 300°C, 400°C and 500°C in a Thermo Scientific Lindberg/Blue Mini-Mite tubular oven, at different ramps as presented in Figure 3-2 (Mena, 2014). A schematic representation of the synthesis steps, their conditions, and levels is presented in Figure 3-3.

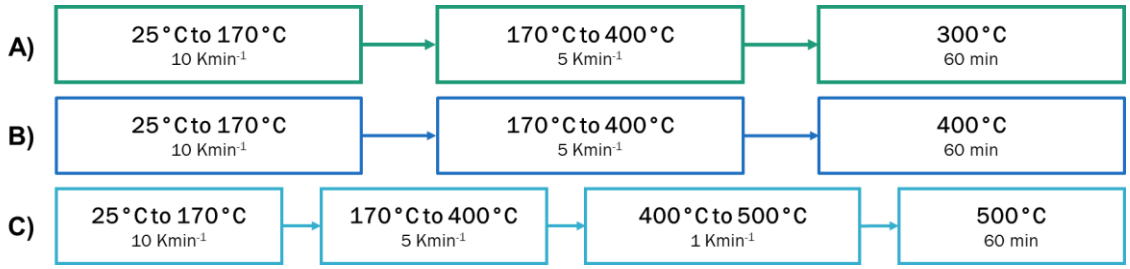

Figure 3-2. Temperature ramps for carbonization in Cassava-Starbon synthesis. A) for CS-300, B for CS-400 and C for CS-500.

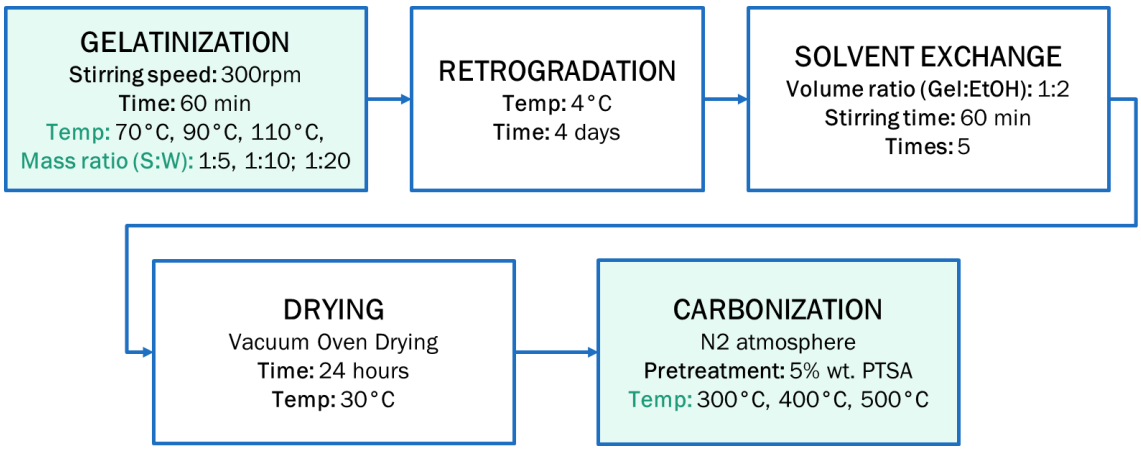

Figure 3-3. Synthesis method for expanded-starch samples and carbonized samples.

3.2.2.3 Samples characterization

Expanded starch samples and carbonized samples were characterized using nitrogen adsorption isotherms at 77K using Quadrasorb (Quantachrome Instruments). The expanded starch samples were outgassed using a vacuum degasser for 24 h at 50 °C and subsequently analysed, while the carbonized starch samples were outgassed at 250°C. The surface area was calculated using Brunauer, Emmett and Teller (BET) method in the relative pressure range from 0.05 to 0.30, with a correction proposed for samples exhibiting a type III isotherm (c<2) (Lowell et al., 2004). Pore size distributions were calculated using the non-linear density function theory (DFT) model for slit-cylindrical pores on carbon materials. From the adsorption and desorption branches of the isotherms, the pore sizes distributions, the average pore size in mesopore region and the total pore volume were obtained.

3.3 Results and discussion

3.3.1 Effect of gelatinization conditions on expanded cassava starches

The pore surface results for the factorial experimental design are presented in **Table 3-3**, detailing the behaviour of the porosity of expanded starch at different conditions. A and B refers to the duplicates in the experiments.

Table 3-3: Factorial experimental design response data for porosity of expanded starch.

Run	X_1	X_2	S_{BET} /m^2g^{-1} (Y_1)		Av. Mesopore size /nm (Y_2)		Total $P_{vol.\ A}$ /cm^3g^{-1} (Y_3)	
			A	B	A	B	A	B
F1	1:5	70	5.4	5.1	14.7	14.6	0.031	0.029
F2	1:10	70	9.6	10.6	14.3	14.8	0.083	0.084
F3	1:20	70	1.4	1.4	22.4	20.8	0.085	0.082
F4	1:5	90	5.8	5.0	15.4	14.6	0.055	0.056
F5	1:10	90	10.0	9.3	14.5	13.6	0.099	0.100
F6	1:20	90	9.7	10.5	14.5	14.1	0.089	0.089
F7	1:5	110	3.3	4.8	18.1	19.8	0.049	0.049
F8	1:10	110	11.2	13.2	14.9	13.3	0.120	0.121
F9	1:20	110	7.5	8.5	13.7	13.1	0.069	0.070

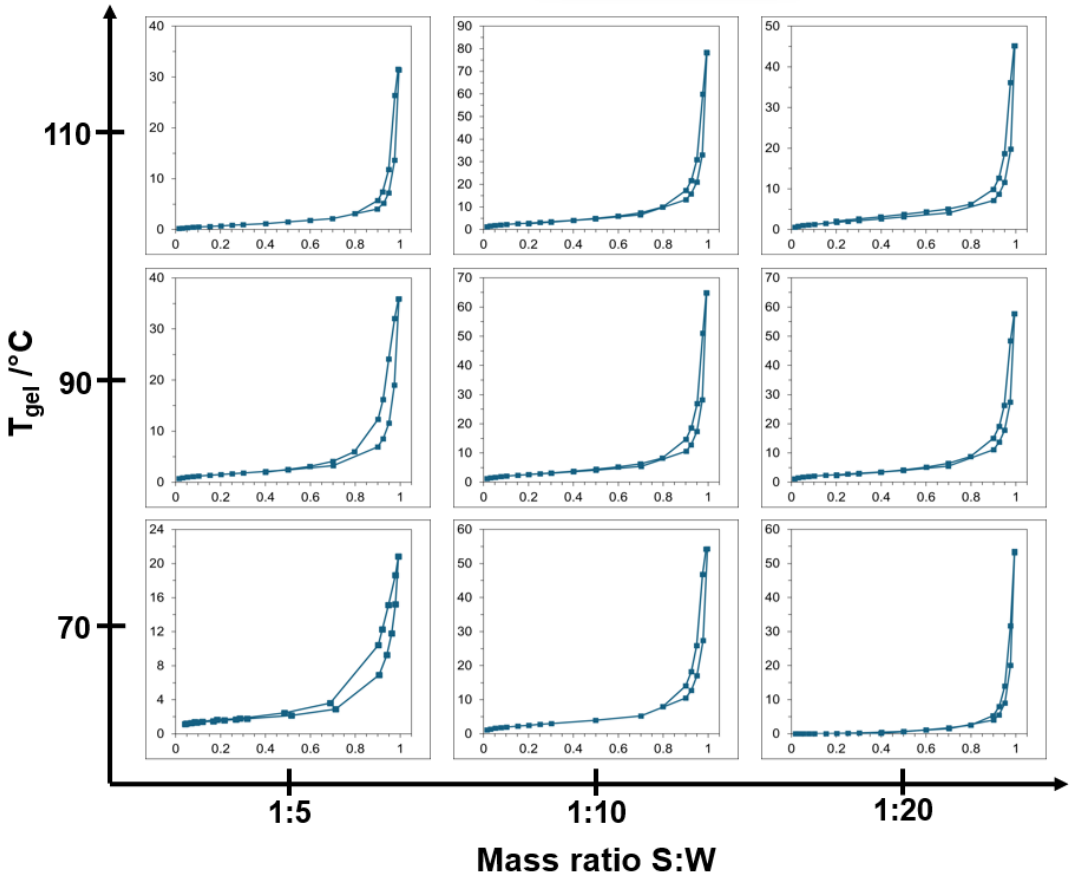

Figure 3-4. Nitrogen isotherm for expanded cassava starch samples in factorial experimental design. P/Po is x-axis of inside plots, and volume @STP in cm^3g^{-1} is y-axis.

Nitrogen isotherms presented in Figure 3-4 exhibit type II and III isotherms with hysteresis which are characteristic of meso and macroporous structures. Although most of the samples look like type III isotherm, it was reported that when C coefficient proposed by Brauner-Emmett-Taylor equation is less than 2, the isotherm corresponds to a type II. This behaviour suggests that a high cohesion force between adsorbate molecule and samples is taking place, and high pressure is required so as to start the adsorption, being associated to macroporous materials. Additionally, samples which present hysteresis imply the existence of mesopores in the materials. In contrast, negligible micropore volume is presented in the expanded starch samples.

Statistical tests were performed to understand the influence of mass ratio and gelatinization temperature on the porosity of the expanded cassava starches. Data was validated to follow

a normal distribution (Appendix C). ANOVA results for surface area, pore volume and pore size are presented in Table 3-4. For each factor and its interactions, p-value resulted to be lower than the significance level defined (0.05), consequently, the means are different for employed mass ratio, gelatinization temperature and their interaction. In this regard, at least one of the levels studied for gelatinization temperature, for mass ratio and one of the interactions between the levels of this factor is having a significant effect over the surface area, the pore volume, and the pore size of the expanded starch materials.

Table 3-4: Results of ANOVA for expanded cassava starches in factorial experimental design.

Source	Degree of Freedom	Sum of squares	Mean square	F value	P value	
Surface area (Y_1)						
Mass ratio	2	105,7	52,8	94,086	<0.0001	Significant
T gel	2	28,36	14,2	25,246	<0.0001	Significant
Interaction	4	63,68	15,9	28,344	<0.0001	Significant
Model	8	197,7	24,7	44,005	<0.0001	Significant
Residuals	9	5,055	0,568			
Total	17	202,3				
Pore size (Y_2)						
Mass ratio	2	17,52	8,76	15,402	0,0012	Significant
T gel	2	18,67	9,33	16,413	0,0009	Significant
Interaction	4	85,33	21,3	37,499	<0.0001	Significant
Model	8	121,5	15,2	26,704	<0.0001	Significant
Residuals	9	5,120	0,569			
Total	17	126,6				
Pore volume (Y_3)						
Mass ratio	2	0,0097	0,0048	4877,7	<0.0001	Significant
T gel	2	8,884E-4	4,44E-4	444,22	<0.0001	Significant
Interaction	4	0,0016	3,99E-4	398,89	<0.0001	Significant
Model	8	0,0122	0,0015	1529,9	<0.0001	Significant
Residuals	9	9,00E-6	1,00E-6			
Total	17	0,0122				

The effect of each factor and their influence over the surface properties was deeper studied through Tukey test, presented in **Table 3-5** and **Table 3-6**. The mean values that share the same letter are not significantly different.

Table 3-5: Tukey test results for individual effects of mass ratio and gelatinization temperature over surface area, pore volume and pore size.

		Mean Surface area /m^2g^{-1}	Mean Pore size /nm	Mean Pore volume /cm^3g^{-1}
Mass ratio	1:5	4.9 (A)	16.2 (A)	0.044 (A)
	1:10	10.7 (B)	14.2 (B)	0.101 (B)
	1:20	6.5 (C)	16.4 (A)	0.081 (C)
Gelatinization temperature	70	5.6 (A)	16.9 (A)	0.066 (A)
	90	8.4 (B)	14.4 (B)	0.081 (B)
	110	8.1 (B)	15.5 (B)	0.079 (B)

Table 3-6: Tukey test results for individual effects of mass ratio and gelatinization temperature over surface area, pore volume and pore size.

Mass ratio	Gelatinization temperature	Mean Surface area /m^2g^{-1}	Mean Pore size /nm	Mean Pore volume /cm^3g^{-1}
10	110	12,2 (A)	14.1 (B)	0.120 (A)
10	70	10,1 (A, B)	14.6 (B)	0.084 (D)
20	90	10,1 (A, B)	14.3 (B)	0.089 (C)
10	90	9,65 (A, B)	14.0 (B)	0.100 (B)
20	110	8 (B,C)	13.4 (B)	0.070 (E)
5	90	5,4 (C,D)	15 (B)	0.056 (F)
5	70	5,25 (C,D)	14.6 (B)	0.030 (H)
5	110	4,05 (D,E)	18,95 (A)	0.049 (G)
20	70	1,4 (E)	21,6 (A)	0.084 (D)

As observed from results, samples exhibited a reduced surface area and a wide pore size distribution in the range of mesopores and macropores. This is interesting considering that a reduction in pore size and the formation of smaller pores might take place when samples are further carbonized, so the macropores can lead to formation of mesopores.

Regarding the ANOVA analysis and analysing the influence of mass ratio on surface area, the means of the three levels studied exhibit significant differences. The use of a mass ratio

of 1:5 results in smaller surfaces compared to mass ratios of 1:10 and 1:20 (1:5 < 1:10 < 1:20). Regarding pore size, there is no significant difference between the means for the 1:5 and 1:20 mass ratios. However, the 1:10 mass ratio shows a significantly smaller pore size (1:10 < 1:5 = 1:20). For the pore volume, the means of the three levels studied are significantly different. A mass ratio of 1:10 presents the highest pore volume, followed by 1:20, with the smallest pore volumes observed for 1:5 (1:5 < 1:20 < 1:10). These results suggest that the optimal ratio for synthesizing cassava starch is 1:10. The use of a higher amount of starch may affect final porosity, as the network formed when gelatinization concludes could consist of several entangled and dispersed amylopectin chains, leaving less space for pore formation. Conversely, dilute starting solutions, such as a 1:20 mass ratio, produce a low-viscosity gel, resulting in higher pore volume due to the increased space available for pore formation but also leading to smaller surfaces.

Concerning gelatinization temperature, no significant differences were found between samples synthesized at 90°C and 110°C, while samples prepared at 70°C exhibited lower surface areas and pore volumes but higher pore sizes. This can be attributed to granule dispersion during gelatinization. Although the gelatinization peak is reached at temperatures lower than 70°C, at this point, the granule has not completed its dispersion in water, and some parts of the envelope remain organized and non-porous. Additionally, the lack of a significant difference between the porosity of materials obtained at 90°C and 110°C could be associated with the total dispersion of the granule at 90°C; therefore, an increase in temperature does not further promote porosity.

The observed interactions demonstrate that the optimal gelatinization conditions that promote higher surface areas and pore volumes are a mass ratio of 1:10 at 110°C. Nevertheless, most interactions between the factors do not exhibit a significant effect on pore size. In addition to Tukey test, the contour plots obtained for the three response variables allow for a visualization of the previously discussed results (Figure 3-5, Figure 3-6, and Figure 3-7).

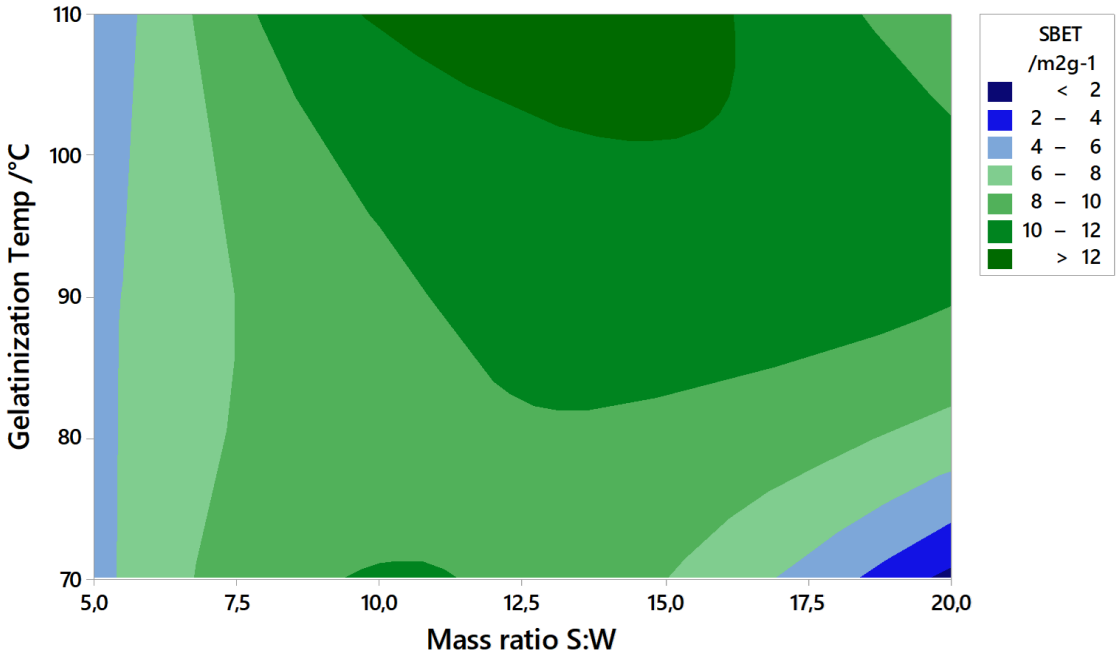

Figure 3-5. Contour plot for surface area as response variable, with mass ratio and gelatinization temperature as factors.

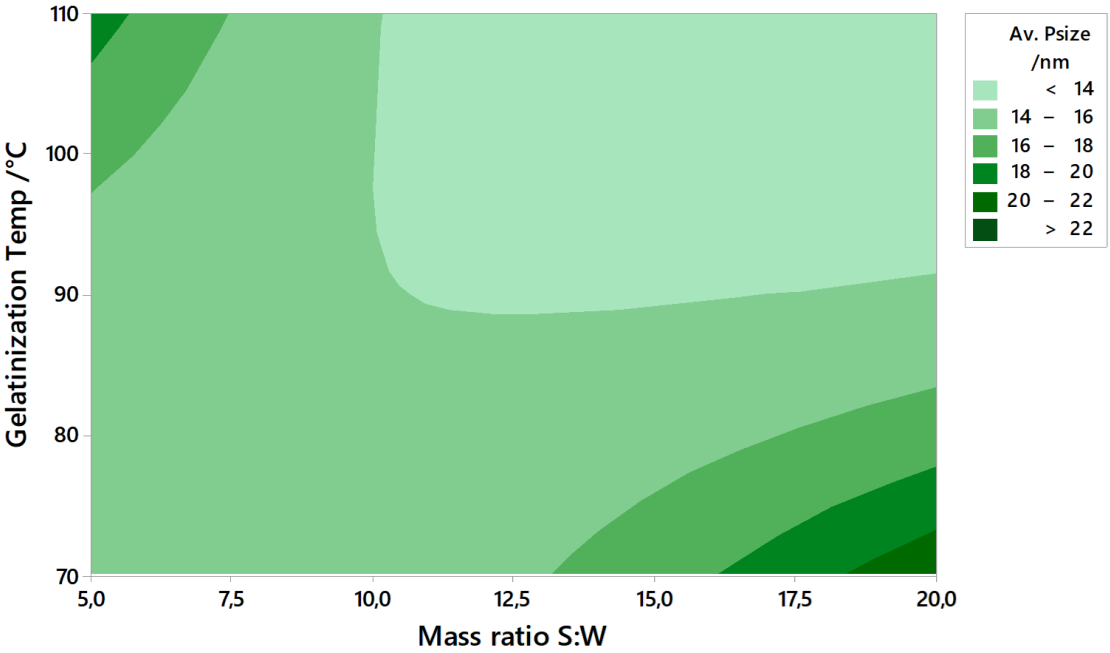

Figure 3-6. Contour plot for pore size as response variable, with mass ratio and gelatinization temperature as factors.

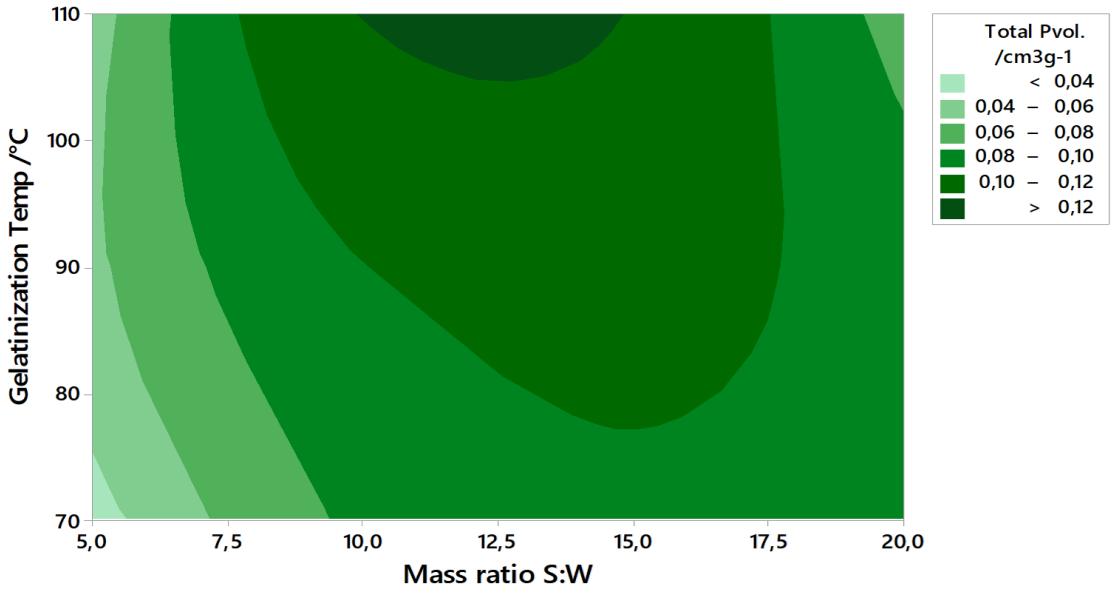

Figure 3-7. Contour plot for pore volume as response variable, with mass ratio and gelatinization temperature as factors.

3.3.2 Effect of carbonization conditions on Cassava-Starbon® synthesis

Previously obtained results regarding expanded cassava-starch samples are complemented with the analysis of their behaviour after carbonization. Surface area, pore volume and pore size results for the Box-Behnken experimental design (BBD) are presented in **Table 3-7**. Additionally, in Figure 3-8 , Figure 3-9, and Figure 3-10 are presented the nitrogen adsorption isotherms obtained for the carbonized materials at 300°C, 400°C and 500°C, respectively.

Isotherms for carbonized samples are a Type II and present an open hysteresis loop. According to Maziarka et. al. 2021, this behaviour is typical for carbonized organic polymers with a flexibility in the framework which causes the gas to not desorb completely during desorption process. Additionally, this shape is common when narrow slit pores or bottle shaped pores are present. Those characteristics causes that the N_2 molecules at 77 K are very slowly moving, and the use of another adsorbent such as CO_2 would be recommended (Maziarka et al., 2021).

Table 3-7: BBD experimental design response data for porosity of Cassava-Starbons.

Run	Mass ratio S:W (X_1)	T_{Gel} /°C (X_2)	T_{Carb} /°C (X_3)	S_{BET} /m^2g^{-1} (Y_1)	Av. P_{size} /nm (Y_2)	Total $P_{vol.}$ /cm^3g^{-1} (Y_3)
BB1	1:5	70	400	2.43	5.7	0.025
BB2	1:20	70	400	<1	ND	0.035
BB3	1:5	110	400	27.8	4.7	0.056
BB4	1:20	110	400	28.04	4.9	0.056
BB5	1:5	90	300	<1	ND	0.012
BB6	1:20	90	300	<1	ND	0.026
BB7	1:5	90	500	76.77	2.7	0.069
BB8	1:20	90	500	1.44	3.2	0.004
BB9	1:10	70	300	<1	ND	0.005
BB10	1:10	110	300	<1	ND	0.013
BB11	1:10	70	500	131.97	2.4	0.230
BB12	1:10	110	500	251.67	2.9	0.175
BB13	1:10	90	400	89.81	4.3	0.135
BB14	1:10	90	400	112.33	3.9	0.143
BB15	1:10	90	400	93.19	4.1	0.140

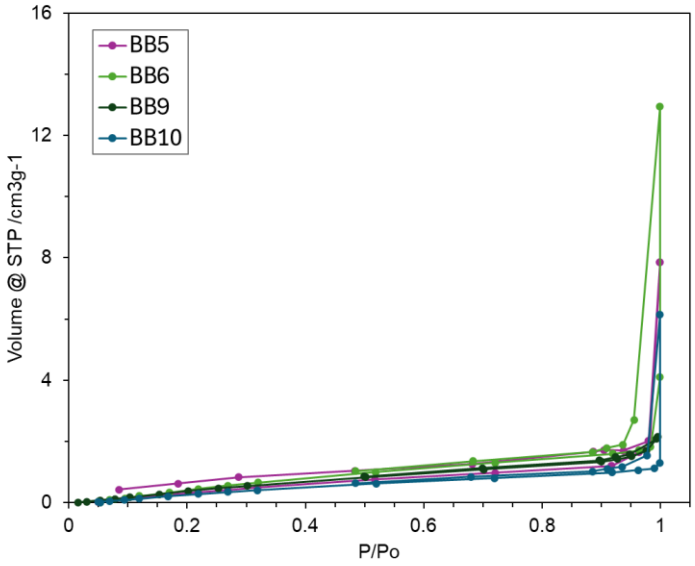

Figure 3-8. Nitrogen adsorption isotherm for samples carbonized at 300°C.

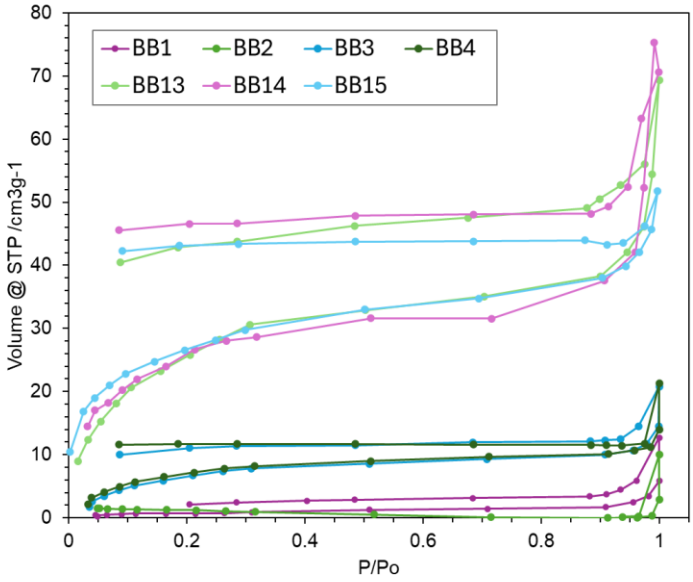

Figure 3-9. Nitrogen adsorption isotherm for samples carbonized at 400°C.

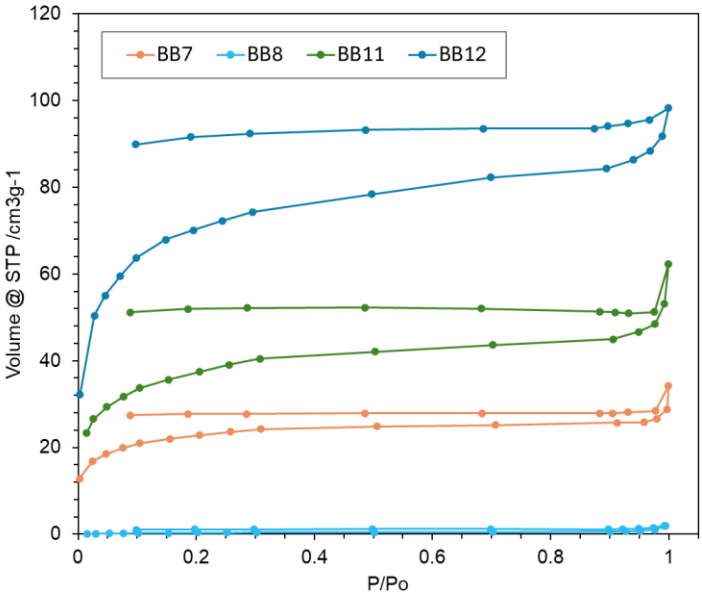

Figure 3-10. Nitrogen adsorption isotherm for samples carbonized at 500°C.

Although it was expected an increase in the pore volume and the creation of microporosity when samples were carbonized, it was found that samples carbonized at 300°C exhibited a decrease in the surface properties, in comparison to the expanded starch precursor. Connected with the isotherm shape, it is possible that those samples suffered a shrinkage

of pores during carbonization and exhibited a porosity which cannot be measured by N_2 sorption. As mesoporosity is the main goal in the synthesis for its use in fatty acid esterification, those materials which might have micro or macroporosity, are analysed as if their surface area and pore sizes were negligible. Similar to conventional Starbons® that typically present higher micropore content as a function of T, samples carbonized at 400°C and 500°C do exhibited higher surface areas and pore volume.

The effect of the gelatinization temperature, the mass ratio and the carbonization temperature over the surface area, pore size and pore volume of carbonized materials was analysed using a surface response method. ANOVA including orthogonal polynomials for lineal and quadratic part of the factors is presented in **Table 3-8**, **Table 3-9** and **Table 3-10**. In the case of ANOVA results for surface area, quadratic interactions between mass ratio, gelatinization temperature and carbonization temperature prove to be relevant with a significant level of 0.05. Additionally, regarding pore size, p-value resulted to be lower than the significance level defined for linear interactions. Nevertheless, in case of pore size the model is not significant and nor linear or quadratic interactions between factors prove to have an effect on this response variable.

Table 3-8: Results of ANOVA for cassava-starbons surface area in BBD experimental design.

Source	DF	Sum of squares	Mean square	F value	P value	
Model	7	50792,0	7256,0	49,20	0,020	Significant
Linear	3	2119,2	706,4	4,79	0,178	
Mass ratio S:W	1	1,2	1,2	0,01	0,936	
Gel. Temp	1	147,9	147,9	1,00	0,422	
Carb. Temp	1	517,8	517,8	3,51	0,202	
Square	2	30856,4	15428,2	104,61	0,009	Significant
Mass ratio S:W*Mass ratio S:W	1	29949,5	29949,5	203,07	0,005	Significant
Gel. Temp*Gel. Temp	1	38,9	38,9	0,26	0,659	
Interactions	2	2945,3	1472,6	9,98	0,091	
Mass ratio S:W*Gel. Temp	1	2224,5	2224,5	15,08	0,060	
Mass ratio S:W*Carb. Temp	1	434,6	434,6	2,95	0,228	
Error	2	295,0	147,5			
Total	9	51086,9				

Table 3-9: Results of ANOVA for cassava-starbons pore size in BBD experimental design.

Source	DF	Sum of squares	Mean square	F value	P value	
Model	7	10,3251	1,47501	38,68	0,025	Significant
Linear	3	3,3985	1,13283	29,71	0,033	Significant
Mass ratio S:W	1	1,0331	1,03309	27,09	0,035	Significant
Gel. Temp	1	0,1245	0,12449	3,26	0,213	
Carb. Temp	1	2,8512	2,85121	74,77	0,013	Significant
Square	2	0,1182	0,05911	1,55	0,392	
Mass ratio S:W*Mass ratio S:W	1	0,1098	0,10977	2,88	0,232	
Gel. Temp*Gel. Temp	1	0,0186	0,01856	0,49	0,558	
Interactions	2	0,7303	0,36514	9,58	0,095	
Mass ratio S:W*Gel. Temp	1	0,6154	0,61544	16,14	0,057	
Mass ratio S:W*Carb. Temp	1	0,6851	0,68513	17,97	0,051	
Error	2	0,0763	0,03813			
Total	9	10,4014				

Table 3-10: Results of ANOVA for cassava-starbons pore volume in BBD experimental design.

Source	DF	Sum of squares	Mean square	F value	P value	
Model	9	0,056955	0,006328	2,20	0,199	
Linear	3	0,018753	0,006251	2,17	0,209	
Mass ratio S:W	1	0,014820	0,014820	5,16	0,072	
Gel. Temp	1	0,000798	0,000798	0,28	0,621	
Carb. Temp	1	0,005874	0,005874	2,04	0,212	
Square	3	0,026769	0,008923	3,10	0,127	
Mass ratio S:W*Mass ratio S:W	1	0,025532	0,025532	8,88	0,031	Significant
Gel. Temp*Gel. Temp	1	0,000319	0,000319	0,11	0,753	
Carb. Temp*Carb. Temp	1	0,002200	0,002200	0,77	0,422	
Interactions	3	0,005501	0,001834	0,64	0,622	
Mass ratio S:W*Gel. Temp	1	0,000007	0,000007	0,00	0,963	
Mass ratio S:W*Carb. Temp	1	0,004494	0,004494	1,56	0,267	
Gel. Temp*Carb. Temp	1	0,001000	0,001000	0,35	0,581	
Error	5	0,014373	0,002875			
Lack of fit	3	0,014334	0,004778	249,39	0,004	Significant
Pure Error	2	0,000038	0,000019			
Total	14	0,071328				

Multiple regression analysis on the experimental data was conducted for the three assessed variables. The coefficient of determination (R^2) value were 0.994, 0.993 and 0.923 for surface area (Y_1), pore size (Y_2) and pore volume (Y_3), respectively.

$$Y_1 = -138 - 1.8X_1 - 3.92X_2 + 0.446X_3 - 2.706X_1^2 + 0.0122X_2^2 + 0.472X_1X_2 + 0.0439X_1X_3 \quad (3.1)$$

$$Y_2 = 27.61 - 1.674X_1 - 0.1136X_2 - 0.3306X_3 + 0.00518X_1^2 + 0.000266X_2^2 + 0.00784X_1X_2 + 0.001745X_1X_3 \quad (3.2)$$

$$Y_3 = -1.444 + 0.0586X_1 + 0.0073X_2 + 0.00368X_3 - 0.001705X_1^2 + 0.000023X_2^2 + 0.000002X_3^2 + 0.000009X_1X_2 - 0.000043X_1X_3 - 0.000008X_2X_3 \quad (3.3)$$

It is essential to test accuracy to get an adequate model. The model accuracy was checked by comparing experimental and predicted surface property respectively (Figure 3-11).

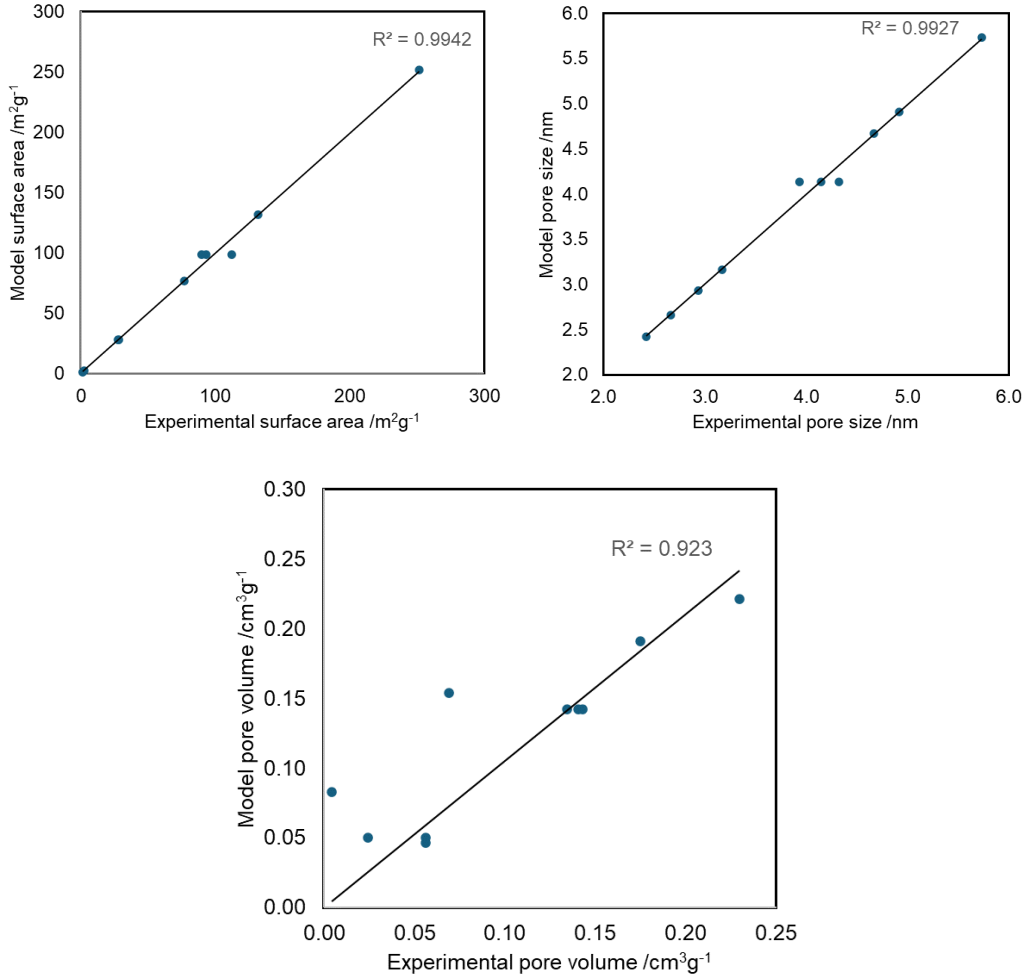

Figure 3-11. Pareto diagrams of model predicted response against experimental response for the surface area, pore size and pore volume.

3.3.3 Optimization of surface parameters of cassava-Starbon

In order to enhance the surface properties of the cassava-starbons, an optimization was conducted considering the three response variables studied. A ponderation of values was proposed. As the obtained pore volume for cassava-starbon materials was limited due to its amylose content, this is the most important variable to maximize through the synthesis conditions and a value of 0.5 was assigned. Subsequently, as it is needed that pores range within the mesoporous region being higher than 4nm so as to avoid the steric hindrance, it was pondered in 0.3. Finally, surface area was assigned with a value of 0.2.

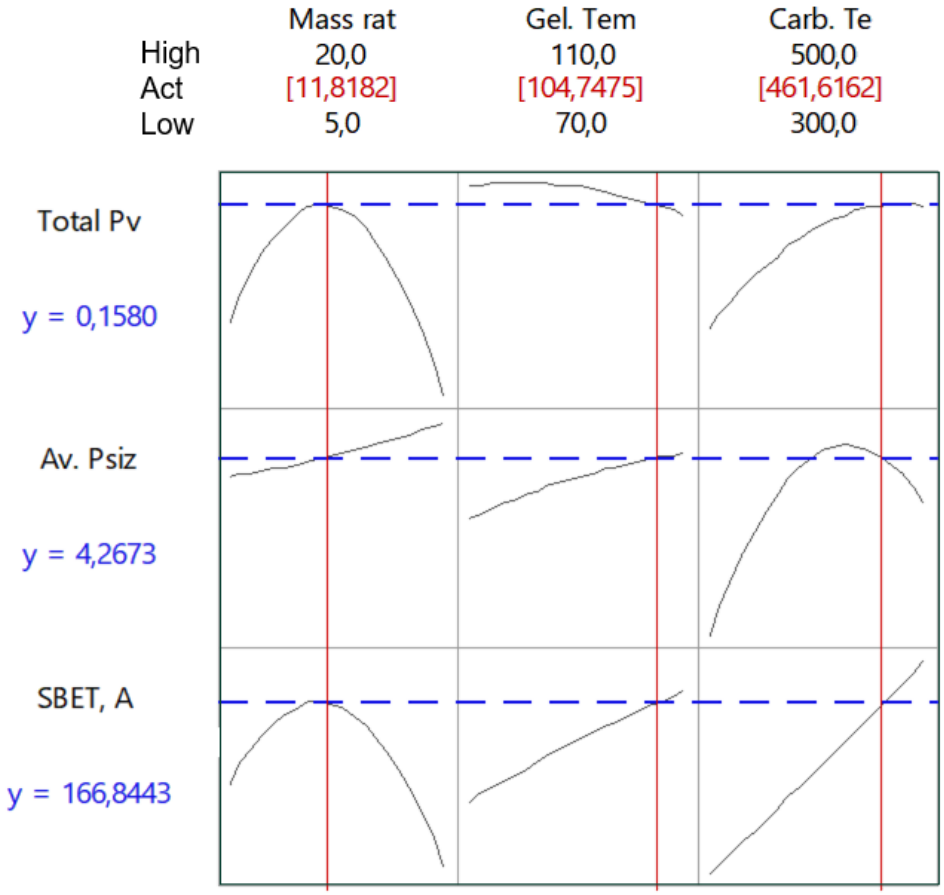

Figure 3-12. Surface properties optimization for Cassava-starbon materials.

Optimization results are presented in Figure 3-12. It was found that a mass ratio of 1:12, gelatinized at 105°C and carbonized at 450°C will maximize the surface properties of the cassava-starbon. This is consistent with the results obtained by the study of factorial design,

which suggests that the higher porosity in the expanded-starch precursor can be obtained when material is synthesized at 1:10 mass ratio at a gelatinization temperature of 110°C. Further studies under these conditions will be carried out to verify the results from the model and to synthesize a suitable cassava-based starbon® for its catalytic application in esterification reactions.

3.4 Conclusions

Factorial 3^2 experimental design and a Box-Behnken experimental design were conducted for assessing the effect of gelatinization and carbonization conditions on Cassava-Starbon synthesis. The comprehensive analysis of experimental data and statistical tests revealed key insights into the factors influencing the porosity of cassava based Starbon® materials. The factorial design demonstrated that a mass ratio of 1:10 and a gelatinization temperature of 110°C are crucial for achieving higher surface area and pore volume. In contrast, smaller and larger mass ratios led to a decrease in porosity. The Tukey test supported these findings, emphasizing the significance of these factors. Additionally, carbonization results, demonstrated that low carbonization temperatures affect the porosity, therefore temperatures of 400°C of higher are desirable. Finally, optimization for maximum surface properties indicated that a mass ratio of 1:12, gelatinization at 105°C, and carbonization at 450°C are the recommended conditions to achieve optimal porosity in cassava-starbons. This aligns with the factorial design results, providing a consistent and suitable method for synthesizing cassava starch based Starbon® materials with enhanced porosity for further use as catalysts in fatty acid esterification.

4. Sulfonated cassava starch-based Starbon® as catalyst for fatty acids esterification

4.1 Introduction

Fatty acid esters (FAEs) are important oleochemicals widely used in the manufacture of food and personal care products, pharmaceuticals, cosmetics, solvents, and biofuels among many other applications. Currently, the global market of FAEs is around $ 3 billion/yr., and it is expected to reach $ 4.5 billion by 2030 (Grand View Research, 2020). FAEs can be produced by Fischer esterification of fatty acids with different alcohols generally using homogeneous catalysts such as sulfuric acid, p-toluenesulfonic acid (PTSA), or methanesulfonic acid (MSA) (Chandane et al., 2017; de Jong et al., 2009; Kastratovic & Bigovic, 2018). To comply with the required specifications of commercial FAEs, complete removal of the homogeneous catalysts is required, and this involves intensive downstream separations, neutralization, and waste generation. Also, homogeneous catalysts promote equipment corrosion and undesired side reactions such as etherification of alcohols, and organics dehydration and oxidation inducing product darkening. As an alternative, commercial heterogeneous acid catalysts such as ion exchange resins have been used in FAE production (Paterson et al., 2013; Yalçinyuva et al., 2008). As the kinetic diameter of FAEs is around 0.8-1.5 nm (Dimian & Rothenberg, 2016), mesoporous macroreticular crosslinked resins are preferred. This is the case of Amberlyst 15 which has an average pore size of 28-30 nm (DuPont de Nemours, 2019; Kunin et al., 1962). Such mesoporosity enhances mobility within the polymeric matrix and accessibility to the active sites. However, polymeric exchange resins exhibit high and selective water absorption, which is a drawback for the synthesis of FAEs considering that esterification conversion is limited by chemical equilibrium. Additionally, and despite they enable easier recovery and reuse, most ion exchange resins can operate up to 120-130°C to avoid degradation of the polymeric matrix and its deactivation, thus limiting achievable reaction rates.

In this regard, in recent years heterogeneous catalysts have been increasingly tailored to overcome operating limitations such as those previously mentioned. In particular, biobased feedstocks have been spotted as flexible and functionalized raw materials for the synthesis of catalysts with specific properties. By exploiting the natural structures of different biobased sources (e.g., seed shells, fibres, husks, bones, seashells, polysaccharides, etc.), or by shaping them into tailored porous matrices, it has been possible to obtain solids with suitable morphologies for different catalytic applications. Besides enhancing activity and selectivity, the use of biobased precursors aids in reducing catalyst life cycle impacts and mitigating issues with used catalyst disposal, thus improving sustainability indicators.

Among the large variety of biobased catalysts, acid-activated carbons have been successfully synthesized and used in the esterification of different carboxylic acids (Borges & Díaz, 2012; Clark et al., 2008; De et al., 2015; Mahajan & Gupta, 2020; Peng et al., 2010; Wenchao et al., 2019; White et al., 2009). In addition to better thermal stability, their hydrophobic nature enables them to reach high conversions despite the presence of water in the reaction media (Peng et al., 2010; Wenchao et al., 2019; White et al., 2009). Particularly, certain activated carbons have demonstrated excellent catalytic performances, notably in biodiesel production, leading to high yields within remarkably short reaction times, typically less than 0.5 hours (Yang et al., 2023). Another alternative approach involves the utilization of biochar catalysts. Those have been obtained from marine macroalgae subjected to thermochemical treatment (180-900°C), followed by activation through physical methods such as steam and CO2 activation, as well as chemical treatments including alkaline, acidic, and oxidative processes. The yields obtained in biodiesel production using these biochar catalysts have proven to be significant, with reaction times varying from 1 to 5 hours depending on the synthesis method and reaction conditions (Yameen et al., 2023). Despite the promising results, further development of synthesis methodologies for carbon-based catalysts is essential to achieve more sustainable alternatives, particularly given the elevated temperatures involved in their production (Yameen et al., 2023; Yang et al., 2023). As a result, several sustainable synthesis approaches have been investigated. Biochar catalysts synthesized via thermochemical treatment of lignin-derived monomers at low temperatures (80°C) have shown promising high yields. However, it is worth noting that the reaction time still extends to approximately 6 hours (Huang et al., 2022). Nonetheless, reaction times using carbon-

based catalysts can be reduced by using combined intensification approaches such as sonication or microwaves. For instance, it has been demonstrated that the reaction time for producing canola-based biodiesel using activated carbon derived from calcinated lime could be reduced to 15 minutes by using microwaves (Bokhari et al., 2019).

As presented in Table 4-1, mesoporous-activated carbons have demonstrated to be effective catalysts in the synthesis of FAEs. Such mesoporous structures have been produced via controlled carbonization of organic materials using sacrificial inorganic templates (e.g., mesoporous silica or alumina) or by direct carbonization of pre-formed structures. In the first case, carbonization at high temperatures is generally required for the chemical digestion of the inorganic template. However, besides destroying the complexity and entropy embedded in the inorganic template, this last step involves the use of hazardous hydrofluoric acid and a large generation of waste making this approach unsustainable for further industrialization.

Table 4-1: Reported studies on the synthesis of biobased mesoporous carbon catalysts for the esterification of fatty acids.

Biobased source	Synthesis conditions	Area m^2/g	D_P[§] (nm)	V_P [¥] (cm^3/g)	Activation	Acidity (meq. H^+/g)	Fatty acid esterification case	Ref.
Sucrose	Impregnation of mesoporous silica, calcination, activation, template removal with HF	808	3.9	0.47	Sulfonation with H_2SO_4	2.3	Oleic acid:Methanol 1:10 mol, Cat 0.7% wt. 353 K, X - 60%, 10h	(Peng et al., 2010)
		318-805	2.8-6.8	0.04-0.25	Attachment of benzenesulfonic acid	1.7-2.6	Oleic acid:Methanol 1:56 mol, Cat 2.9% wt. 338 K, X - 90%, 2.5h	(Geng et al., 2011)
Starch	Sulfonation of Starbon® 300	66-77	11-15	-	Sulfonation with H_2SO_4	1.1-2.3	Oleic acid:Ethanol 1:10 mol, Cat 1.3% wt. 353 K, X - 90%, 10h	(Aldana et al., 2012)
Cleargum starch	Gelling, drying, carbonization, activation	32	30	0.16	Sulfonation with H_2SO_4	0.82	Lauric acid:Methanol 1:15 mol, Cat 3% wt. 343 K, X – 77%, 12h	(Mena & Macquarrie, 2014)

-	Impregnation of mesoporous γ-alumina, calcination, activation, template removal with HF	493-616	3.3-3.8	0.35-0.44	Phosphorylation with H_3PO_4	0.56-1.12	Oleic acid:Methanol 1:15 mol, Cat 1.8% wt. 353 K, X - 70%, 5h	(L. Wang et al., 2014)
Pongamia galabra seed cake	Activation-carbonization, sulfonation	483	4.7	0.58	Sulfonation with 4-benzene-diazonium sulfonate	3.62	Acid oil:Methanol, 1:40 mol, Cat 0.9% wt. 393 K, X - 93%, 2h	(Konwar et al., 2019)
Bamboo	Carbonization, activation	226	10-20	0.12	Attachment of sulfanilic acid	1.69	Oleic acid:Ethanol 1:7 mol, Cat 5.6% wt. 358 K, X - 96%, 3h	(Niu et al., 2018)

§ Average pore diameter
¥ Pore volume
Cat – Catalyst loading with respect to total weight
X – Conversion

To prevent this, the generation of template-free mesoporous carbons has been achieved via pre-formation and subsequent carbonization of organic aerogels, xerogels, and cryogels. This approach has enabled to obtain catalysts of improved mechanical resistance with high surface area per volume unit (Członka et al., 2018; F. Liu et al., 2016; Mena, 2014). Whereas they were initially obtained from fossil-based resources (Członka et al., 2018), they were eventually produced from storage and structural polysaccharides such as starches, glycogen, cellulose, chitin, and pectin. Such biobased materials are widely available at low cost, they contain useful functional groups, and they can form structured aqueous gels. Recently, starch-based mesoporous activated carbons became commercial and are currently traded under the name Starbon® (Budarin, Clark, Luque, & Macquarrie, 2007). They have been tested in different acid-catalyzed reactions exhibiting high stability, reusability, and high reaction rates, conversions, and selectivity (Budarin, Luque, et al., 2007; Mena, 2014; White et al., 2009).

An additional advantage of Starbons® is that they can be produced using second-generation starches coming from food wastes, thus enabling to exploit circular economy principles. This is of paramount importance for countries like Colombia, where nearly 30% (i.e., 1.5 Mt) of starch-rich roots and tubers produced annually are discarded and wasted because they do not meet quality standards (DPN, 2016). Also, large starchy waste streams

are discarded in some agro-industrial processing, particularly in the processing of cassava (Manihot esculenta) (García et al., 2020; Torres et al., 2005). Then, as a suitable valorization alternative for such food wastes, this work explored the synthesis of sulfonated Starbon® catalysts using cassava and corn starch as feedstock. The aim is to use them in the esterification of fatty acids, particularly for the production of cosmetic FAEs such as isopropyl stearate. The process involved gelation and retrogradation of starches, aqueous to organic solvent exchange, freeze drying, and final carbonization under controlled temperature. Subsequently, the biobased carbon was subjected to activation via sulfonation with sulfuric acid, and the obtained materials were characterized and further evaluated as catalysts in the esterification of stearic acid with isopropanol. For comparison purposes, a set of commercial homogeneous (H2SO4, p-toluene sulfonic acid, methane sulfonic acid) and heterogenous (Lewatit K2629 and Amberlyst 15, 35, and 70) catalysts were also evaluated in the esterification processes under equivalent acid loadings.

4.2 Materials and methods

4.2.1 Materials

Corn starch was purchased from an industrial supplier (Hylon VII, Ingredion®) and it contained 68-70% wt. amylose and ~30% wt. amylopectin. Cassava starch corresponded to a commercial product (Yucarina, Unilever®) and it was used without further purification. Deionized water used for the gelation process was obtained in the laboratory. Ethanol (99.7% wt., PanReac AppliChem ITW Reagents) was used for solvent exchange, and p-toluenesulfonic acid monohydrate (97% wt., Fisher Scientific) was used to dope the material before carbonization and also as homogeneous catalysts. Triple-pressed stearic acid (95% wt., Legaquímicos) and isopropyl alcohol (99.90% wt., J.T. Baker) were used in the esterification tests. Solutions of 0.1 and 0.25 M NaOH (99% wt., PanReac AppliChem ITW Reagents) were prepared for ion exchange capacity measurement and acid value monitoring, respectively. Ethanol (99.5% wt., PanReac AppliChem ITW Reagents) and toluene (99.5% wt., PanReac AppliChem ITW Reagents) were used as solvents during acid value determination. Sulfuric acid (98% wt., PanReac AppliChem ITW Reagents), p-toluenesulfonic acid monohydrate (97% wt., Thermo Fisher Scientific), and methanesulfonic acid (70% wt., Fisher Scientific) were also used as homogeneous

catalysts during esterification. Commercial heterogeneous catalysts used in the comparative assessment of esterification were Amberlyst 15 (Dow Chem.), Amberlyst 35 (Dow Chem.), Amberlyst 70 (Dow Chem.), and Lewatit K 2629 (Lanxess). Some physicochemical properties of the assessed heterogeneous catalysts are reported in **Table 4-2**.

Table 4-2: Properties of the heterogeneous catalysts tested in the esterification of stearic acid with isopropanol (Dow Chemical Company, 2020; Lanxess Energizing Chemistry, 2011; Rohm & Haas, 2005; Rohm and Haas, 2006).

Catalyst	Amberlyst™ 15WET	Amberlyst™ 35WET	Amberlyst™ 70	Lewatit® K2629
Moisture (%)	52-57	51-57	53-59	50-55
BET surface area (m^2/g)	53	50	36	40
Average pore diameter (nm)	30	30	22	40
Total pore volume (cm^3/g)	0.40	0.35	Not reported	0.30

4.2.2 Methods

4.2.2.1 Preparation of Starbon® type materials

As the specification was not available, commercial cassava starch used as precursor was initially characterized to determine amylopectin and amylose content using an enzymatic method (i.e., K-AMYL 06/18) (Megazyme, 2018). High amylose corn (HACS) mesoporous carbons were synthesized according to a method reported in the literature for conventional Starbons® (Budarin et al., 2006; Mena, 2014). Initially, a defined amount of the HACS was added to deionized water in a 1:10 mass ratio, and the mixture was heated at 140°C under atmospheric pressure for 1 hour. Subsequently, the resulting gel was retrograded at 4 °C for 48 h. Later, a solvent exchange was done by adding tert-butyl alcohol up to 30% wt. in the mixture and *p*-toluenesulfonic acid (5% wt.) as a doping agent. Then, the material was freeze-dried at -107°C and 1 mbar to yield the expanded starch. Once obtained, the resulting material was carbonized at 450 °C (from 25°C to 170°C at 10 $K \cdot min^{-1}$), from 170°C to 400°C at 5 $K \cdot min^{-1}$ and from 400°C to 450°C at 1 $K \cdot min^{-1}$), under an inert atmosphere of nitrogen to enable suitable hydrophobicity/hydrophilicity characteristics for esterification reactions (Członka et al., 2018).

Cassava-based mesoporous carbon was synthesized following the route proposed as result of the optimization in previous chapters. Gels were synthesized stirring cassava starch in deionized water in a 1:10 mass ratio, for 1h at 110°C in a three-neck round-bottom flask using a half-moon overhead stirrer. The obtained gel was put in a freezer for its retrogradation at 4°C for 4 days. Subsequently, solvent exchange using ethanol was performed, 1:2 volume ratio of ethanol respect to the initial water was added to the gel, blended, and subsequently stirred magnetically at 500 rpm for 1h at room temperature. It was filtered under vacuum to remove water-ethanol solvent. New ethanol (1:2 vol.) was added, and the procedure was repeated. Five solvent exchanges were performed. Sample was then placed in a vacuum oven at 30°C for 24h. Dried material was doped using 5% wt. of p-TSA dissolved in a small volume of acetone as promotor of carbonization. Carbonization was executed at 450°C (from 25°C to 170°C at 10 $K \cdot min^{-1}$, from 170°C to 400°C at 5 $K \cdot min^{-1}$ and from 400°C to 450°C at 1 $K \cdot min^{-1}$), in a Thermo Scientific Lindberg/Blue Mini-Mite tubular oven. Herein, these Starbon® type materials are referred to as S450 for corn-based material, and CS450 for cassava-based carbon.

4.2.2.2 Functionalization

The obtained Starbon® type materials were sulfonated in concentrated sulfuric acid (98% wt. purity) in a ratio of 10:1 volume (ml) of acid to mass (g) of carbonized material at 80°C for 8 hours. The sulfonated material was washed several times with distilled water until sulphates were no longer detected in the washing water through a test with barium chloride. Finally, it was dried overnight in an oven at 100°C. The corresponding activated carbons are referred to as S450-SO3H for corn-based starch and CS450-SO3H for cassava-based material, respectively.

The complete preparation and functionalization protocol is schematically described in Figure 4-1.

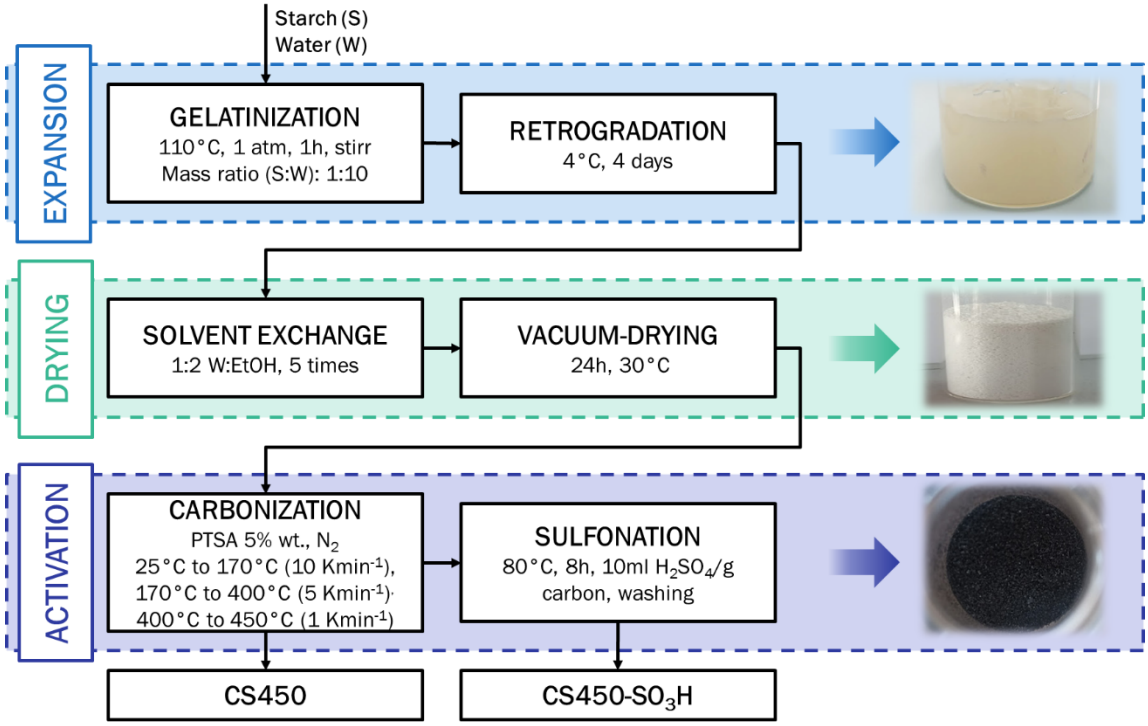

Figure 4-1. Cassava-starbon catalyst preparation methodology.

4.2.2.3 Determination of ion exchange capacity

The ion exchange capacity of sulfonated Starbons® and the other heterogeneous catalysts was determined by back titration by adding 1g of the dried material in a solution of NaOH 0.1 M and stirring for 5 hours at room temperature. Subsequently, the solution was filtrated to remove the catalyst and titrated to determine the final concentration. The ion exchange capacity of sulfonated Starbons® was also tested after their use as catalysts in esterification. In this case the catalysts were filtered out from the reactive medium, washed using anhydrous ethanol and dried until constant weight.

4.2.2.4 Characterization

The surface area and porosimetry of sulfonated Starbons® were determined by measurement of nitrogen adsorption isotherm at -195.5 °C using an ASAP 2020 V4.02 volumetric adsorption analyser (Micromeritics). Samples were degassed for 24 hours before absorption measurements. Data interpretation was done by the application of the multi-point Brunauer-Emmett-Teller (BET) equation and the pore size distribution was determined via the Barrett, Joyner, and Halenda (BJH) model. The morphology and pore structure of the solids were analysed by scanning electron microscopy (SEM) using FEI

Quanta 200 equipment. The catalyst sample was sputter-coated with a thin gold film, and micrographs were obtained at different magnifications (5000X, 10000X).

The nature of the organic groups in the carbon-based materials were characterized by Fourier-transform infrared spectra (FT-IR). In this case a Perkin Elmer FT-IR 1760 Spectrometer was used, and the spectra were measured in the wavenumber range from 4000 cm-1 to 500 cm−1. The thermal stability of the material was tested by thermogravimetric analysis (TGA). The analysis was conducted using a Mettler Toledo TGA 1/SF/1100/268, and a 4.5 mg sample was used in all tests. The operation was performed from 30 to 1000 ºC at a heating rate of 10 ºC·min-1 under nitrogen atmosphere.

4.2.2.5 Esterification tests

Esterification of stearic acid with isopropyl alcohol (1:2 molar ratio) was carried out at 70°C and atmospheric pressure for 5 hours. The reaction was carried out in a 200 ml jacketed three-necked glass reactor under total reflux, connected to a 200 mm 19/26 Graham condenser, and stirred with a teflon-coated magnet at 450 rpm (Figure 4-2).

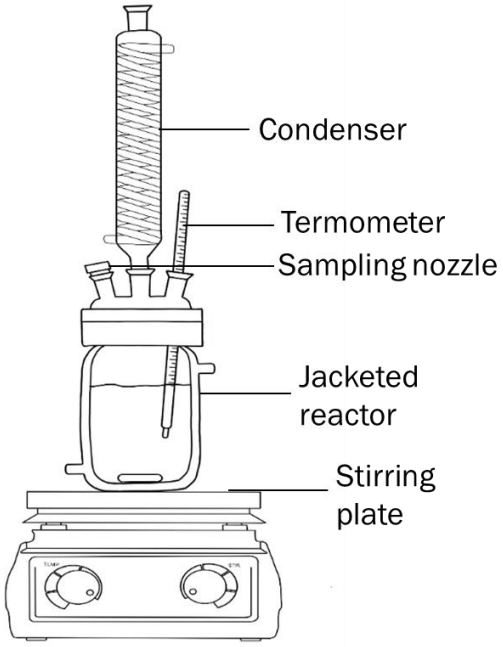

Figure 4-2. Scheme of reactor for esterification tests.

Initially, preliminary experiments were carried out with H_2SO_4 as a benchmark catalyst. It is the most typical homogeneous catalyst used in industrial esterification at loadings of 0.5% wt. and 1% wt. with respect to the stearic acid. Subsequently, esterification experiments with all other catalysts were done using the same number of acid equivalents to a 1% wt. sulfuric acid loading. Acid equivalents were calculated considering the corresponding ion exchange capacity of the solid catalysts. The reaction was followed by taking samples from the reactor at different time intervals using a preheated pipette to avoid stearic acid solidification during sampling. Collected reaction samples were characterized by measuring acid value (AV) according to ISO 660 E (International Organization for Standatization, 2009). Reaction conversion (X) along time was determined with Equation 4.1

$$X = \frac{AV_0 - AV}{AV_0} \quad (4.1)$$

Here, AV_0 is the initial acid value of the triple pressed stearic acid (207.11 mg KOH/g sample), and AV is the acid value of the reaction sample on an alcohol- and water-free basis. In the particular case of commercial ion exchange resins, prior use they were washed with EtOH in a stirred glass container for 2 h using a volumetric ratio EtOH/resin of 4:1, and the washing process was repeated three times. Subsequently, the catalysts were rinsed with deionized water, filtered, and dried under vacuum at 60°C until constant weight. The dry materials were stored in dark and hermetic containers within a desiccator before use.

4.3 Results and discussion

4.3.1 Characterization of biobased activated carbons

Based upon the initial characterization of the commercial cassava starch, it was found that it contains 20.7% wt. amylose and 79.3% wt. amylopectin. This represents a challenge because high amylose starches are preferred for Starbon® synthesis (Budarin et al., 2006; Clark et al., 2008; White et al., 2009). Nevertheless, it has been reported that low amylose starches could also be used as feedstock, but they generally produce activated carbons with lower pore diameters and surface areas (Brouwer, 2017; Uriburu-Gray et al., 2020). In this regard, the corresponding nitrogen adsorption isotherms for high amylose corn-based (S450) and cassava-based (CS450) carbons are presented in Figure 4-3A.

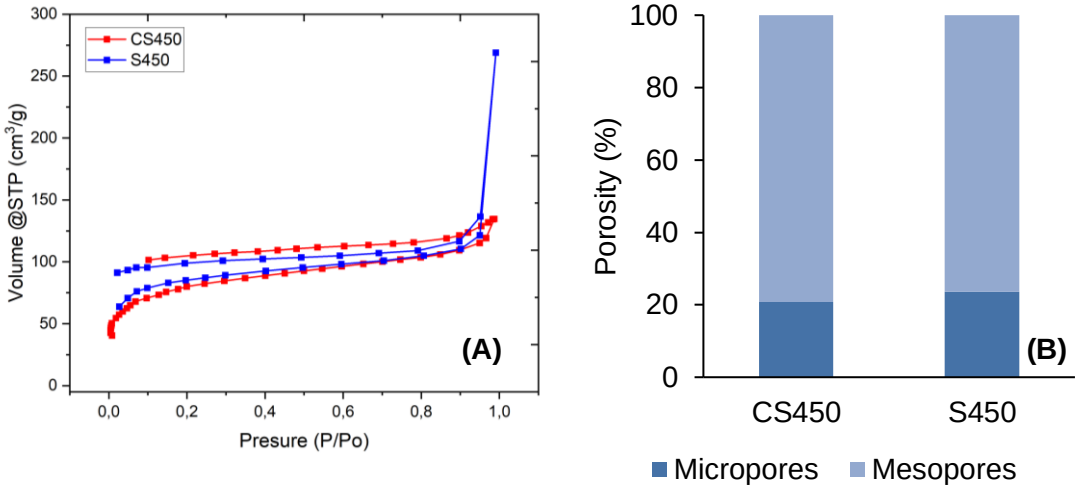

Figure 4-3. Nitrogen adsorption isotherms (A) and porosity histogram (B) for sulfonated cassava-based (CS450-SO_3H) and corn-based (S450-SO_3H) carbon materials.

As observed, isotherms of both Starbon®-type materials can be classified as type II, with a H3-type hysteresis. This behaviour reveals a mixed microporous-mesoporous structure of slit-shaped pores, which is typical for this type of carbons (Leofanti et al., 1998). Both materials exhibited a wide pore distribution, being predominantly mesoporous (Figure 4-3B). Conventional Starbon® from HACS exhibited a BET surface area of 281 m^2g^{-1}, with an average BJH pore size of 5.2 nm and a pore volume of 0.36cm^3g^{-1}, while cassava-Starbon® exhibited a surface area of a surface area of 263 m^2g^{-1}, with an average BJH pore size of 3.7nm and a total pore volume of 0.20 cm^3g^{-1}. The complete set of results from the surface and porosity analysis are presented in Table 4-3.

Table 4-3: Surface area and porosity of assessed sulfonated corn-based (S450-SO_3H) and cassava-based (CS450-SO_3H) carbons catalysts.

Property	S450-SO_3H	CS450-SO_3H
BET surface area /m^2g^{-1}	281	263
BJH average pore diameter /nm	5.2	3.7
Micropore content /cm^3g^{-1}	0.08	0.04
Total pore volume /cm^3g^{-1}	0.36	0.20

The morphology and particle sizes for CS450-SO_3H and S450-SO_3H can be observed on the SEM micrographs of Figure 4-4.

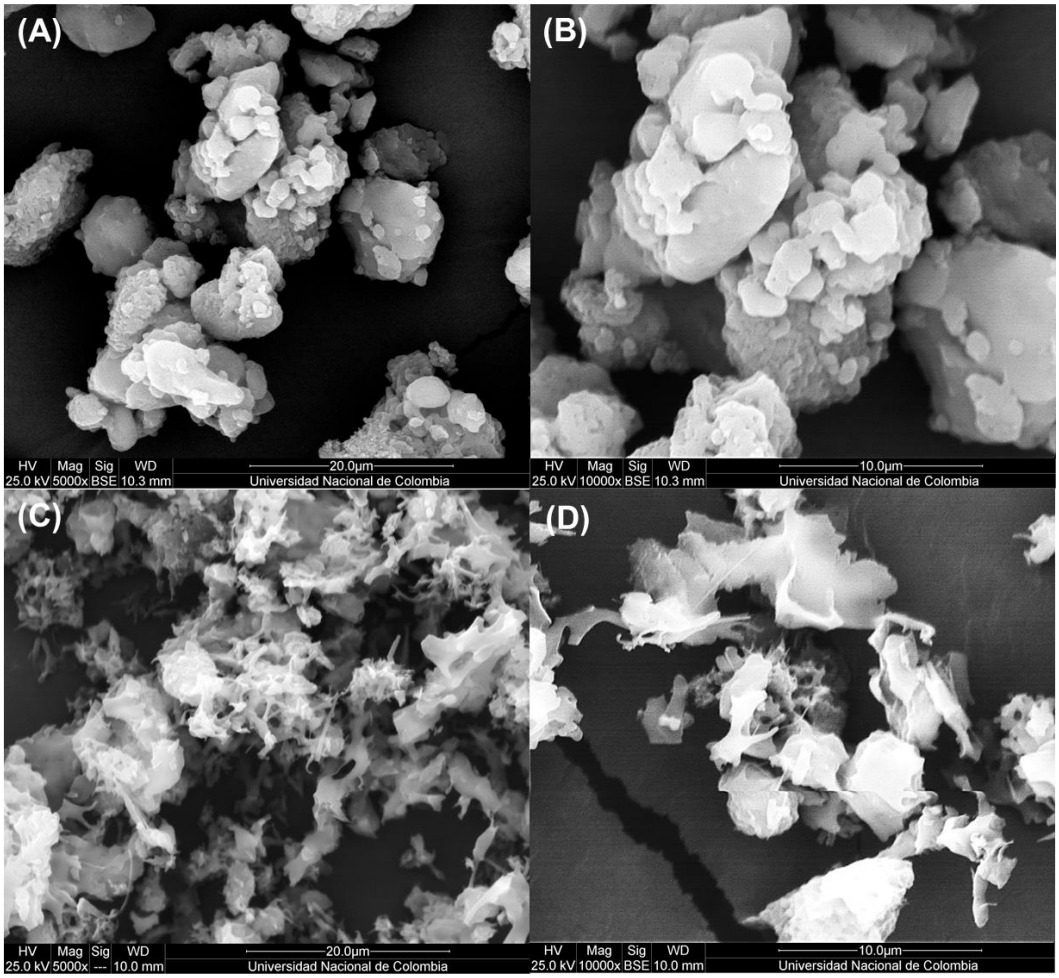

Figure 4-4. SEM micrographs obtained at different magnifications (5000X left and 10000X right) for S450-SO3H (A, B) and CS450-SO3H (C, D)

For HACS-based Starbon® (Figure 4-4A and Figure 4-4B), the particle morphology preserves the granulated form of the starting starch, whereas, in the case of the Cassava Starbon® (Figure 4-4C and Figure 4-4D), the granular shape completely disappeared. Considering the scaffolding action of amylose, its lower content in cassava generated a lack of supporting action causing the collapse of the gel structure during the solvent exchange and drying process. This collapse generated a filament- and sponge-like material with a lower surface. Subsequent sulfonation of such a weak structure probably generated additional damage and degradation of the material. Then, it is expected for CS450-SO_3H catalysts to have issues of reduced mechanical strength and lower recoverability after reaction due to erosion. Additionally, the particle size from SEM images for S450-SO3H is estimated in the range of 12-20 µm, and the formation of agglomerates will lead to a more

stable material in comparison with CS450-SO3H, whose particle size varies from 4 to 18 µm.

FT-IR spectra of CS450-SO_3H and S450-SO_3H are presented in Figure 4-5. The one corresponding to CS450 is also included to enable identifying alterations occurred in the material after sulfonation. In all cases, the broad band at the range of 3200-3600 cm^{-1} is attributable to the O-H stretching vibrations (Silverstein & Webster, 1996) arising from carboxylic acids, the hydroxy groups from the original saccharides present in the starch-based material. Also, this broad band comes from the hydroxyls in phenolic groups formed during the carbonization of the starch precursor, and from adsorbed water (Chen & Fang, 2011). Notably, both CS450-SO_3H and S450-SO_3H exhibit a distinct peak at 1024 cm^{-1}, which corresponds to the vibrational mode of SO3- groups (Silverstein & Webster, 1996), confirming the successful acidification of the material. This is also verified by the large increase around 1150 cm^{-1}, which correspond to S=O groups. Vibrational bands associated with carbonyl C=O and C=C stretching vibrations assigned to 1705 cm^{-1} and 1600 cm^{-1}, respectively (Silverstein & Webster, 1996), are observed in all three materials. Furthermore, peaks at 1456 cm^{-1} correspond to the C-C skeleton stretching vibrations of aromatic rings (Silverstein & Webster, 1996). All these are typical characteristics of sulfonated carbons.

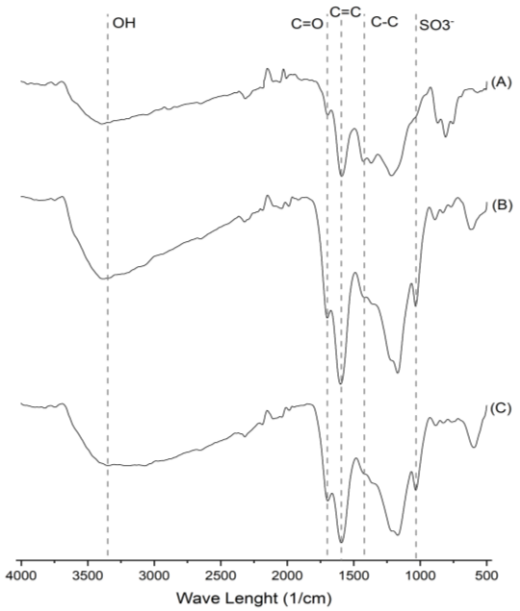

Figure 4-5. FT-IR spectra for CS450 (A), CS450-SO3H (B) and S450-SO3H (C)

The corresponding ion exchange capacities of the different assessed catalysts are reported in Table 4-4. Despite the values for the commercial ion exchange resins are reported in the technical data sheets, they were measured on a dry basis for confirmation and comparison purposes. As observed, the sulfonation of the starch-based materials was less effective in the case of the cassava catalysts. As the gel structure collapsed during the synthesis of CS450-SO_3H, there were less stable anchoring sites for the sulfonic groups within the mesoporous structure. Besides, even if produced, sulfonic groups were most probably bonded to structures that detached from the solid during the sulfonation process and were leached during the rinsing step.

Table 4-4. Ion exchange capacity of assessed heterogeneous catalysts

Catalyst	Exchange capacity – dry basis (Eq H^+/kg)
Amberlyst 15	4.56
Amberlyst 35	3.85
Amberlyst™ 70	2.78
Lewatit® K2629	4.33
S450-SO_3H	2.31
CS450-SO_3H	1.64

4.3.2 Reaction tests

As a preliminary assessment of the process, kinetic profiles during the esterification of stearic acid with isopropanol using H_2SO_4 as catalyst are presented in Figure 4-6. For comparison purposes, these profiles were obtained with catalysts loading of 0% (i.e. self-catalytic), 0.5% and 1% wt. with respect to stearic acid. As observed, using H_2SO_4 as catalyst, the reaction reaches equilibrium condition in 5 h of reaction. Comparatively, the uncatalyzed reaction remains below a 4% conversion during the same period. To obtain a quantitative indicator, reaction rates were calculated at time zero with respect to the acid equivalents of the catalyst. This enabled to verify an increase in the turnover frequency (TOF) from 0.49 to 0.79 mol/s H^+Eq when changing from 0.5 to 1% wt. H_2SO_4 loading, and those were one or two orders of magnitude higher than the corresponding for the self-catalytic reaction.

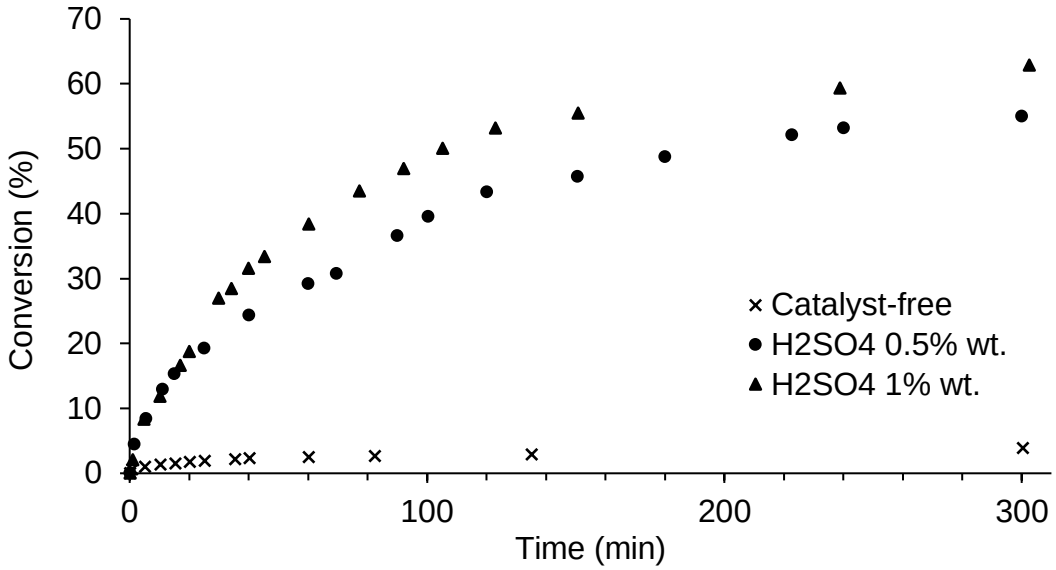

Figure 4-6. Effect of H_2SO_4 catalyst loading on the esterification of stearic acid (SA) with isopropyl alcohol (IPA) (T=70°C, molar ratio 1:2 SA/IPA)

This behavior was similar to that observed in the synthesis of isopropyl myristate (de Jong et al., 2009), so the self-catalytic effect could be neglected at the assessed temperature when using H_2SO_4 as catalyst. Despite a higher loading could be used, it has been reported that industrial esterification of fatty acids is carried out with H_2SO_4 up to 1% wt. to avoid product darkening and equipment corrosion (Markley, 1983). Then, subsequent experiments with other homogeneous and heterogeneous catalysts were carried out using the same acid equivalents of a 1% wt. H_2SO_4 loading. The required amount of each catalyst was determined based on the corresponding ion exchange capacities reported in Table 4-4. The kinetic profiles during the esterification of stearic acid with isopropyl alcohol using the different assessed catalysts are presented in Figure 4-7.

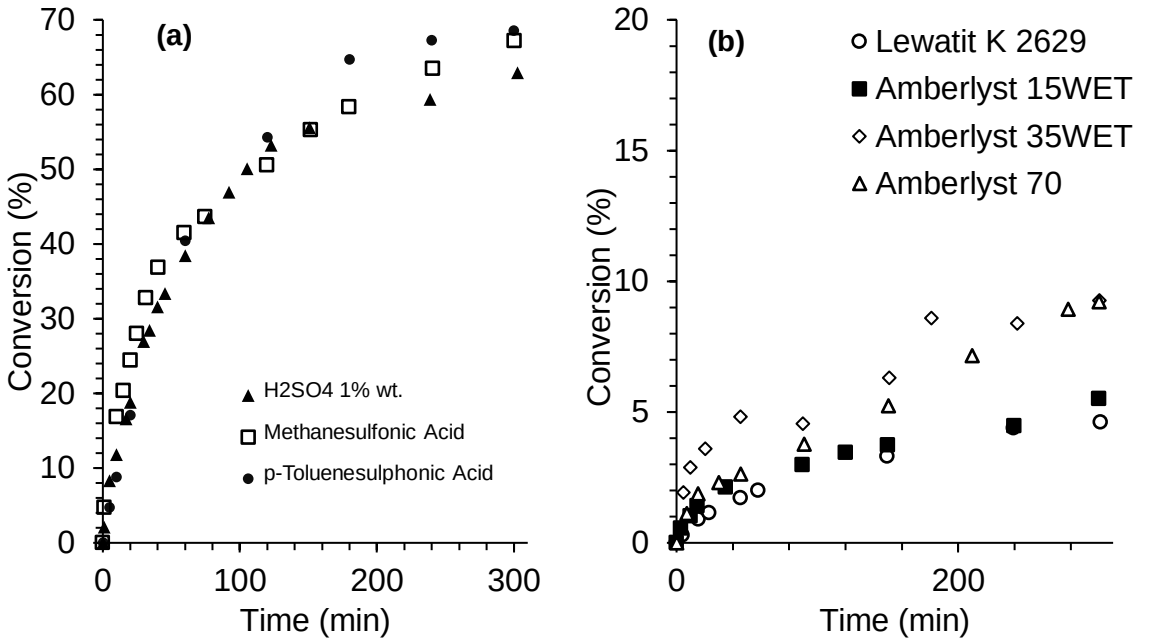

Figure 4-7. Kinetic profiles during esterification of stearic acid (SA) with isopropanol (IPA) (T=70°C, molar ratio 1:2 SA/IPA) using homogeneous (a) and heterogeneous commercial (b) catalysts. Catalyst loading corresponding to acid equivalents of H_2SO_4 at 1% wt. with respect to fatty acid

As expected, all homogeneous catalysts enabled to obtain higher reaction rates and conversions. Interestingly, methanesulfonic acid (MSA) enabled similar and slightly better results in comparison to H_2SO_4, but with lower colour degradation in the final product. This can be related to a lack of affinity of H_2SO_4 for the mostly organic reactive media, which could allow only a partial dissociation of the second proton in sulfuric acid, thus reducing their catalytic activity. In comparison, MSA and *p*-Toluene sulfonic acid contain an organic structure with a better affinity for the reactive media (i.e. fatty acid and alcohol), and they can dissociate their only proton. The corresponding TOF of MSA and *p*-Toluene sulfonic acid, calculated with respect to the initial reaction rate, were 0.47 and 0.49 mol/s H^+Eq, respectively.

Comparatively, commercial macroreticular ion exchange resins showed very poor catalytic activity in reaction. In this case, all resins enabled to obtain only slightly better results than the self-catalytic process, with conversions below 10% in 5 h, and TOFs below 0.05 mol/s H^+Eq. This result has been previously observed in the esterification of fatty acids (de Jong et al., 2009; Yalçinyuva et al., 2008), and similar to those reports, no pore diffusion limitation

was expected to hinder reaction rates considering that pore openings lie within the mesoporous region. Then, the poor catalytic activity was related to the selective absorption of produced water preventing reagents from accessing the active sulfonic groups. Also, a slight shrinking effect of the polymeric matrix can occur when put in contact with organic compounds, and this might induce a steric hindrance for the adsorption/desorption of the long alkyl chain fatty acid into the active sites of the catalysts.

As observed in Figure 4-8, corn-based sulfonated Starbon® (S450-SO_3H) showed the best performance among the assessed heterogeneous catalysts. The reaction rate was three times higher due to the available surface area, which is considerably larger than the obtained for other macroporous commercial resins. Additionally, the pore diameter profile of the material allows the fatty acid molecules to reach active sites. Correspondingly, the TOF for this catalyst was 0.08 mol/s H^+Eq. On the other hand, the performance obtained by using the sulfonated cassava Starbon (CS450-SO_3H) on reaction is still poor and similar to the obtained using the tested ion exchange resin. Nonetheless, the TOF for CS450-SO_3H was higher than the obtained for the other heterogeneous catalysts (i.e. 0.15 mol/s H^+Eq). This indicates that while activity is good, further explorations are required to improve the structural stability of cassava-based Starbons.

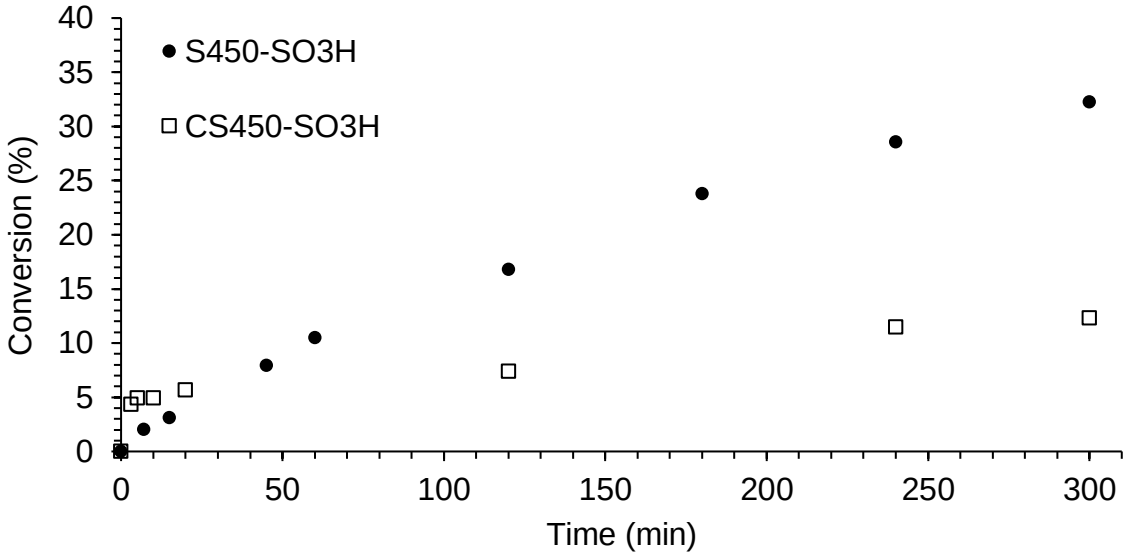

Figure 4-8. Kinetic profiles during esterification of stearic acid (SA) with isopropanol (IPA) (T=70°C, molar ratio 1:2 SA/IPA) using corn- (S450-SO_3H) and cassava-based (CS450-SO_3H) catalysts

The corresponding results of the thermogravimetric analysis (TGA) of the sulfonated materials is presented in Figure 4-9. Both, S450-SO3H and CS450-SO3H, exhibited an initial stage of moisture elimination from room temperature to 100°C (10.98% and 14.43%, respectively). The residual dry weight of both samples remained constant until reaching 200°C. Subsequently, in the temperature range of 200°C to 1000°C, the loss of mass is associated with the degradation of organic compounds on the surface of the material and the formation of aromatic rings. Upon reaching a temperature of 1000°C, a substantial transformation of the samples into a carbonaceous structure was observed. Specifically, for S450-SO3H, 56.81% of the dry mass remained after thermal treatment, while for CS450-SO3 it remained 55.13% of the original material. These results indicate that the catalysts could be used in reactions up to 200°C in order to preserve the sulfonic groups in the surface, the hydrophilic-hydrophobic ratio and the mechanical structure of the materials.

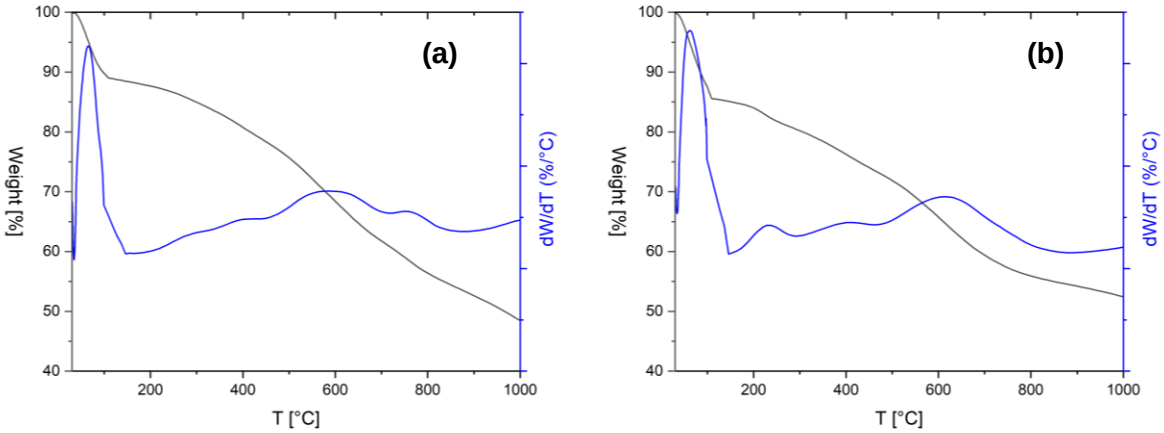

Figure 4-9. TGA and DTG curves for S450-SO3H (A) and CS450-SO3H (B).

In order to assess the potential reusability of the Starbon® type catalysts, the acidity of the sulfonated materials was measured after the esterification process. The corresponding acidity decreased to 2.26 Eq H^+/kg in the case of S450-SO3H (a reduction of 2.25%) and to 1.59 Eq H^+/kg in the case of CS450-SO3H (a reduction of 3.11%). These slight reductions indicate that the materials remained relatively stable and that they could be used in further reaction cycles. Nevertheless, only the corn-based material (i.e. S450-SO3H) seems suitable for further exploration, and the synthesis procedures could be further optimized to enhance the performance in the esterification of fatty acids.

4.4 Conclusions

Starbon®-type activated carbons were produced using HACS and cassava starches as feedstock and they were activated via sulfonation for catalytic purposes. The obtained materials exhibited a highly mesoporous structure with average pore diameters above 8 nm. The area and pore volume of the cassava-based catalysts (CS450-SO_3H) was lower (263 m^2/g, 0.2 cm^3/g) than for the corn-based (S450-SO_3H) (281 m^2/g, 0.4 cm^3/g), the pore volume was lower (0.22 cm^3/g). Based upon the SEM characterization, it was verified that the S450-SO_3H activated carbon retained the mesoporous structure of the gelled starch while the CS450-SO_3H material collapsed. This was related to the lower content of amylose that affected the stability of the gel structure after the solvent exchange, drying and carbonization. Also, sulfonation was less effective in the cassava material mainly due to the lack of stable anchoring points that leached during the rinsing process. This resulted in an ion exchange capacity of 1.64 Eq H^+/kg which was lower in comparison with the corn-based catalysts (2.31 Eq H^+/kg). After a further evaluation of the synthesized catalysts in the esterification of stearic acid with isopropanol, it was found that S450-SO_3H enabled higher rates of reaction than more commercial ion exchange resins. Nonetheless, they were still well below most typical homogeneous catalysts, in particular methanesulfonic acid which exhibited the best performance in reaction. In the case of the CS450-SO_3H catalyst, it exhibited slightly better performance than all heterogeneous catalysts, but its activity was much lower in comparison with the conventional Starbon® catalyst. The thermal analysis of the materials suggests a similar stability for S450-SO_3H and CS450-SO_3H, which can be used in reactions up to 200°C. Additionally, there was no significant decrease on the acidity of the materials after their use in reaction (~ 3%). Results indicate that while CS450-SO_3H has a high TOF compared with other heterogeneous catalysts, there is a need for further improve the synthesis of the cassava-based material, mainly focusing on preserving the gel structure and the sulfonation process and to enhance the activity for fatty acids esterification.

5. Conclusions and perspectives

5.1 Conclusions

This research endeavors to advance the synthesis of Starbon® material using cassava starch as a locally abundant and sustainable precursor in Colombia, thus aligning with the principles of circular economy and green chemistry. The experimental phase unfolded in three segments. Initially, the conventional synthesis method, as reported by Budarin and colleagues (2006), was implemented using Colombian cassava starch. However, the resulting samples lacked the expected porosity and surface area due to the high-amylose nature of the reported methodology, which did not suit the low-amylose content (20.75% wt.) of Colombian cassava starch. To overcome this challenge, a meticulous exploration of gelatinization, retrogradation, solvent exchange, and carbonization conditions was conducted.

In case of gelatinization, the results suggested that the best conditions are related to the use of a 1:10 mass ratio at temperatures between 90°C and 110°C, as lower temperatures lead to incomplete dispersion of starch network and higher temperatures could promote the amylopectin depolymerization also destroying the network. Subsequently, retrogradation was found to produce a pore shrinkage due to the increase of organization of molecules during the cooling. Particularly for cassava starch, samples retrograded longer times resulted in lower surface areas, so shorter retrogradation times are desirable. Regarding solvent exchange, two methods were assessed, and it was interestingly found that the use of each method conducted to materials with different surface properties. Ethanol and vacuum oven utilization produced materials with higher pore sizes, while freeze-drying and TBA led to smaller pores with higher surfaces. During carbonization, the use of an acid precursor proved effective in preserving the material's porous structure. Additionally, it was found that at 300°C the produced porosity was nulled by the carbonization process and higher synthesis temperatures were needed for obtaining porous materials from cassava.

The optimized conditions for cassava-derived Starbon® synthesis included a gelatinization mass ratio of 1:10, a gelatinization temperature of 110°C and a carbonization at 450°C, supported by both factorial and Box-Behnken designs. The resulting cassava-derived Starbon® exhibited notable surface area (263 m^2/g), pore volume (0.2 cm^3/g), and pore sizes (4 nm) at 450°C with ethanol solvent exchange. While these properties fell short of the capabilities of conventional Starbon® materials, the methodology proved successful, especially considering the low amylose content of the cassava precursor.

Furthermore, sulfonation was employed for the use of the synthesized starch for catalytic purposes, for the esterification of long chain fatty acids. However, although the cassava-Starbon® catalysts (CS450-SO3H) exhibited an ion exchange capacity of 1.64 Eq H+/kg, the cassava material demonstrated slightly better catalytic performance than other heterogeneous catalysts in the esterification of stearic acid with isopropanol, therefore being susceptible to improvements.

In conclusion, this research provides valuable insights into the synthesis and optimization of cassava-derived Starbon® materials. The adapted methodology showcases its applicability to low-amylose starches, contributing to the utilization of agricultural waste in Colombia. Additionally, the proposed methods result in an easier and cheaper route for the production of Starbon® materials which can be implemented without the requirement of complex equipment. The comprehensive exploration of experimental variables and statistical analyses offers a robust foundation for further advancements in catalytic applications, fostering sustainability in the Colombian agro-industry. Nevertheless, the material still is susceptible to modifications and improvement for making it suitable for catalyzing esterification reactions.

5.2 Perspectives

For a better understanding, the cassava-derived Starbon® prepared and sulphonated under the conditions previously defined could be assessed as catalyst for different reactions with smaller molecules to understand the cause of their poor performance in the esterification of isopropanol. Additionally, changes in the reaction conditions such as increasing the

amount of alcohol used in the esterification can lead to higher conversions and a better understanding of the catalyst.

Moving forward, there is a need for continuous refinement of the synthesis process to enhance the porosity and surface characteristics of cassava-derived Starbon®. This involves exploring additional factors influencing the synthesis, such as variations in the solvent exchange method by changing the amount of EtOH used or preparing the starch gel directly in TBA.

Regarding the lack of available information for the prediction of gels formation or surface properties, mathematical and computational modelling of the behaviour of porosity for different starch and stages is needed for promoting the use of this material.

On the other hand, while cassava starch has proven to be a viable precursor, future research could investigate the use of other local starches such as canna starch. Exploring a variety of precursors may provide opportunities to develop Starbon® materials with diverse properties, catering to specific applications in catalysis or other fields.

Additionally, scaling up the synthesis process for cassava-derived Starbon® is crucial for practical applications and industrial adoption. Investigating the feasibility of large-scale production, cost-effectiveness, and reproducibility will be essential for integrating this material into industrial processes.

A. Appendix: BET modification for the determination of surface area in materials with Type III isotherm

Typically, for mesoporous materials, BET surface area is calculated through the use of the following equation:

$$\frac{1}{W\left[\frac{P}{P_0}-1\right]}=\frac{1}{W_m C}+\frac{C-1}{W_m C}\left[\frac{P}{P_0}\right] \qquad (A.1)$$

Where P_0 is the relative pressure at which a monolayer is formed on the material's surface, P is the adsorption pressure, W correspond to the weight of N_2 adsorbed, W_m refers to the adsorb weight in a monolayer, and C is a constant determined from the slope of the isotherm in the monolayer region.

Therefore, when $1/W[P_0/P -1]$ is plotted vs. P/P_0, it will yield to a straight line, where the slope m and intercept i are, respectively:

$$s=\frac{C-1}{W_m C} \qquad (A.2)$$

$$i=\frac{1}{W_m C} \qquad (A.3)$$

C and Wm can be obtained through equations A.2 and A.3. Then, the total surface area can be calculated as:

$$S_{BET}=\frac{W_m N_A A_X}{MW} \qquad (A.4)$$

Where Ax is the cross-sectional adsorbate area, MW is the adsorbate molecular weight, and N_A is Avogadro's number. This method is applicable in the range of P/P_0 of 0.05 to 0.3.

When type III isotherm is presented, the BET surface method should be corrected. This is noticed when C constant is lower than 2 (C<2). In those cases, $W=W_m$, and $(P/P_0)_m$ need to be estimated as:

$$\left(\frac{P}{P_0}\right)_m = \frac{\sqrt{C}-1}{C-1} \qquad (A.5)$$

At this monolayer relative pressure, the adsorbed weight in monolayer is obtained from raw data and used in equation A.4 for the determination of BET surface (Lowell et al., 2004)

B. Appendix: Statistical analysis supports

Statistical analysis presented in Chapter III were validated. Verification of normality was performed for result variables of factorial and Box-Behnken experimental designs.

3^2 Factorial Experimental Design

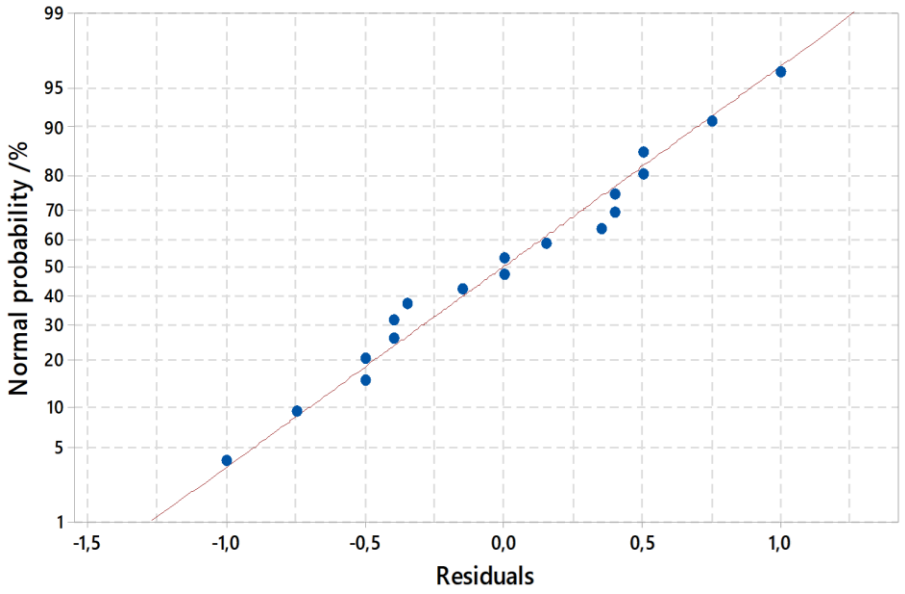

Figure B-1. Normal plot of residuals for Area BET results in factorial 3^2 experimental design.

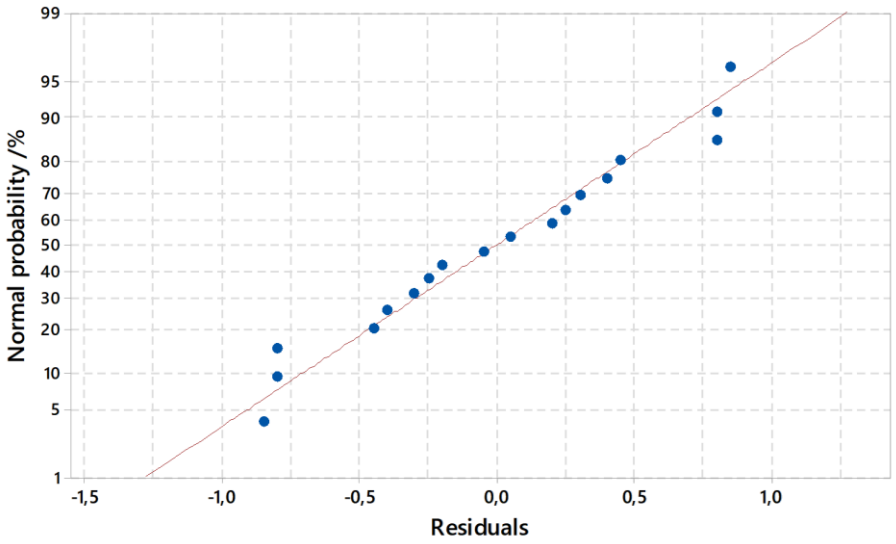

Figure B-2. Normal plot of residuals for pore size results in factorial 3^2 experimental design.

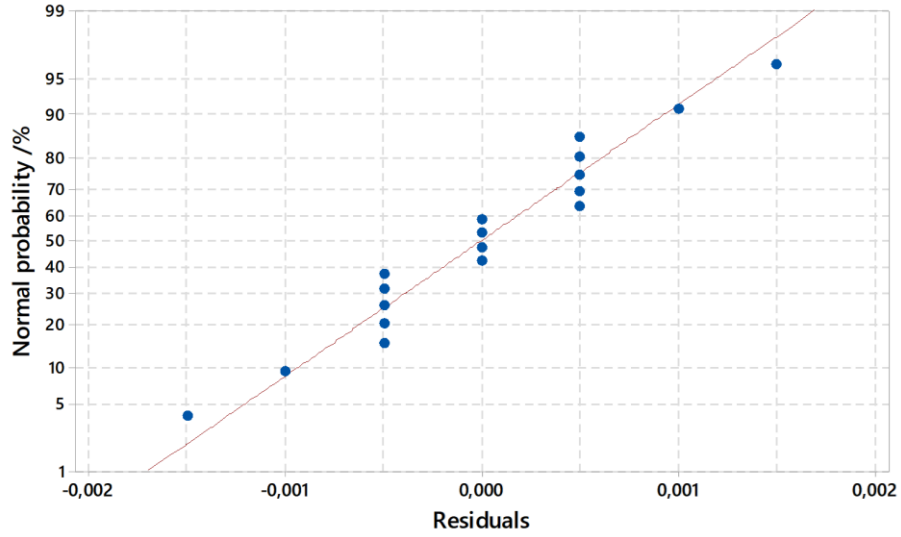

Figure B-3. Normal plot of residuals for pore volume results in factorial 3^2 experimental design.

According to normal probability plots presented in Figure B-1, Figure B-2 and Figure B-3, most of the values for surface area, pore size and pore volume are located over the normal probability line. Therefore, validating that data follow a normal distribution. Shapiro-Wilk test was performed to verify the assumption with a significant level of 0.05. P-values were found to be 0.299, 0.872 and 0.600 for surface area, pore size and pore volume respectively. As

p-value is higher than the significance level defined, there is no evidence to reject the H_0 and the data fits a normal distribution.

Box-Behnken Experimental Design (BBD)

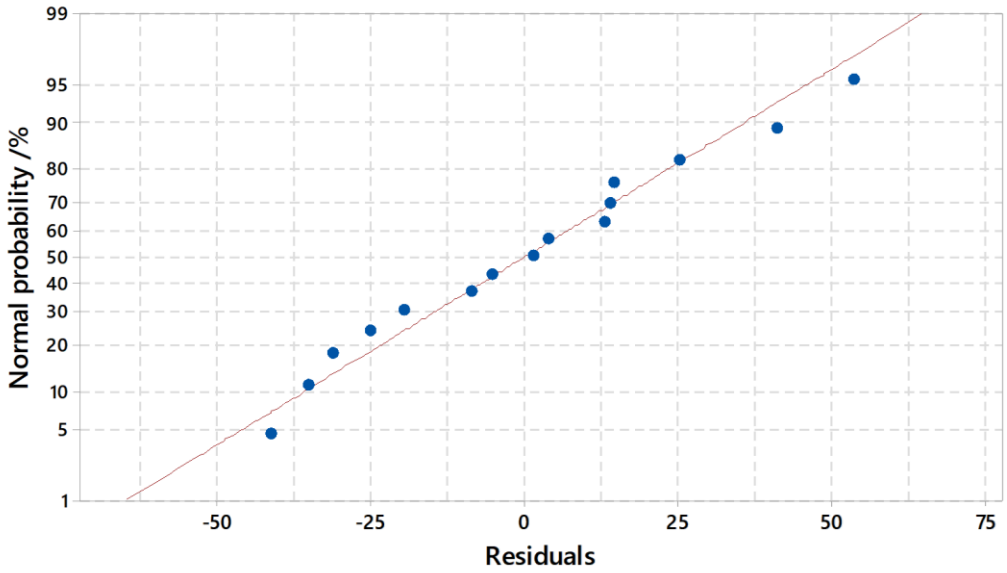

Figure B-4. Normal plot of residuals for Area BET results in BBD experimental design.

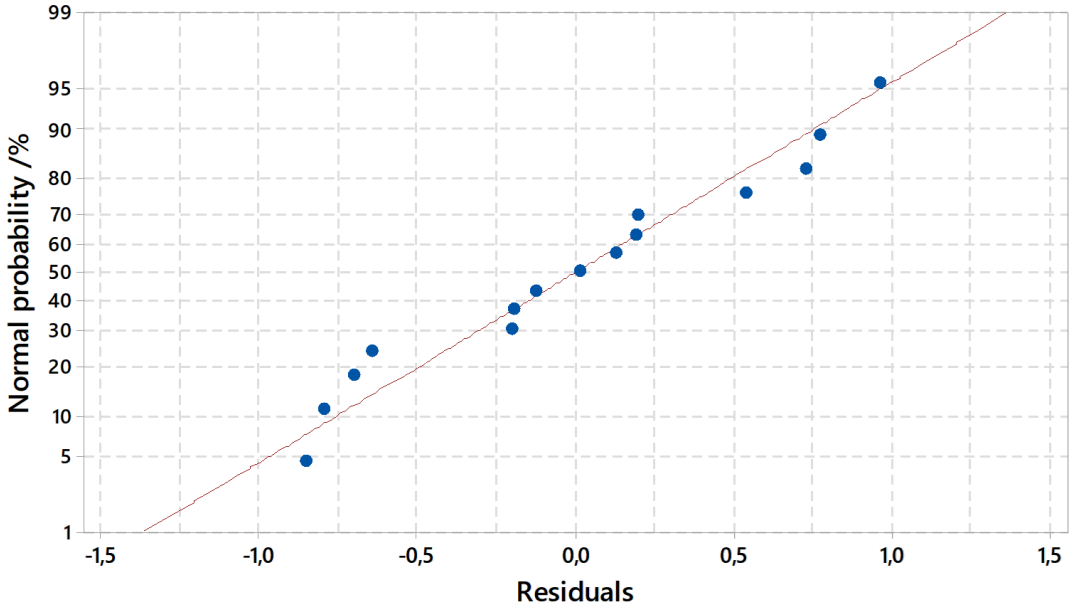

Figure B-5. Normal plot of residuals for pore size results in BBD experimental design.

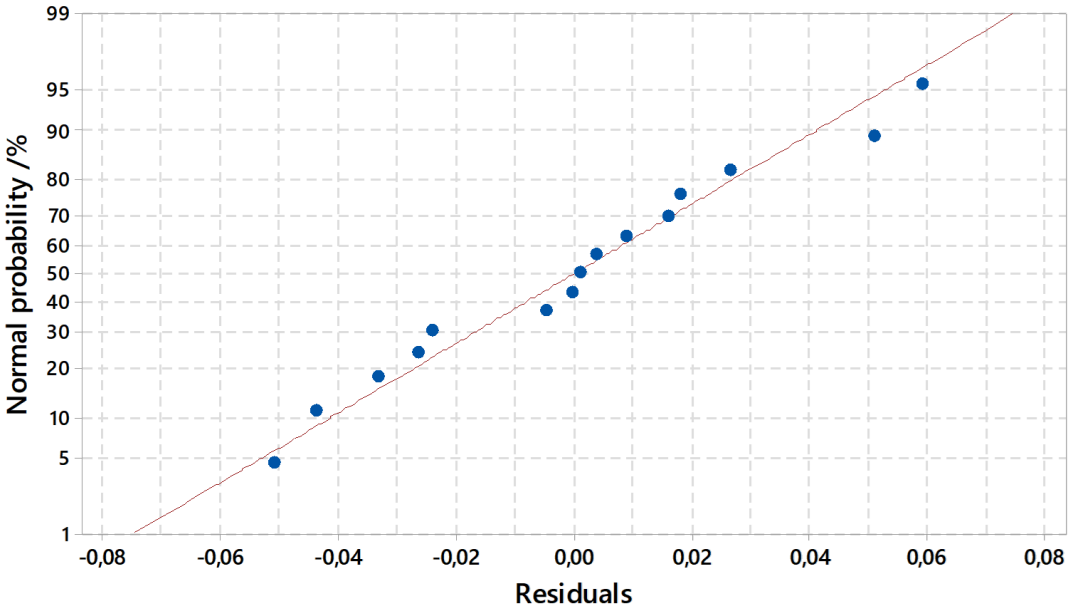

Figure B-6. Normal plot of residuals for pore volume results in BBD experimental design.

According to normal probability plots presented in Figure B-4, Figure B-5 and Figure B-6, most of the values for surface area, pore size and pore volume are located over the normal probability line, validating that data follow a normal distribution. Shapiro-Wilk test was performed to verify the assumption with a significant level of 0.05. P-values were found to be 0.012, 0.032 and 0.026 for surface area, pore size and pore volume respectively. As p-value is higher than the significance level defined, there is no evidence to reject the H_0 and the data fits a normal distribution.

References

Aldana, A., Lartundo, L., Gómez, R., & Niño, M. (2012). Sulfonic groups anchored on mesoporous carbon Starbons-300 and its use for the esterification of oleic acid. *Fuel*, *100*, 128–138. https://doi.org/10.1016/j.fuel.2012.02.025

Auer, E., Freund, A., Pietsch, J., & Tacke, T. (1998). Carbons as supports for industrial precious metal catalysts. *Applied Catalysis A: General*, *173*(2), 259–271. https://doi.org/10.1016/S0926-860X(98)00184-7

Bazuła, P., Lu, A. H., Nitz, J., & Schüth, F. (2008). Surface and pore structure modification of ordered mesoporous carbons via a chemical oxidation approach. *Microporous and Mesoporous Materials*, *108*(1–3), 266–275. https://doi.org/10.1016/j.micromeso.2007.04.008

Bekyarova, E., & Kaneko, K. (2000). Structure and physical properties of tailor-made Ce,Zr-doped carbon aerogels. *Advanced Materials*, *12*(21), 1625–1628. https://doi.org/10.1002/1521-4095(200011)12:21<1625::AID-ADMA1625>3.0.CO;2-9

Biliaderis, C., Page, C., Slade, L., & Sirett, R. (1985). Thermal Behavior of Amylose-Lipid Complexes. *Carbohydrate Polymers*, *55*, 367–389.

Bokhari, A., Chuah, L., Michelle, L., Asif, S., Shahbaz, M., Akbar, M., Inayat, A., Jami, F., Naqvi, S., & Yusup, S. (2019). Microwave enhanced catalytic conversion of canola-based methyl ester: Optimization and parametric study. In *Advanced Biofuels: Applications, Technologies and Environmental Sustainability*. Elsevier Ltd. https://doi.org/10.1016/B978-0-08-102791-2.00006-4

Borges, M. E., & Díaz, L. (2012). Recent developments on heterogeneous catalysts for biodiesel production by oil esterification and transesterification reactions: A review. *Renewable and Sustainable Energy Reviews*, *16*(5), 2839–2849. https://doi.org/10.1016/j.rser.2012.01.071

Borisova, A., De Bruyn, M., Budarin, V., Shuttleworth, P., Dodson, J., Segatto, M., & Clark, J. (2015). A Sustainable freeze-drying route to porous polysaccharides with tailored hierarchical meso- and macroporosity. *Macromolecular Rapid Communications*, *36*(8), 774–779. https://doi.org/10.1002/marc.201400680

Bosley, J. (1997). Turning upases into industrial biocatalysts. *Biochemical Society Transactions*, *25*(1), 174–178. https://doi.org/10.1042/bst0250174

Brouwer, T. (2017). *Determining the influence of the starch amylose content on the mesoporosity of starbons* (Issue September 2016) [Wageningen University].

https://edepot.wur.nl/409082

Budarin, V., Clark, J., Hardy, J., Luque, R., Milkowski, K., Tavener, S., & Wilson, A. (2006). Starbons: New starch-derived mesoporous carbonaceous materials with tunable properties. *Angewandte Chemie - International Edition*, *45*(23), 3782–3786. https://doi.org/10.1002/anie.200600460

Budarin, V., Clark, J., Luque, R., & Macquarrie, D. (2007). Versatile mesoporous carbonaceous materials for acid catalysis. *Chemical Communications*, *6*, 634–636. https://doi.org/10.1039/b614537j

Budarin, V., Clark, J., Luque, R., Macquarrie, D., Koutinas, A., & Webb, C. (2007). Tunable mesoporous materials optimised for aqueous phase esterifications. *Green Chemistry*, *9*(9), 992–999. https://doi.org/10.1039/b704055e

Budarin, V., Clark, J., Luque, R., Macquarrie, D., Milkowski, K., & White, R. (2007). *Carbonaceous materials* (Patent No. WO 2007/104798 A2).

Budarin, V., Luque, R., Macquarrie, D., & Clark, J. (2007). Towards a bio-based industry: Benign catalytic esterifications of succinic acid in the presence of water. *Chemistry - A European Journal*, *13*(24), 6914–6919. https://doi.org/10.1002/chem.200700037

Canales, N., & Trujillo, M. (2021). The value chain of cassava and its potential in the bioeconomy of Colombia [in Spanish]. In *Stockholm Environment Institute*. https://cdn.sei.org/wp-content/uploads/2021/05/workingpaperyucabioeconomia-canalestrujillo-mayo21.pdf

Chandane, V., Rathod, A., Wasewar, K., & Sonawane, S. (2017). Response Surface Optimization and Kinetics of Isopropyl Palmitate Synthesis using Homogeneous Acid Catalyst. *International Journal of Chemical Reactor Engineering*, *15*(3), 1–10. https://doi.org/10.1515/ijcre-2016-0111

Chen, G., & Fang, B. (2011). Preparation of solid acid catalyst from glucose-starch mixture for biodiesel production. *Bioresource Technology*, *102*(3), 2635–2640. https://doi.org/10.1016/j.biortech.2010.10.099

Cheng, Y., McPherson, A., Radosavljevic, M., Lee, V., Wong, K., & Jane, J. (1998). *Effects of starch chemical structures on gelatinization and pasting properties*. *4*(17), 63–71.

Choi, S., Drese, J., & Jones, C. (2009). Adsorbent materials for carbon dioxide capture from large anthropogenic point sources. *ChemSusChem*, *2*(9), 796–854. https://doi.org/10.1002/cssc.200900036

Clark, J. (2002). Solid acids for green chemistry. *Accounts of Chemical Research*, *35*(9), 791–797. https://doi.org/10.1021/ar010072a

Clark, J., Budarin, V., Dugmore, T., Luque, R., Macquarrie, D., & Strelko, V. (2008). Catalytic performance of carbonaceous materials in the esterification of succinic acid. *Catalysis Communications*, *9*(8), 1709–1714. https://doi.org/10.1016/j.catcom.2008.01.037

Clohessy, J., & Kwapinski, W. (2020). Carbon-based catalysts for biodiesel production-A

review. *Applied Sciences (Switzerland)*, *10*(3), 1–17. https://doi.org/10.3390/app10030918

Cruz, J., Silverio, J., Eliasson, A., & Larsson, K. (1996). A comparative study of gelatinization of cassava and potato starch in an aqueous lipid phase (L2) compared to water. *Food Hydrocolloids*, *10*(3), 317–322. https://doi.org/10.1016/S0268-005X(96)80007-5

Członka, S., Bertino, M., Kośny, J., & Shukla, N. (2018). Freeze-drying method as a new approach to the synthesis of polyurea aerogels from isocyanate and water. *Journal of Sol-Gel Science and Technology*, *87*(3), 685–695. https://doi.org/10.1007/s10971-018-4769-9

de Jong, M., Feijt, R., Zondervan, E., Nijhuis, T., & de Haan, A. (2009). Reaction kinetics of the esterification of myristic acid with isopropanol and n-propanol using p-toluene sulphonic acid as catalyst. *Applied Catalysis A: General*, *365*(1), 141–147. https://doi.org/10.1016/j.apcata.2009.06.009

De, S., Balu, A., van der Waal, J., & Luque, R. (2015). Biomass-derived porous carbon materials: Synthesis and catalytic applications. *ChemCatChem*, *7*(11), 1608–1629. https://doi.org/10.1002/cctc.201500081

Díaz, I., Márquez, C., Mohino, F., Pérez, J., & Sastre, E. (2000). Combined Alkyl and Sulfonic Acid Functionalization of MCM-41-Type Silica. *Journal of Catalysis*, *193*(2), 295–302. https://doi.org/10.1006/jcat.2000.2899

Dimian, A., & Rothenberg, G. (2016). An effective modular process for biodiesel manufacturing using heterogeneous catalysis. *Catalysis Science & Technology*, *6*(15), 6097–6108. https://doi.org/10.1039/C6CY00426A

Dome, K., Podgorbunskikh, E., Bychkov, A., & Lomovsky, O. (2020). Changes in the crystallinity degree of starch having different types of crystal structure after mechanical pretreatment. *Polymers*, *12*(3), 1–12. https://doi.org/10.3390/polym12030641

Dow Chemical Company. (2020). *Amberlyst 15WET Product Data Sheet*. *177.03087-0313*, 2. https://www.lenntech.com/Data-sheets/Dow-Amberlyst-15-wet-L.pdf

DPN. (2016). *Lost and waste of food in Colombia [in Spanish]* (Vol. 39).

DuPont de Nemours, I. (2019). *AMBERLYST™ 15DRY Polymeric Catalyst*. *45*, 1–2.

Elkhatat, A., & Al, S. (2011). Advances in tailoring resorcinol-formaldehyde organic and carbon gels. *Advanced Materials*, *23*(26), 2887–2903. https://doi.org/10.1002/adma.201100283

Fallahi, P., Muthukumarappan, K., & Rosentrater, K. (2016). Functional and structural properties of corn, potato, and cassava starches as affected by a single-screw extruder. *International Journal of Food Properties*, *19*(4), 768–788. https://doi.org/10.1080/10942912.2015.1042112

Folgueras, M., Rodríguez, S., Maza, N., & Oliva, M. (2012). Harvest, processing, and preservation of cassava (Manihot esculenta Crantz). II: Preservation methods, packaging and transportation, and root harvesting systems [in Spanish]. *Revista Científica UDO Agrícola*, *12*(4), 749–758.

Fu, Z., Wan, H., Hu, X., Cui, Q., & Guan, G. (2012). Preparation and catalytic performance of a carbon-based solid acid catalyst with high specific surface area. *Reaction Kinetics, Mechanisms and Catalysis*, *107*(1), 203–213. https://doi.org/10.1007/s11144-012-0466-9

García, M., Cardona, A., & García, C. (2020). Diagnosis of cassava bran management in the department of Sucre [in Spanish]. *Innovación En La Región Caribe de Colombia: Aportes Teóricos y Buenas Prácticas*. https://doi.org/10.21892/9789585547858.9

Geng, L., Wang, Y., Yu, G., & Zhu, Y. (2011). Efficient carbon-based solid acid catalysts for the esterification of oleic acid. *Catalysis Communications*, *13*(1), 26–30. https://doi.org/10.1016/j.catcom.2011.06.014

Grand View Research. (2020). *Fatty Acid Ester Market Size, Share & Trends Analysis Report 2020 - 2027*. https://www.grandviewresearch.com/industry-analysis/fatty-acid-esters-market

Gregg, S., & Sing, K. (1982). *Adsorption, Surface Area and Porosity* (Second edi).

Guan, J., & Hanna, M. (2004). Extruding foams from corn starch acetate and native corn starch. *Biomacromolecules*, *5*(6), 2329–2339. https://doi.org/10.1021/bm049512m

Hanzawa, Y., Kaneko, K., Pekala, R., & Dresselhaus, M. (1996). Activated carbon aerogels. *Langmuir*, *12*(26), 6167–6169. https://doi.org/10.1021/la960481t

Hara, M., Yoshida, T., Takagaki, A., Takata, T., Kondo, J., Hayashi, S., & Domen, K. (2004). A carbon material as a strong protonic acid. *Angewandte Chemie - International Edition*, *43*(22), 2955–2958. https://doi.org/10.1002/anie.200453947

Hernández, M., Torruco, J., Chel, L., & Betancur, D. (2008). Physicochemical Characterization of Starches from Tubers Cultivated in Yucatán, Mexico [in Spanish]. *Ciência e Tecnologia de Alimentos*, *28*(3), 718–726. https://doi.org/10.1590/s0101-20612008000300031

Hu, B., Yu, S.-H., Wang, K., Liu, L., & Xu, X. (2008). Functional carbonaceous materials from hydrothermal carbonization of biomass: an effective chemical process. *Dalton Transactions*, *9226*(40), 5414–5423. https://doi.org/10.1039/b804644c

Huang, J., Jian, Y., Li, H., & Fang, Z. (2022). Lignin-derived layered 3D biochar with controllable acidity for enhanced catalytic upgrading of Jatropha oil to biodiesel. *Catalysis Today*, *404*(August 2021), 35–48. https://doi.org/10.1016/j.cattod.2022.04.016

Inagaki, M. (2013). Advanced Carbon Materials. In *Handbook of Advanced Ceramics: Materials, Applications, Processing, and Properties* (Second Edt, pp. 25–60). Elsevier Inc. https://doi.org/10.1016/B978-0-12-385469-8.00002-2

Inagaki, M., & Kang, F. (2016). *Materials Science and Engineering of Carbon:*

Characterization. Tsinghua University Press Limited. https://doi.org/10.1016/B978-0-12-805256-3.00001-5

International Organization for Standatization. (2009). *ISO 660 (E). Animal and Vegetable Fats and Oils. Determination of Acid Value and Acidity.* (p. 14).

Intriago, M., & Muñoz, G. (2014). *Feasibility Study for the Establishment of a Company Producing Cassava Starch as a Raw Material for the Guayaquil Market [in Spanish]* [Universidad Católica de Santiago de Guayaquil]. http://repositorio.ucsg.edu.ec/handle/3317/2257

Ji, J., Zhang, G., Chen, H., Wang, S., Zhang, G., Zhang, F., & Fan, X. (2011). Sulfonated graphene as water-tolerant solid acid catalyst. *Chemical Science*, *2*(3), 484–487. https://doi.org/10.1039/c0sc00484g

Jia, R., Ren, J., Liu, X., Lu, G., & Wang, Y. (2014). Design and synthesis of sulfonated carbons with amphiphilic properties. *Journal of Materials Chemistry A*, *2*(29), 11195–11201. https://doi.org/10.1039/c4ta01836b

Joo, S., Choi, S., Oh, I., Kwak, J., Liu, Z., Terasaki, O., & Ryoo, R. (2001). Ordered nanoporous arrays of carbon supporting high dispersions of platinum nanoparticles. *Nature*, *412*(6843), 169–172. https://doi.org/10.1038/35084046

Jun, S., Joo, S., Ryoo, R., Kruk, M., Jaroniec, M., Liu, Z., Ohsuna, T., & Terasaki, O. (2000). Synthesis of new, nanoporous carbon with hexagonally ordered mesostructure. *Journal of the American Chemical Society*, *122*(43), 10712–10713. https://doi.org/10.1021/ja002261e

Juszczak, L., Fortuna, T., & Wodnicka, K. (2002). Characteristics of cereal starch granules surface using nitrogen adsorption. *Journal of Food Engineering*, *54*(2), 103–110. https://doi.org/10.1016/S0260-8774(01)00190-X

Kastratovic, V., & Bigovic, M. (2018). Esterification of stearic acid with lower monohydroxylic alcohols. *Chemical Industry and Chemical Engineering Quarterly*, *24*(3), 283–291. https://doi.org/10.2298/CICEQ170327040K

Kistler, S. (1932). Coherent expanded aerogels. *Journal of Physical Chemistry*, *36*(1), 52–64. https://doi.org/10.1021/j150331a003

Kitano, M., Arai, K., Kodama, A., Kousaka, T., Nakajima, K., Hayashi, S., & Hara, M. (2009). Preparation of a sulfonated porous carbon catalyst with high specific surface area. *Catalysis Letters*, *131*(1–2), 242–249. https://doi.org/10.1007/s10562-009-0062-4

Knorr, D., Heinz, V., & Buckow, R. (2006). High pressure application for food biopolymers. *Biochimica et Biophysica Acta - Proteins and Proteomics*, *1764*(3), 619–631. https://doi.org/10.1016/j.bbapap.2006.01.017

Konwar, L., Mäki, P., & Mikkola, J. (2019). SO3H-Containing Functional Carbon Materials: Synthesis, Structure, and Acid Catalysis. *Chemical Reviews*, *119*(22), 11576–11630. https://doi.org/10.1021/acs.chemrev.9b00199

Kosonen, H., Valkama, S., Nykänen, A., Toivanen, M., Brinke, G., Ruokolainen, J., & Ikkala, O. (2006). Functional porous structures based on the pyrolysis of cured templates of block copolymer and phenolic resin. *Advanced Materials*, *18*(2), 201–205. https://doi.org/10.1002/adma.200401110

Kruk, M., Jaroniec, M., Ryoo, R., & Joo, S. (2000). Characterization of ordered mesoporous carbons synthesized using MCM-48 silicas as templates. *Journal of Physical Chemistry B*, *104*(33), 7960–7968. https://doi.org/10.1021/jp000861u

Kunin, R., Meitzner, E. A., Oline, J. A., Fisher, S. A., & Frisch, N. (1962). Characterization of Amberlyst 15. Macroreticular Sulfonic Acid Cation Exchange Resin. *I&EC Product Research and Development*, *1*(2), 140–144. https://doi.org/10.1021/i360002a016

Labelle, M., Ispas, P., Tajer, S., Xiao, Y., Barbeau, B., & Mateescu, M. (2023). Anionic and Ampholytic High-Amylose Starch Derivatives as Excipients for Pharmaceutical and Biopharmaceutical Applications: Structure-Properties Correlations. *Pharmaceutics*, *15*(3). https://doi.org/10.3390/pharmaceutics15030834

Lanxess Energizing Chemistry. (2011). *Product Information Lewatit® K 2629*. 3. https://www.lenntech.com/Data-sheets/Lewatit-K-2629-L.pdf

Leofanti, G., Padovan, M., Tozzola, G., & Venturelli, B. (1998). Surface area and pore texture of catalysts. *Catalysis Today*, *41*(1–3), 207–219. https://doi.org/10.1016/S0920-5861(98)00050-9

Li, W., Yue, Q., Deng, Y., & Zhao, D. (2013). Ordered mesoporous materials based on interfacial assembly and engineering. *Advanced Materials*, *25*(37), 5129–5152. https://doi.org/10.1002/adma.201302184

Liang, C., Hong, K., Guiochon, G., Mays, J., & Dai, S. (2004). Synthesis of a large-scale highly ordered porous carbon film by self-assembly of block copolymers. *Angewandte Chemie - International Edition*, *43*(43), 5785–5789. https://doi.org/10.1002/anie.200461051

Liu, F., Li, B., Liu, C., Kong, W., Yi, X., Zheng, A., & Qi, C. (2016). Template-free synthesis of porous carbonaceous solid acids with controllable acid sites and their excellent activity for catalyzing the synthesis of biofuels and fine chemicals. *Catalysis Science and Technology*, *6*(9), 2995–3007. https://doi.org/10.1039/c5cy01226k

Liu, X., Huang, M., Ma, H., Zhang, Z., Gao, J., Zhu, Y., Han, X., & Guo, X. (2010). Preparation of a carbon-based solid acid catalyst by sulfonating activated carbon in a chemical reduction process. *Molecules*, *15*(10), 7188–7196. https://doi.org/10.3390/molecules15107188

Lowell, S., Shields, J., Martin, T., & Thommes, M. (2004). Surface Area Analysis from the Langmuir and BET Theories. In *Characterization of Porous Solids and Powders: Surface Area, Pore Size and Density*.

Lu, A. H., Li, W. C., Schmidt, W., & Schüth, F. (2005). Template synthesis of large pore ordered mesoporous carbon. *Microporous and Mesoporous Materials*, *80*(1–3), 117–128. https://doi.org/10.1016/j.micromeso.2004.12.007

Luque, R. (2010). Catalizadores de diseño para la producción de compuestos químicos de alto valor añadido y biocombustibles a partir de biomasa. *Anales de La Real Sociedad Española de Química*, *106*(4), 296–303. http://dialnet.unirioja.es/servlet/articulo?codigo=3347192

Luque, R., Budarin, V., Clark, J., Shuttleworth, P., & White, R. (2011). Starbon® acids in alkylation and acetylation reactions: Effect of the Brönsted-Lewis acidity. *Catalysis Communications*, *12*(15), 1471–1476. https://doi.org/10.1016/j.catcom.2011.06.008

Luque, R., Budarin, V., Shuttleworthb, P., & Clark, J. (2012). A new Starch is born: Starbons as biomass-derived mesoporous carbonaceous materials. *Bol. Grupe Espanol Carbón*, *June 2014*, 1–5.

Luque, R., & Clark, J. (2010). Water-tolerant Ru-Starbon® materials for the hydrogenation of organic acids in aqueous ethanol. *Catalysis Communications*, *11*(10), 928–931. https://doi.org/10.1016/j.catcom.2010.03.015

Luque, R., & Clark, J. (2011). Biodiesel-Like biofuels from simultaneous transesterification/esterification of waste oils with a biomass-derived solid acid catalyst. *ChemCatChem*, *3*(3), 594–597. https://doi.org/10.1002/cctc.201000280

Luque, R., Clark, J., Yoshida, K., & Gai, P. (2009). Efficient aqueous hydrogenation of biomass platform molecules using supported metal nanoparticles on Starbons®. *Chemical Communications*, *35*, 5305–5307. https://doi.org/10.1039/b911877b

Mahajan, A., & Gupta, P. (2020). Carbon-based solid acids: a review. *Environmental Chemistry Letters*, *18*(2), 299–314. https://doi.org/10.1007/s10311-019-00940-7

Manrique, N. (2006). *Production of pregelatinized starches from blends of starches from unconventional sources using a twin-screw extruder [in Spanish]*. Instituto Politécnico Nacional.

Markley, K. (1983). *Fatty acids: their chemistry properties production and uses* (Second edi). Krieger Publishing.

Marziano, N., Tortato, C., Ronchin, L., & Bianchi, C. (1998). On the acidity of liquid and solid acid catalysts: Part 1. A thermodynamic point of view. *Catalysis Letters*, *56*(2), 159–164. https://doi.org/10.1023/a:1019096726458

Maziarka, P., Wurzer, C., Arauzo, P. J., Dieguez-Alonso, A., Mašek, O., & Ronsse, F. (2021). Do you BET on routine? The reliability of N2 physisorption for the quantitative assessment of biochar's surface area. *Chemical Engineering Journal*, *418*(March). https://doi.org/10.1016/j.cej.2021.129234

Megazyme. (2018). Amylose/Amylopectin: Assay Procedure K-AMYL 06/18. *Megazyme Data Booklet*, *6*, 11. https://www.megazyme.com/amylose-amylopectin-assay-kit?sSearch=amylose

Mena, C. (2014). *Synthesis and characterisation of sulfonated Starbons®, biobased catalysts* (Issue August). University of York Chemistry.

Mena, C., & Macquarrie, D. (2014). Esterification of lauric acid with methanol using sulfonated Starbons. *Research Journal of Chemistry and Environment*, *18*(8), 1–6.

Milescu, R., Dennis, M., McElroy, R., Macquarrie, D., Matharu, A., Smith, M., Clark, J., & Budarin, V. (2020). The role of surface functionality of sustainable mesoporous materials Starbon® on the adsorption of toxic ammonia and sulphur gasses. *Sustainable Chemistry and Pharmacy*, *15*(February). https://doi.org/10.1016/j.scp.2020.100230

Mohan, D., & Pittman, C. (2006). Activated carbons and low cost adsorbents for remediation of tri- and hexavalent chromium from water. *Journal of Hazardous Materials*, *137*(2), 762–811. https://doi.org/10.1016/j.jhazmat.2006.06.060

Morishita, T., Ishihara, K., Kato, M., & Inagaki, M. (2007). Preparation of a carbon with a 2 nm pore size and of a carbon with a bi-modal pore size distribution. *Carbon*, *45*(1), 209–211. https://doi.org/10.1016/j.carbon.2006.09.032

Morishita, T., Ishihara, K., Kato, M., Tsumura, T., & Inagaki, M. (2007). Mesoporous carbons prepared from mixtures of magnesium citrate with poly (vinyl alcohol). *Tanso*, *2007*(226), 19–24. https://doi.org/10.7209/tanso.2007.19

Morishita, T., Tsumura, T., Toyoda, M., Przepiórski, J., Morawski, A., Konno, H., & Inagaki, M. (2010). A review of the control of pore structure in MgO-templated nanoporous carbons. *Carbon*, *48*(10), 2690–2707. https://doi.org/10.1016/j.carbon.2010.03.064

Niu, S., Ning, Y., Lu, C., Han, K., Yu, H., & Zhou, Y. (2018). Esterification of oleic acid to produce biodiesel catalyzed by sulfonated activated carbon from bamboo. *Energy Conversion and Management*, *163*(17923), 59–65. https://doi.org/10.1016/j.enconman.2018.02.055

Okamoto, Y., & Yashima, E. (1998). Polysaccharide Derivatives for Chromatographic Separation of Enantiomers. *Angewandte Chemie International Edition*, *37*(8), 1020–1043.

Okamura, M., Takagaki, A., Toda, M., Kondo, J., Domen, K., Tatsumi, T., Hara, M., & Hayashi, S. (2006). Acid-catalyzed reactions on flexible polycyclic aromatic carbon in amorphous carbon. *Chemistry of Materials*, *18*(13), 3039–3045. https://doi.org/10.1021/cm0605623

Ouyang, S., Kuang, X., Xu, Q., & Yin, D. (2014). Preparation of a Carbon-Based Solid Acid with High Acid Density via a Novel Method. *Journal of Materials Science and Chemical Engineering*, *02*(06), 4–8. https://doi.org/10.4236/msce.2014.26002

Pandolfo, A., & Hollenkamp, A. (2006). Carbon properties and their role in supercapacitors. *Journal of Power Sources*, *157*(1), 11–27. https://doi.org/10.1016/j.jpowsour.2006.02.065

Pang, Q., Wang, L., Yang, H., Jia, L., Pan, X., & Qiu, C. (2014). Cellulose-derived carbon bearing -Cl and -SO3H groups as a highly selective catalyst for the hydrolysis of cellulose to glucose. *RSC Advances*, *40*(78), 41212–41218. https://doi.org/10.1039/c4ra05520a

Parker, H. (2013). *Recovery from Waste Streams: Working Towards a Sustainable Future*. *April*. http://etheses.whiterose.ac.uk/4176/1/Helen_Parker_PhD_Thesis.pdf

Parker, H., Budarin, V., Clark, J., & Hunt, A. (2013). Use of starbon for the adsorption and desorption of phenols. *ACS Sustainable Chemistry and Engineering*, *1*(10), 1311–1318. https://doi.org/10.1021/sc4001675

Parker, H., Hunt, A., Budarin, V., Shuttleworth, P., Miller, K., & Clark, J. (2012). The importance of being porous: Polysaccharide-derived mesoporous materials for use in dye adsorption. *RSC Advances*, *2*(24), 8992–8997. https://doi.org/10.1039/c2ra21367b

Paterson, G., Issariyakul, T., Baroi, C., Bassi, A., & Dalai, A. (2013). Ion-exchange resins as catalysts in transesterification of triolein. *Catalysis Today*, *212*, 157–163. https://doi.org/10.1016/j.cattod.2012.10.013

Pekala, R. (1989). Organic aerogels from the polycondensation of resorcinol with formaldehyde. *Journal of Materials Science*, *24*(9), 3221–3227. https://doi.org/10.1007/BF01139044

Pekala, R., Alviso, C., Kong, F., & Hulsey, S. (1991). Aerogels Derived from Multifunctional Organic Monomers. *Third International SymPosium on Aerogels*, 21.

Peng, L., Philippaerts, A., Ke, X., Van Noyen, J., De Clippel, F., Van Tendeloo, G., Jacobs, P., & Sels, B. (2010). Preparation of sulfonated ordered mesoporous carbon and its use for the esterification of fatty acids. *Catalysis Today*, *150*(1–2), 140–146. https://doi.org/10.1016/j.cattod.2009.07.066

Rodriguez, F. (1998). The role of carbon materials in heterogeneous catalysis. *Carbon*, *36*(3), 159–175. https://doi.org/https://doi.org/10.1016/S0008-6223(97)00173-5

Rohm & Haas. (2005). Amberlyst™ 70 Product Data Sheet. *Rohm & Haas: Philadelphia, PA, USA*, 1–2.

Rohm and Haas. (2006). *Amberlyst™ 35WET Product Data Sheet*.

Saha, D., Payzant, A., Kumbhar, A., & Naskar, A. (2013). Sustainable mesoporous carbons as storage and controlled-delivery media for functional molecules. *ACS Applied Materials and Interfaces*, *5*(12), 5868–5874. https://doi.org/10.1021/am401661f

Sandhu, K., & Singh, N. (2007). Some properties of corn starches II: Physicochemical, gelatinization, retrogradation, pasting and gel textural properties. *Food Chemistry*, *101*(4), 1499–1507. https://doi.org/10.1016/j.foodchem.2006.01.060

Shi, Y., & Seib, P. (1992). The structure of four waxy starches related to gelatinization and retrogradation. *Carbohydrate Research*, *227*(C), 131–145. https://doi.org/10.1016/0008-6215(92)85066-9

Shuttleworth, P., Budarin, V., White, R., Gun'Ko, V., Luque, R., & Clark, J. (2013). Molecular-level understanding of the carbonisation of polysaccharides. *Chemistry - A*

European Journal, *19*(28), 9351–9357. https://doi.org/10.1002/chem.201300825

Silverstein, R. M., & Webster, F. X. (1996). Spectrometric Identification Of Organic Compounds 6th Edition. In *John Wiley & Sons Ltd* (Vol. 6, pp. 1–482).

Sing, K., Everett, D., Haul, R., Moscou, L., Pierotti, R., Rouquérol, J., & Siemieniewska, T. (1985). Reporting phisisorption data for gas/solid systems. *Pure and Applied Chemistry*, *57*(4), 603–619.

Sreedhar, I., Aniruddha, R., & Malik, S. (2019). Carbon capture using amine modified porous carbons derived from starch (Starbons®). *SN Applied Sciences*, *1*(5), 1–11. https://doi.org/10.1007/s42452-019-0482-8

Suganuma, S., Nakajima, K., Kitano, M., Yamaguchi, D., Kato, H., Hayashi, S., & Hara, M. (2008). Hydrolysis of Cellulose by Amorphous Carbon Bearing SO3H, COOH, and OH Groups. *Journal of the American Chemical Society*, *130*(38), 12787–12793. https://doi.org/10.1021/la8040506

Takagaki, A., Toda, M., Okamura, M., Kondo, J., Hayashi, S., Domen, K., & Hara, M. (2006). Esterification of higher fatty acids by a novel strong solid acid. *Catalysis Today*, *116*(2 SPEC. ISS.), 157–161. https://doi.org/10.1016/j.cattod.2006.01.037

Tamon, H., Ishizaka, H., Yamamoto, T., & Suzuki, T. (1999). Preparation of mesoporous carbon by freeze drying. *Carbon*, *37*(12), 2049–2055. https://doi.org/10.1016/S0008-6223(99)00089-5

Tanaka, S., Nishiyama, N., Egashira, Y., & Ueyama, K. (2005). Synthesis of ordered mesoporous carbons with channel structure from an organic-organic nanocomposite. *Chemical Communications*, *16*, 2125–2127. https://doi.org/10.1039/b501259g

Tang, M., & Copeland, L. (2007). Investigation of starch retrogradation using atomic force microscopy. *Carbohydrate Polymers*, *70*(1), 1–7. https://doi.org/10.1016/j.carbpol.2007.02.025

Tian, Y., Li, Y., Xu, X., & Jin, Z. (2011). Starch retrogradation studied by thermogravimetric analysis (TGA). *Carbohydrate Polymers*, *84*(3), 1165–1168. https://doi.org/10.1016/j.carbpol.2011.01.006

Titirici, M., White, R., Brun, N., Budarin, V., Su, D., Del Monte, F., Clark, J., & MacLachlan, M. (2015). Sustainable carbon materials. *Chemical Society Reviews*, *44*(1), 250–290. https://doi.org/10.1039/c4cs00232f

Toda, M., Takagaki, A., Okamura, M., Kondo, J., Hayashi, S., Domen, K., & Hara, M. (2005). Biodiesel made with sugar catalyst. *Nature Communications*, *438*, 178. https://doi.org/10.1038/438178

Torres, P., Rodríguez, J., & Rojas, O. (2005). Extracción de almidón de yuca. Manejo integral y control de la contaminación hídrica. *Livestock Research for Rural Development*, *17*(7), 2005.

Uriburu-Gray, M., Pinar-Serrano, A., Cavus, G., Knipping, E., Aucher, C., Conesa-Cabeza, A., Satti, A., Amantia, D., & Martínez-Crespiera, S. (2020). Mesoporous carbons from polysaccharides and their use in li-o2 batteries. *Nanomaterials*, *10*(10),

1–18. https://doi.org/10.3390/nano10102036

van Soest, J., de Wit, D., Tournois, H., & Vliegenthart, J. (1994). The influence of glycerol on structural changes in waxy maize starch as studied by Fourier transform infra-red spectroscopy. *Polymer*, *35*(22), 4722–4727. https://doi.org/10.1016/0032-3861(94)90724-2

Wang, L., Dong, X., Jiang, H., Li, G., & Zhang, M. (2014). Phosphorylated ordered mesoporous carbon as a novel solid acid catalyst for the esterification of oleic acid. *Catalysis Communications*, *56*, 164–167. https://doi.org/10.1016/j.catcom.2014.07.008

Wang, S., & Copeland, L. (2013). Molecular disassembly of starch granules during gelatinization and its effect on starch digestibility: A review. *Food and Function*, *4*(11), 1564–1580. https://doi.org/10.1039/c3fo60258c

Wang, S., Li, C., Copeland, L., Niu, Q., & Wang, S. (2015). Starch Retrogradation: A Comprehensive Review. *Comprehensive Reviews in Food Science and Food Safety*, *14*(5), 568–585. https://doi.org/10.1111/1541-4337.12143

Wenchao, W., Fashe, L., & Ying, L. (2019). Kinetics and the fluidity of the stearic acid esters with different carbon backbones. *Green Process Synth*, *8*, 776–785. https://doi.org/https://doi.org/10.1515/gps-2019-0046

White, R., Brun, N., Budarin, V., Clark, J., & Titirici, M. (2014). Always look on the “light” side of life: Sustainable carbon aerogels. *ChemSusChem*, *7*(3), 670–689. https://doi.org/10.1002/cssc.201300961

White, R., Budarin, V., & Clark, J. (2008). Tuneable mesoporous materials from alpha-D-polysaccharides. *ChemSusChem*, *1*(5), 408–411. https://doi.org/10.1002/cssc.200800012

White, R., Budarin, V., Luque, R., Clark, J., & Macquarrie, D. (2009). Tuneable porous carbonaceous materials from renewable resources. *Chemical Society Reviews*, *38*(12), 3401–3418. https://doi.org/10.1039/b822668g

White, R., & Clark, J. (2015). Porous carbon materials from sustainable precursors. In *RSC Green Chemistry No. 32* (Vol. 32).

White, R., Shuttleworth, P., Budarin, V., De Bruyn, M., Fischer, A., & Clark, J. (2016). An Interesting Class of Porous Polymer - Revisiting the Structure of Mesoporous α- D - Polysaccharide Gels. *ChemSusChem*, *9*(3), 280–288. https://doi.org/10.1002/cssc.201501354

Yalçinyuva, T., Deligöz, H., Boz, İ., & Ali, M. (2008). Kinetics and mechanism of myristic acid and isopropyl alcohol esterification reaction with homogeneous and heterogeneous catalysts. *International Journal of Chemical Kinetics*, *40*(3), 136–144. https://doi.org/10.1002/kin.20293

Yamamoto, T., Nishimura, T., Suzuki, T., & Tamon, H. (2001). Control of mesoporosity of carbon gels prepared by sol-gel polycondensation and freeze drying. *Journal of Non-*

Crystalline Solids, *288*(1–3), 46–55. https://doi.org/10.1016/S0022-3093(01)00619-6

Yameen, M., AlMohamadi, H., Naqvi, S., Noor, T., Chen, W., & Amin, N. (2023). Advances in production & activation of marine macroalgae-derived biochar catalyst for sustainable biodiesel production. *Fuel*, *337*(December 2022), 127215. https://doi.org/10.1016/j.fuel.2022.127215

Yang, N., Sheng, X., Ti, L., Jia, H., Ping, Q., & Li, N. (2023). Ball-milling as effective and economical process for biodiesel production under Kraft lignin activated carbon stabilized potassium carbonate. *Bioresource Technology*, *369*(November 2022), 128379. https://doi.org/10.1016/j.biortech.2022.128379

Zhan, S., Tao, X., Cai, L., Liu, X., & Liu, T. (2014). The carbon material functionalized with NH2+ and SO3H groups catalyzed esterification with high activity and selectivity. *Green Chemistry*, *16*(11), 4649–4653. https://doi.org/10.1039/c4gc01395f

Zhang, B., Ren, J., Liu, X., Guo, Y., Guo, Y., Lu, G., & Wang, Y. (2010). Novel sulfonated carbonaceous materials from p-toluenesulfonic acid/glucose as a high-performance solid-acid catalyst. *Catalysis Communications*, *11*(7), 629–632. https://doi.org/10.1016/j.catcom.2010.01.010

Zhang, F., Meng, Y., Gu, D., Yan, Y., Yu, C., Tu, B., & Zhao, D. (2005). A facile aqueous route to synthesize highly ordered mesoporous polymers and carbon frameworks with Ia3d bicontinuous cubic structure. *Journal of the American Chemical Society*, *127*(39), 13508–13509. https://doi.org/10.1021/ja0545721

Zobel, H. (1988). Molecules to Granules: A Comprehensive Starch Review. *Starch - Stärke*, *40*(2), 44–50. https://doi.org/10.1002/star.19880400203

Zong, M., Duan, Z., Lou, W., Smith, T., & Wu, H. (2007). Preparation of a sugar catalyst and its use for highly efficient production of biodiesel. *Green Chemistry*, *9*(5), 434–443. https://doi.org/10.1039/b615447f